Savannah River National Laboratory®

A U.S. DEPARTMENT OF ENERGY NATIONAL LAB • SAVANNAH RIVER SITE • AIKEN, SC • USA

Refinement of Pitting Factor Basis to Support the Corrosion Control Program – Interim Report

J. T. Boerstler

June 2023

SRNL-STI-2023-00061, Revision 0

DISCLAIMER

Printed in the United States of America

Prepared for
U.S. Department of Energy

SRNL-STI-2023-00061
Revision 0

Keywords: *pitting factor, salt dissolution, pitting corrosion*

Retention: *Permanent*

Refinement of Pitting Factor Basis to Support the Corrosion Control Program – Interim Report

J. T. Boerstler

June 2023

Savannah River National Laboratory is operated by Battelle Savannah River Alliance for the U.S. Department of Energy under Contract No. 89303321CEM000080.

REVIEWS AND APPROVALS

AUTHORS:

JOSHUA BOERSTLER (Affiliate) Digitally signed by JOSHUA BOERSTLER (Affiliate)
Date: 2023.06.06 09:23:59 -04'00'

J. T. Boerstler, Applied Materials Research, SRNL Date

TECHNICAL REVIEW:

BRUCE WIERSMA (Affiliate) Digitally signed by BRUCE WIERSMA (Affiliate)
Date: 2023.06.06 09:33:45 -04'00'

B. J. Wiersma, Applied Materials Research, SRNL, Reviewed per E7 2.60 Date

KEISHA MARTIN (Affiliate) Digitally signed by KEISHA MARTIN (Affiliate)
Date: 2023.06.06 10:03:48 -04'00'

K. B. Martin, Safety Programs and Regulatory, SRMC Date

APPROVAL:

ALEX COZZI (Affiliate) Digitally signed by ALEX COZZI (Affiliate)
Date: 2023.06.07 09:25:00 -04'00'

A. D. Cozzi, Manager, Applied Materials Research, SRNL Date

FRANK PENNEBAKER (Affiliate) Digitally signed by FRANK PENNEBAKER (Affiliate)
Date: 2023.06.07 10:27:25 -04'00'

F. M. Pennebaker, Director, Chemical Processing and Characterization, SRNL Date

Andrew Marvel Digitally signed by Andrew Marvel
Date: 2023.06.07 10:34:53 -04'00'

A. J. Marvel, Manager, Safety Programs and Regulatory Date

ACKNOWLEDGEMENTS

The author gratefully acknowledges the assistance of B. Hill and C. Rasmussen in the execution of the testing program. The author would also like to acknowledge Dr. Stephen Harris for his assistance with the statistical design for the experiments.

EXECUTIVE SUMMARY

At Savannah River Site (SRS), High-Level Waste is stored in below-grade tanks constructed of carbon steel. This waste is composed of sludge, salt cake, and/or supernate. In part, preparation of this waste for future processing involves dissolution of the salt cake layer. The salt dissolution process can create conditions that leave the carbon steel tanks susceptible to a number of corrosion processes. The salt to be dissolved contains high concentrations of nitrate, that once released, create an environment that may be conducive to pitting corrosion or stress corrosion cracking (SCC) of carbon steel. Additionally, during the salt dissolution process, in the absence of mixing, stratification of the supernatant liquid may occur. This can result in less dense, more dilute waste layers occurring higher in the tank. In these more dilute waste layers, the susceptibility to localized corrosion could potentially differ from that of the more concentrated salt solutions evaluated in previous testing, as the amount of inhibiting and aggressive species, not just the ratios, can affect susceptibility. Evaluation of the susceptibility to localized corrosion in these more dilute waste chemistries could provide insight into the amount of inhibitors required to effectively mitigate pitting corrosion in stagnant salt dissolution environments, as well as other tank farm operations involving dilute waste streams.

The current Corrosion Control Program dictates minimum inhibitor requirements based upon the concentration of nitrate present in the waste. Instead of focusing on multiple limits based on the nitrate concentration, this work seeks to utilize a single value, the Pitting Factor (PF), as a metric for the prediction of localized corrosion. This metric uses the weighted ratios of inhibiting species (hydroxide and nitrite) to aggressive species (nitrate and chloride) as a predictive metric for susceptibility to localized corrosion.

The chemistry envelope evaluated in previous works considered conditions at both the Hanford and Savannah River sites, which considered significantly higher chloride concentrations than are present in SRS tanks. In addition, this work focused on the highly concentrated salt solutions that are present during the salt dissolution process. Considering that chloride concentrations are an order of magnitude lower at SRS than the maximum chloride previously tested, it has been proposed that the control limits be refined to determine if a reduction in the minimum nitrite requirement is warranted in more dilute solutions and those with chloride concentrations more indicative of waste tank chemistries at SRS. The test matrix developed for this work focuses in particular on more dilute chemistries than previous testing campaigns. In addition, because pitting corrosion, not SCC, is the focus of this work, only temperatures up to 50 °C were considered.

Through the use of cyclic potentiodynamic polarization and Modified ASTM G192 testing methods, the susceptibility of A537 carbon steel to pitting corrosion was evaluated. The Pitting Factor was shown to accurately predict pitting susceptibility throughout the chemistry envelope evaluated. In addition, it was shown that nitrite is not required for inhibition of pitting corrosion in tank conditions with chloride concentrations observed at SRS and up to 4 M nitrate. Based upon these findings, new control limits were proposed that removed the minimum nitrite requirement within the chemistry envelope evaluated up to 50 °C. In addition, a comparison of the hydroxide required to effectively inhibit pitting corrosion using the proposed control limits and limits imposed by the current Corrosion Control Program was conducted. Additional analysis will be conducted and documented in the Final Report that will cover the effects of nitrite/nitrate ratio and the amount, not just the ratios, of inhibiting and aggressive species on pitting susceptibility. A statistical analysis will also be performed to determine if the coefficients used previously in the Pitting Factor equation would need to be adjusted over the compositional range tested in this work.

TABLE OF CONTENTS

LIST OF TABLES

LIST OF FIGURES

LIST OF ABBREVIATIONS

°C	Degrees Celsius
μA	microamperes
A	Amperes
A537	A537 Low Carbon Steel
ASTM	American Society for Testing and Materials
CPP	Cyclic Potentiodynamic Polarization
M	Molar (moles/Liter)
mV	Millivolts
OCP	Open Circuit Potential
SCC	Stress Corrosion Cracking
SCE	Saturated Calomel Electrode
SiC	Silicon Carbide
SRS	Savannah River Site
V	Volts

1.0 Introduction

At Savannah River Site (SRS), High-Level Waste is stored in below-grade tanks constructed of carbon steel. This waste is composed of sludge, salt cake, and/or supernate. In part, preparation of this waste for future processing involves dissolution of the salt cake layer. The salt dissolution process can create conditions that leave the carbon steel tanks susceptible to localized corrosion (e.g., pitting or stress corrosion cracking (SCC)). The salt to be dissolved contains high concentrations of nitrate, that once released, create an aggressive environment.

An administrative control program is in place that dictates the amount of inhibitor required for tank chemistries based on the concentration of nitrate (and also chloride and sulfate when nitrate is less than 1 M) present [1]. The inhibitor concentration limits used by this program are shown in Table 1-1. This program is based on experimental programs that have evaluated the susceptibility of A537 and A285 carbon steels to pitting corrosion and SCC in high nitrate concentration solutions with low concentrations of inhibitors [2-4].

Table 1-1: Current Corrosion Control Program Inhibitor Concentration Limits [1].

Table 1. Minimum Corrosion Inhibitor Concentration Limits

Applicability	Limit		Parameter	Minimum Needed	Units
$5.5M < [NO_3^-] \leq 8.5M$	1		$[OH^-]$	0.6	Molar
			$[OH^-] + [NO_2^-]$	1.1	Molar
$2.75M < [NO_3^-] \leq 5.5M$	2		$[OH^-]$	0.3	Molar
			$[OH^-] + [NO_2^-]$	1.1	Molar
$1.0M \leq [NO_3^-] \leq 2.75M$	3		$[OH^-]$	$0.1[NO_3^-]$	Molar
			$[OH^-] + [NO_2^-]$	$0.4[NO_3^-]$	Molar
$0.02M < [NO_3^-] < 1.0M$ AND $[OH^-] < 1.0M$ (See Note 2)	4	4a	$[OH^-]$	1.0	Molar
			OR		
		4b	$[NO_2^-]$	$0.038 \cdot [NO_3^-] \cdot 10^{1.64}$	Molar
		4c	AND $[NO_2^-]$	$6.11 \cdot 10^{[1.64+1.34*\log[Cl-]]}$	Molar
		4d	AND $[NO_2^-]$	$0.04 \cdot 10^{[1.64+0.84*\log[SO4-2]]}$	Molar
		4e	AND pH	10.3	pH
$[NO_3^-] \leq 0.02$ M AND $[OH^-] < 1.0$ M (See Note 2)	5	5a	$[OH^-]$	1.0	Molar
			OR		
		5b	$[NO_2^-]$ (if $[Cl^-]$ & $[SO_4^{-2}]$ is not known)	0.033	Molar
			OR		
		5c	$[NO_2^-]$	$0.038 \cdot [NO_3^-] \cdot 10^{1.64}$	Molar
		5d	AND $[NO_2^-]$	$6.11 \cdot 10^{[1.64+1.34*\log[Cl-]]}$	Molar
		5e	AND $[NO_2^-]$	$0.04 \cdot 10^{[1.64+0.84*\log[SO4-2]]}$	Molar
		5f	AND pH	10.3	pH

These control limits were revisited previously to evaluate the corrosion susceptibility of carbon steel in environments that more closely resemble current operating conditions at the SRS [5]. Instead of focusing on multiple limits based on the nitrate concentration, this work sought to utilize a single value, the Pitting Factor (PF), as a metric for the prediction of localized corrosion. The equation for calculating the Pitting Factor is presented below.

$$\text{Pitting Factor} = \frac{8.06\,[\mathrm{OH^-}] + 1.55\,[\mathrm{NO_2^-}]}{[\mathrm{NO_3^-}] + 16.7\,[\mathrm{Cl^-}]}$$

To develop this metric, logistic regression of the results of several series of tests was conducted to evaluate the susceptibility to pitting corrosion [6]. Through this analysis, species that affected susceptibility to localized corrosion were identified (both inhibiting and aggressive species) and their relative impacts on pitting susceptibility weighted. The concentration of these species, in addition to their weighting coefficients from this model were then used as the basis for the development of the empirical pitting factor to be used as a predictive metric for pitting susceptibility. In its current form, the pitting factor uses the weighted ratios of inhibiting species (hydroxide and nitrite) to aggressive species (nitrate and chloride) to predict conditions where susceptibility to localized corrosion exists. A pitting factor of 1.2 or greater indicates a low susceptibility to pitting corrosion, whereas a pitting factor of less than 1.2 indicates a chemistry in which pitting may occur. The chemistry envelope evaluated and the proposed control limits from this previous work are presented in Table 1-2.

Table 1-2: Summary of Chemistry Envelope and Proposed Corrosion Control Limits for Pitting Corrosion Utilizing Pitting Factor Methodology [5].

Chemistry Envelope Tested	
Nitrate [M]	0 – 7
Chloride [M]	0 – 0.4
Hydroxide [M]	0.0001 – 0.6
Nitrite [M]	0.0 – 0.6
Proposed Control Limits	
Minimum pH	12
Minimum Pitting Factor	1.2
Minimum Nitrite [M]	0.2
Maximum Temperature [°C]	75

The chemistry envelope evaluated considered conditions at both the Hanford and Savannah River sites, which considered significantly higher chloride concentrations than are present in SRS tanks. In addition, this work focused on the highly concentrated salt solutions that are present during the salt dissolution process. Considering that chloride concentrations are an order of magnitude lower at SRS than the maximum chloride previously tested, the objective of these test was to further refine the Proposed Control Limits to determine if a reduction in the minimum nitrite requirement is warranted in more dilute solutions and those with chloride concentrations more indicative of waste tank chemistries at SRS. Additional details about the scope of work can be found in the Task Technical Request and Task Technical and Quality Assurance Plan [7, 8]. The chemistry envelope for proposed testing is presented in Table 1-3. The test matrix developed focuses specifically on more dilute chemistries than previous testing campaigns. In addition, because pitting corrosion, not SCC, is the focus of this work in this report, only temperatures up to 50 °C were considered.

Table 1-3: Chemistry Envelope for CPP Testing.

	Minimum	Maximum
Temperature [°C]	30	50
Nitrate [M]	0.008	4
Hydroxide [M]	0.01	0.7
Nitrite [M]	0	0.2
Chloride [M]	0.0005	0.03

Electrodes of A537 carbon steel were subjected to cyclic potentiodynamic polarization (CPP) to determine their susceptibility to pitting corrosion in waste tank simulants. Previous testing evaluated the pitting susceptibility of both A537 and A285 carbon steels, with A537 having shown to be slightly more susceptible to pitting corrosion [5]. Therefore, A537 carbon steel was determined to be bounding for the two materials and only A537 was evaluated in this work. In several cases, a mixed hysteresis on the CPP test in addition to the absence of pitting on the boldly exposed surface made determination of the pass/fail status of a trial inconclusive. In these cases, Modified ASTM G192 was used to attempt to clarify the susceptibility to pitting corrosion. In a number of these cases as well, the results were impacted by crevice corrosion in both the CPP and Modified ASTM G192 tests. As a result, CPP tests were carried out using A537 bullet electrodes, which have no creviced area. With these two techniques and two electrode configurations, all trials could be assessed, and the PF and minimum nitrite limit were evaluated in terms of their applicability in the more dilute, lower chloride chemistry envelope.

2.0 Experimental Procedure

2.1 Cyclic Potentiodynamic Polarization of Carbon Steel Electrodes

A common method used to assess the pitting susceptibility of an alloy in a given environment is CPP. The resulting polarization curve from a CPP test can be found in Figure 2-1 for reference. This method involves first exposing the electrode to the solution for 2 hours while the open circuit potential (OCP) is measured. The OCP after 2 hours of exposure then serves as a reference point for the scan range of the CPP test. The test initiates at 100 mV below this open circuit value and is scanned at a slow rate (0.167 mV/s) toward more positive potentials and the current response is measured. This occurs until the potential limit (1.2 V) or the current density limit (1 mA/cm^2) is reached, at which point the potential scan is reversed and continued towards more negative potentials while continuing to measure the current response. The test is concluded once the potential reaches the original OCP measured at two hours of exposure. From the resulting current-potential plot, a number of assessments can be made about the susceptibility of the material to pitting corrosion in that environment. The first characteristic value is the breakdown potential or pitting potential. This is typified by the large increase in current from the passive current that occurs as a result of increased anodic dissolution rates. The next characteristic that can be assessed is the nature of the hysteresis. A positive hysteresis, the reverse scan having higher current than the forward scan at the same potential value, indicates that pitting has occurred, and pits continue to grow even below the breakdown potential. A negative or no hysteresis likely indicates that no localized corrosion has occurred, or pit growth is no longer stable when the potential decreases. Lastly, the repassivation potential could be obtained if solution conditions are such that repassivation of active pits can occur. This parameter may not be possible to obtain if chemistries conducive to repassivation are not present or if repassivation occurs below the corrosion potential.

The open circuit potential or corrosion potential of the material, along with the repassivation potential and breakdown potential, can be used to assess the severity of the material's susceptibility to pitting corrosion in a given environment. The relative positions of the corrosion and breakdown potentials indicates how much the material must be polarized to support stable pit growth into the material. If the breakdown potential is close to the corrosion potential, pitting is more likely in the event of polarization of the material or if there is an increase in the OCP of the material with exposure time. The relative positions of the breakdown and repassivation potentials essentially indicates the range over which initiated pits will continue to grow, if pits are present. Therefore, materials with repassivation potentials closer to the breakdown potential are desirable. Lastly, the relationship of the corrosion potential and the repassivation potential is an indicator of the likelihood of pitting in a material. If the repassivation potential is near the corrosion potential, there is an increased likelihood that the repassivation potential could be exceeded, and pits that initiated will continue to grow so long as the corrosion potential remains above the repassivation potential.

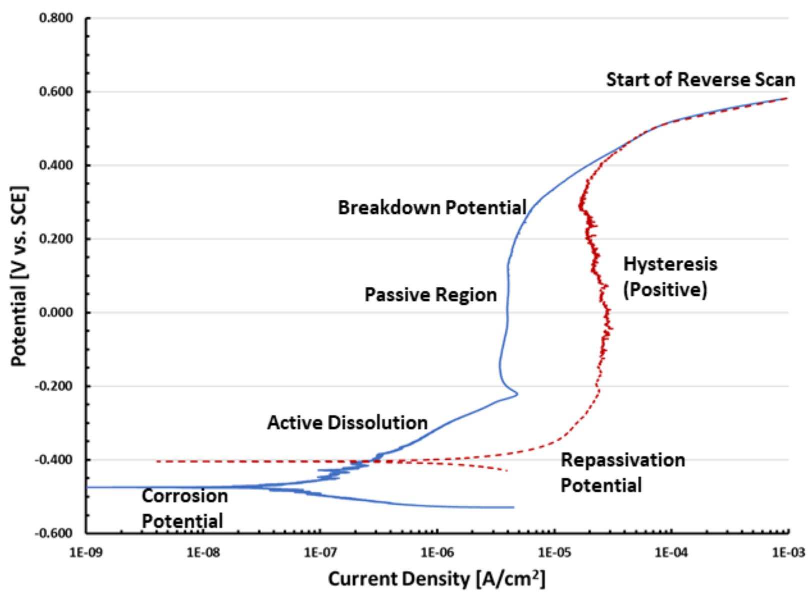

Figure 2-1: Example of CPP curve with regions and values of interest labelled. Solid blue line represents the forward scan, and dashed red line represents the reverse scan.

Three outcomes are possible based upon the presence or absence of stable localized corrosion during the polarization. The first is a positive hysteresis, which is shown in Figure 2-2.

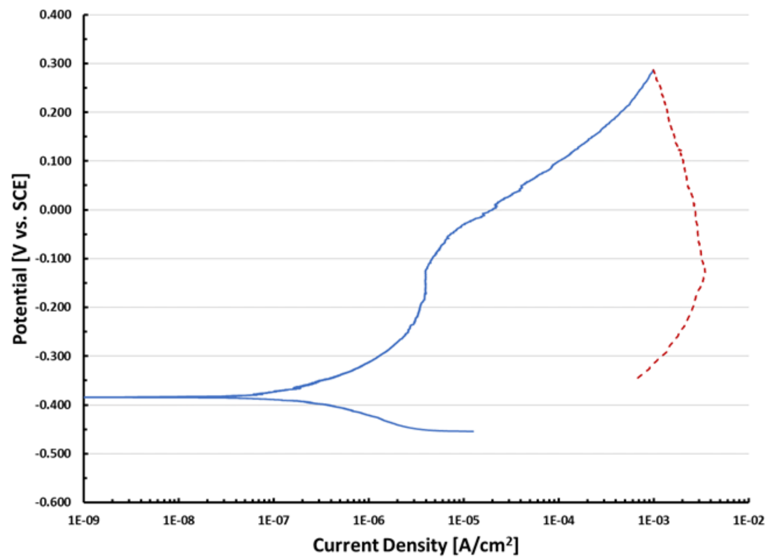

Figure 2-2: Example of a positive hysteresis, defined as the current density from the reverse scan being greater than that of the forward scan. Solid blue line represents the forward scan, and dashed red line represents the reverse scan.

A positive hysteresis is defined by the current of the reverse scan being greater than that of the forward scan. With these cases, the current density of the reverse scan should remain higher than the passive current density within the potential range of the passive region with the exception of decreases in current associated with repassivation, illustrated in Figure 2-1. This is indicative of stable localized corrosion taking place, which could be the result of pitting or crevice corrosion. If the positive hysteresis is the result of crevice corrosion, this does not indicate a failure, as the result is due to an artifact of experimental design. Based upon these conditions and those used to assess the results of CPP testing from previous works, failure is determined if the following three conditions are met [9]:

1. A positive or mixed hysteresis was present on the CPP curve.
2. Pitting, not crevice, corrosion was observed on the electrode surface.
3. Repassivation potential was not observed or the difference between repassivation potential and corrosion potential is less than 200 mV.

Pitting corrosion can only occur at potentials above the repassivation potential. Below this potential, any pits that were present would be passivated, meaning that a passive film is stable, and no further dissolution would occur. Therefore, the difference between the corrosion potential and the repassivation potential indicates how likely pitting corrosion would occur for a given material in an environment. A difference of more than 200 mV indicates that conditions favorable for pitting to occur are not anticipated absent any outside influence polarizing the surface substantially beyond typical OCP drift.

A negative hysteresis is defined by the current density on the reverse scan being less than the current on the forward scan. An example is shown in Figure 2-3.

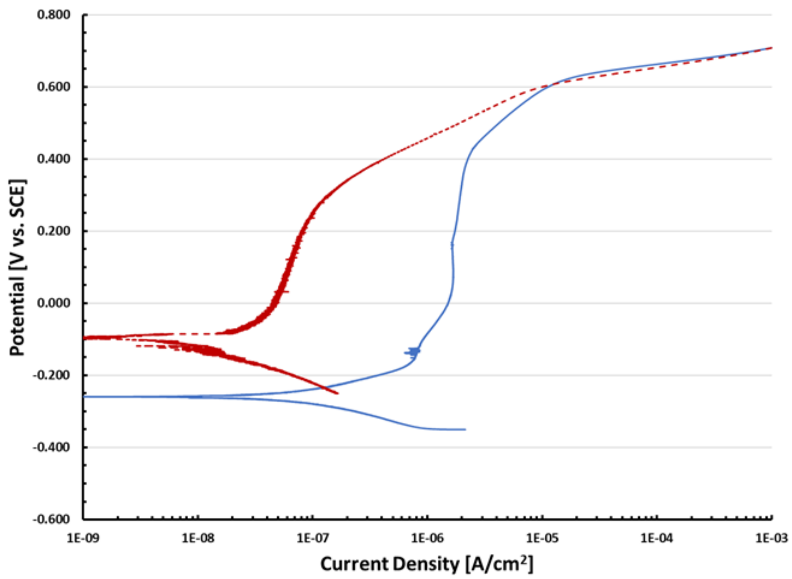

Figure 2-3: Example of a negative hysteresis, defined as the current density from the reverse scan being less than that of the forward scan. Solid blue line represents the forward scan, and dashed red line represents the reverse scan.

A negative hysteresis indicates that stable localized corrosion has not occurred during polarization. Neither pitting nor crevice corrosion was present in these cases. As such, trials with a negative hysteresis are defined as a pass condition.

The final possible outcome is a mixed hysteresis, shown in Figure 2-4.

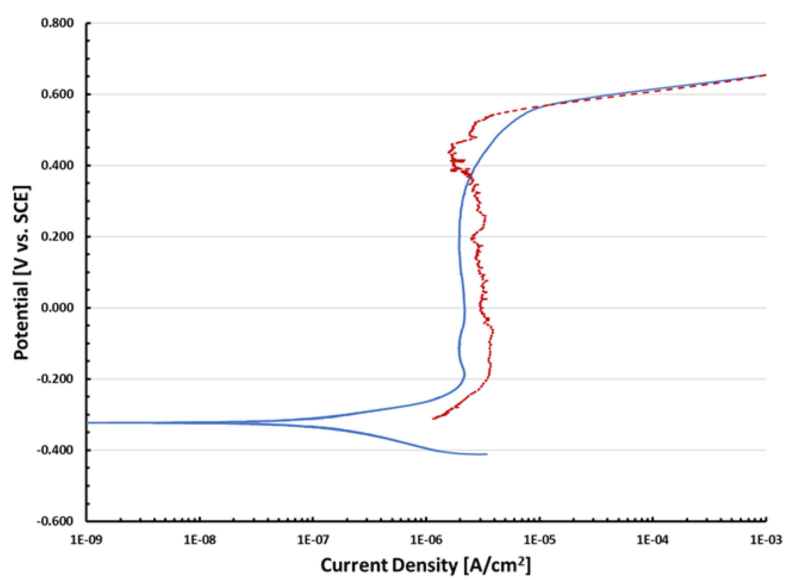

Figure 2-4: Example of a mixed hysteresis, defined as the current density from the reverse scan exhibiting behavior of both a positive and negative hysteresis. Solid blue line represents the forward scan, and dashed red line represents the reverse scan.

A mixed hysteresis represents a condition in which the current density during the reverse scan displays behavior of both positive and negative hysteresis during portions of the reverse scan. This could occur due to localized corrosion to a lesser extent or because of changes to the electrode surface oxide during the forward scan that result in slightly different kinetics for dissolution on the reverse scan. These instances require further examination to determine whether a passing or failing condition for susceptibility to pitting corrosion has occurred. First, the electrode was examined for the presence of pitting or crevice corrosion. If this examination was still inconclusive, meaning there is no clear indication of pitting or crevice corrosion, the electrode was subjected then to a Modified ASTM G192 test, which will be discussed further in the next section.

Two carbon steel electrode configurations were utilized to characterize the pitting behavior of Type IIIA waste tank material of construction; square A537 electrodes mounted in acrylic and A537 bullet electrodes. Squares (approximately 0.75-inch by 0.75-inch) were cut from rectangular bar stock using a slow speed saw. Insulated lead wires were affixed to the back side of electrodes with conductive silver epoxy to create an electrical connection outside of the test cell. The wired electrodes were then cold mounted using acrylic to protect the electrical connection, exposing only the top face of the electrode, and to provide a means of handling the electrodes for further electrode preparation. Both the mounted electrodes and bullet electrodes were ground to 800-grit using progressively higher grit silicon carbide (SiC) paper with water as lubrication to obtain a flat, uniform surface. The final grinding step was conducted within one hour of testing to prevent the development of corrosion products on the test surface due to residual moisture or humid ambient conditions. Finally, the electrodes were rinsed with ethyl alcohol and blown dry to remove any residual organic material and water from the electrode surface. An example of each electrode is shown below in Figure 2-5.

Figure 2-5: Examples of A537 square (top) and bullet (bottom) electrodes used for CPP experiments.

A schematic of the experimental setup is shown in Figure 2-6. 750 mL of test solution was batched for each test. Test solutions were made within 24 hours of testing to prevent precipitation of salts at room temperature during storage. In general solutions were made at their respective test temperature with stirring using a magnetic stir bar on a hotplate/stirrer. However, exceptions were made dependent upon solution chemistry. The prepared solution was then added to a test vessel with ports for the working electrode, a salt bridge containing a reference electrode, two graphite rods to serve as counter electrodes, and thermocouples to monitor test temperature and prevent overheating of the solution. The solution was heated on a hotplate with stirring until a steady test temperature was achieved. The hotplate contained an additional thermocouple to provide feedback for maintaining test temperature. After test temperature was achieved, the working electrode, counter electrodes, and salt bridge containing the reference electrode and a 0.1 M sodium nitrate solution were inserted into the test cell. Two graphite counter electrodes were used to promote more uniform current distribution to the working electrode. A saturated calomel electrode (SCE) was used as the reference electrode.

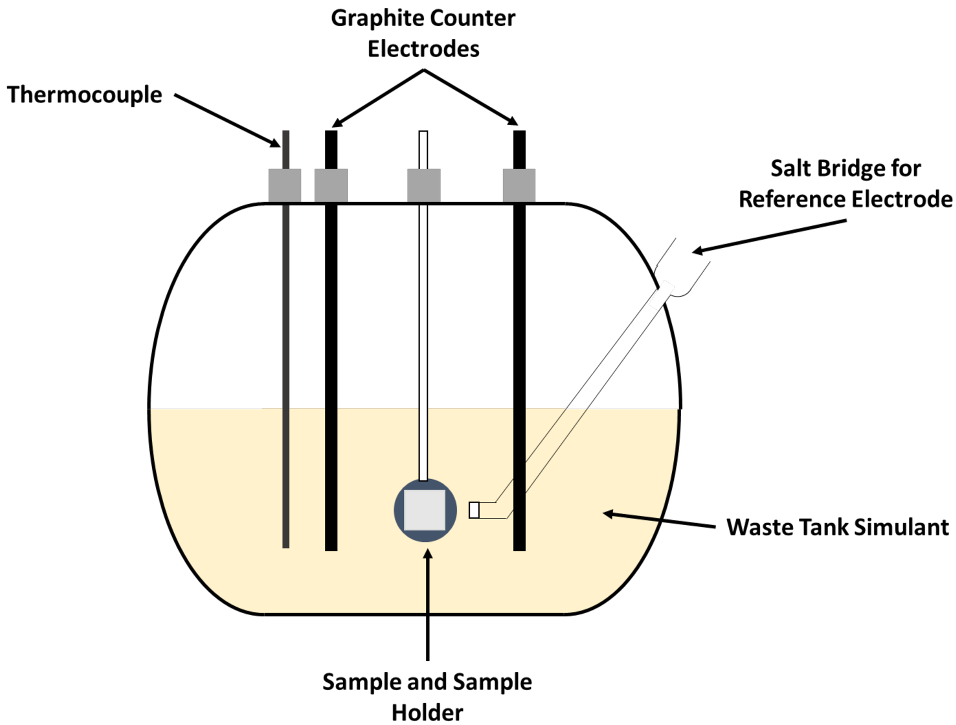

Figure 2-6: Schematic of experimental setup used for CPP and Modified ASTM G192 tests. Note: Schematic shows use of mounted electrode. Some CPP tests utilized a bullet electrode.

After the proper test conditions were established and the test apparatus was prepared, an OCP delay was initiated. The potential was measured once per second for a total of two hours. This was followed by the CPP experiment. The following parameters for the polarization were used [10]:

Scan rate:	0.167 mV/s
Initial potential:	-0.1 V versus OCP
Final potential:	1.2 V versus reference electrode
Current density limit:	1 mA/cm^2
Reverse scan rate:	0.167 mV/s
End potential:	0.0 V versus OCP

The forward scan proceeded until either the final potential or the current density limit was reached, which was the current density limit in all cases. At this point the scan direction was reversed, and the reverse scan proceeded until the OCP at the beginning of the test was reached. The applied potential and the measured current were monitored for the duration of the CPP test. After completion of the test, the electrode was removed from the test solution, rinsed with deionized water, and dried. Electrodes were visually inspected for the presence of pitting and crevice corrosion and then placed in a desiccator for storage.

2.2 Modified ASTM G192

Results from CPP experiments were not always conclusive (i.e., mixed hysteresis). In such cases, a secondary test method was used to clarify the pitting susceptibility of the material. Modified ASTM G192 is a test method by which the protection potential or repassivation potential can be determined [11,12]. This method involves potentiodynamically polarizing the electrode until a potential or current density limit is reached (similar to the forward scan of CPP tests), galvanostatically maintaining that current to allow for stable pit growth, and then finally progressing through a series of potentiostatic holds where the applied potential is reduced in a step-wise manner until the current density becomes less than the current density measured on the forward scan. The potential at which the current density on the reverse scan becomes less than the passive current density on the forward scan is defined as the protection potential (E_{prot}) or the repassivation potential. Electrode preparation and setup for this test were carried out in an identical manner as the CPP tests through the two-hour OCP delay. The following test parameters were used:

Potentiodynamic	
Initial potential:	-0.1 V vs. OCP
Final potential:	1.5 V vs. reference electrode
Current density limit:	50 μA/cm^2
Scan Rate:	0.1667 mV/s
Galvanostatic	
Hold current density:	50μA/cm^2
Hold time:	240 min
Potentiostatic Staircase	
Potential step decrement:	25 mV
Potential hold time:	120 min

The potential and the current were monitored for the duration of the test for all steps. After completion of the test, the electrode was removed from the test solution, rinsed with deionized water, and dried. The electrode was visually inspected for the presence of pitting and crevice corrosion and then placed in a desiccator for storage.

2.3 Quality Assurance

Data for this project was recorded in the electronic laboratory notebook system, notebook number G1720-00424-03.

Requirements for performing reviews of technical reports and the extent of review are established in manual E7 2.60. SRNL documents the extent and type of review using the SRNL Technical Report Design Checklist contained in WSRC-IM-2002-00011, Rev. 2. The design checklist document can be found in Appendix B.

3.0 Results and Discussion

A total of 105 CPP trials were carried out during the course of testing. The test matrix can be found in Table 3-1 in its entirety. Trials 1-100 were determined by a statistical design using the chemistry envelope outlined in Table 1-1. The emphasis of these trials was on evaluating more dilute chemistries than previously tested, in addition to chemistries indicative of more general tank conditions [8]. Another emphasis of this matrix compared to previous work was determining if a reduction in the minimum nitrite requirement was achievable in the chloride range of SRS tanks and in more dilute chemistries. The matrix therefore covers the compositional space of nitrite less than or equal to 0.2 M (the current minimum using the PF methodology). Additionally, as the focus of this reduction in the minimum nitrite requirement is on pitting corrosion (additional nitrite is required at elevated temperatures to prevent SCC), the temperature range tested was from 30 – 50 °C.

Table 3-1: Experimental Test Matrix for CPP Testing.

Trial	Temperature [°C]	Nitrate [M]	Hydroxide [M]	Nitrite [M]	Chloride [M]	Pitting Factor
1	50	4.0000	0.7000	0.2000	0.0005	1.48
2	30	0.0080	0.0708	0.0740	0.0158	2.51
3	50	0.0080	0.7000	0.2000	0.0005	364.04
4	30	0.4606	0.0860	0.1160	0.0206	1.09
5	30	3.4494	0.3431	0.1336	0.0158	0.80
6	50	0.4016	0.1924	0.0880	0.0194	2.33
7	50	0.3622	0.0176	0.1580	0.0135	0.66
8	50	4.0000	0.0100	0.0250	0.0300	0.03
9	30	0.4213	0.1848	0.1300	0.0064	3.20
10	30	0.2833	0.1766	0.0914	0.0290	2.04
11	30	0.0080	0.0100	0.0250	0.0300	0.23
12	50	0.0080	0.7000	0.0250	0.0300	11.16
13	30	0.0080	0.0100	0.0250	0.0005	7.30
14	30	4.0000	0.0100	0.2000	0.0300	0.09
15	30	0.0080	0.7000	0.0250	0.0005	347.45
16	50	0.1457	0.4621	0.1155	0.0127	10.91
17	30	4.0000	0.7000	0.2000	0.0005	1.48
18	30	1.7975	0.6524	0.0672	0.0025	2.91
19	50	4.0000	0.7000	0.2000	0.0300	1.32
20	30	0.0080	0.0100	0.0250	0.0300	0.23
21	50	0.0080	0.0100	0.0250	0.0005	7.30
22	30	0.1261	0.1468	0.1650	0.0005	10.70
23	50	0.0080	0.7000	0.0250	0.0300	11.16
24	50	4.0000	0.0100	0.2000	0.0300	0.09
25	30	4.0000	0.7000	0.0250	0.0300	1.26
26	50	0.1458	0.1316	0.0250	0.0182	2.44
27	30	3.0364	0.3669	0.0310	0.0107	0.93
28	50	4.0000	0.7000	0.0250	0.0005	1.42

Trial	Temperature [°C]	Nitrate [M]	Hydroxide [M]	Nitrite [M]	Chloride [M]	Pitting Factor
29	50	0.4410	0.0936	0.0670	0.0300	0.91
30	50	0.0080	0.0100	0.2000	0.0005	23.89
31	30	0.0080	0.0100	0.2000	0.0005	23.89
32	30	1.6599	0.5572	0.1517	0.0249	2.28
33	50	2.8988	0.6048	0.1698	0.0259	1.54
34	30	4.0000	0.0100	0.0250	0.0300	0.03
35	30	0.0080	0.4859	0.1095	0.0015	122.56
36	50	2.3481	0.5334	0.0612	0.0056	1.80
37	50	0.2245	0.0100	0.0460	0.0088	0.41
38	50	2.6234	0.1290	0.0250	0.0117	0.38
39	50	4.0000	0.0100	0.2000	0.0005	0.10
40	50	0.0080	0.0100	0.2000	0.0300	0.77
41	30	0.2638	0.1696	0.1860	0.0229	2.56
42	50	0.0474	0.1164	0.0950	0.0052	8.07
43	30	0.0080	0.7000	0.2000	0.0300	11.69
44	30	4.0000	0.7000	0.2000	0.0005	1.48
45	50	3.7247	0.0338	0.1216	0.0076	0.12
46	50	0.3819	0.0784	0.0810	0.0123	1.29
47	50	0.0080	0.7000	0.0250	0.0005	347.45
48	50	0.0080	0.0100	0.2000	0.0300	0.77
49	50	0.8339	0.1052	0.0552	0.0208	0.79
50	30	0.0080	0.7000	0.0250	0.0300	11.16
51	30	0.0080	0.7000	0.0250	0.0005	347.45
52	30	4.0000	0.7000	0.2000	0.0300	1.32
53	50	4.0000	0.0100	0.0250	0.0005	0.03
54	30	0.3426	0.0556	0.1020	0.0029	1.55
55	50	4.0000	0.2955	0.1940	0.0168	0.63
56	30	0.0080	0.7000	0.2000	0.0005	364.04
57	30	2.7611	0.2479	0.1819	0.0005	0.82
58	50	4.0000	0.0100	0.2000	0.0005	0.10
59	30	3.1741	0.2717	0.0733	0.0300	0.63
60	50	0.0080	0.0100	0.0250	0.0005	7.30
61	50	2.2105	0.1528	0.1457	0.0229	0.56
62	30	0.0080	0.0100	0.2000	0.0005	23.89
63	50	0.2048	0.1088	0.1930	0.0111	3.01
64	50	0.0080	0.7000	0.2000	0.0005	364.04
65	50	1.2469	0.0814	0.0974	0.0036	0.62
66	50	0.4210	0.0576	0.1759	0.0178	1.03
67	30	0.0867	0.0632	0.2000	0.0170	2.21
68	50	4.0000	0.7000	0.0250	0.0005	1.42

Trial	Temperature [°C]	Nitrate [M]	Hydroxide [M]	Nitrite [M]	Chloride [M]	Pitting Factor
69	50	0.0080	0.7000	0.2000	0.0300	11.69
70	30	4.0000	0.0100	0.2000	0.0005	0.10
71	30	0.3032	0.1620	0.0530	0.0265	1.86
72	50	0.1064	0.0252	0.1090	0.0217	0.79
73	50	0.5586	0.4383	0.1638	0.0269	3.75
74	50	3.8623	0.3907	0.0853	0.0188	0.79
75	30	4.0000	0.0100	0.0250	0.0005	0.03
76	30	2.0728	0.0100	0.1034	0.0147	0.10
77	50	4.0000	0.0100	0.0250	0.0300	0.03
78	30	0.6963	0.2003	0.0371	0.0066	2.07
79	30	4.0000	0.0100	0.0250	0.0005	0.03
80	50	0.3229	0.2000	0.1510	0.0040	4.73
81	30	0.0277	0.1544	0.1230	0.0241	3.34
82	30	0.9716	0.3193	0.1578	0.0097	2.49
83	50	0.0080	0.0100	0.0250	0.0300	0.23
84	50	4.0000	0.7000	0.2000	0.0300	1.32
85	50	0.2835	0.1012	0.1720	0.0288	1.42
86	30	2.4858	0.2241	0.1879	0.0280	0.71
87	30	0.1851	0.0480	0.1370	0.0253	0.99
88	50	3.5870	0.6286	0.1397	0.0046	1.44
89	50	1.9352	0.5810	0.0491	0.0239	2.04
90	30	0.4803	0.1240	0.0320	0.0099	1.62
91	30	3.3117	0.6762	0.0793	0.0219	1.52
92	30	0.2442	0.0404	0.0390	0.0276	0.55
93	30	0.1654	0.1772	0.0600	0.0076	5.21
94	50	0.5000	0.1392	0.1790	0.0147	1.88
95	30	4.0000	0.7000	0.0250	0.0300	1.26
96	30	0.0080	0.0100	0.2000	0.0300	0.77
97	50	0.0670	0.0328	0.1440	0.0017	5.13
98	30	1.3846	0.7000	0.1276	0.0137	3.62
99	50	4.0000	0.7000	0.0250	0.0300	1.26
100	30	4.0000	0.7000	0.0250	0.0005	1.42
101	50	4.0000	0.6800	0.0000	0.0300	1.22
102	50	3.0000	0.5300	0.0000	0.0300	1.22
103	50	2.0000	0.3800	0.0000	0.0300	1.22
104	50	1.0000	0.2300	0.0000	0.0300	1.24
105	50	0.0080	0.0760	0.0000	0.0300	1.20

Figure 3-1 gives a visual depiction of trials 1 – 100 within the compositional space of the test matrix. This matrix was composed of three submatrices. The first is the Full Factorial submatrix, which occupies the upper and lower bounds of the ranges for two variables within the multivariable system. The Space

Filler for Full Factorial submatrix then populates the compositional space between the minima and maxima for each variable. Finally, the Space Filler for Subspace submatrix populates, with more density of trials, the areas of emphasis for the test matrix, in particular more dilute solutions. For example, it can be seen in Figure 3-1 that for the variables of nitrate and hydroxide concentrations, there is a higher density of trials at more dilute concentrations. The remaining five trials, 101-105, were included to evaluate whether a need for nitrite in the prevention of pitting corrosion existed if all other control limits were in compliance. These trials span the range of nitrate concentration tested to ensure that any minimum concentration of nitrite determined would be applicable and both dilute and more concentrated chemistries.

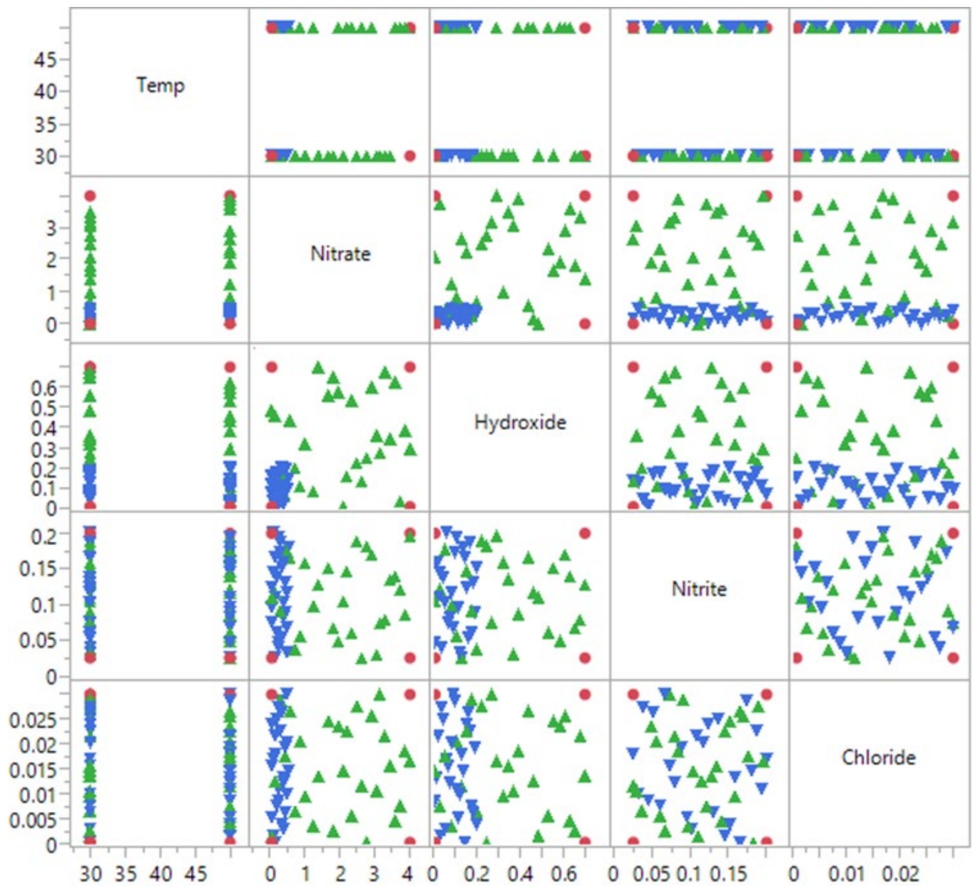

Figure 3-1: Statistical Design of Test Matrix for CPP Testing. The red circles indicate the Full Factorial submatrix, the green triangles indicate the Space Filler for Full Factorial submatrix, and the blue triangles indicate the Space Filler for Subspace submatrix.

While CPP of square electrodes mounted in acrylic was the primary working electrode configuration used for determination of pitting susceptibility, several tests were affected by crevice corrosion. This resulted in inconclusive results as to the pass/fail status of the trial, as a positive hysteresis would be observed in the absence of pitting. This occurred for trials 17, 19, 25, 28, 33, 36, 88, 91, and 94. An example of the CPP curve and corresponding crevice attack is shown in Figure 3-2.

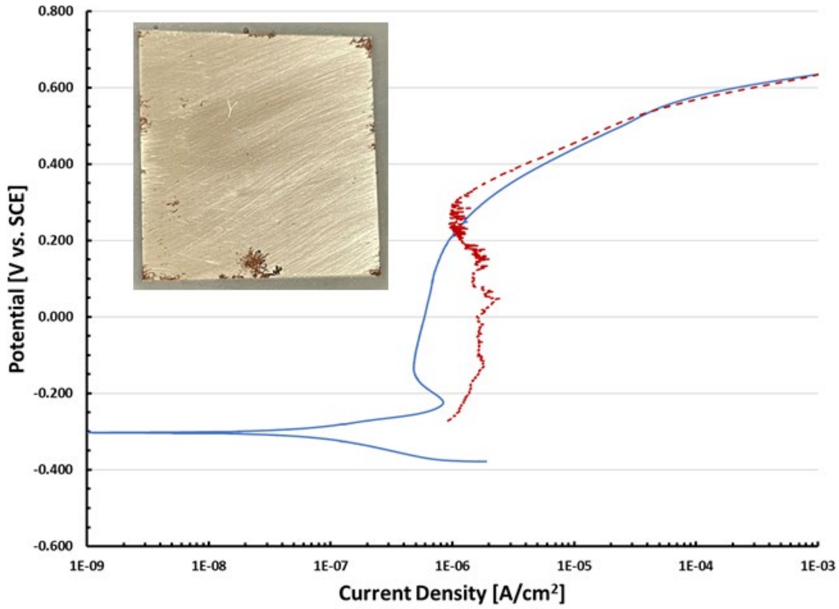

Figure 3-2: Example of CPP curve and Corresponding Crevice Attack in Trial Affected by Crevice Corrosion. CPP curve for Trial 17 mounted electrode is shown.

Because crevice corrosion was an artifact of the test electrode design and does not indicate a susceptibility to pitting corrosion, the trial was re-run utilizing the Modified ASTM G192 test method. This was conducted for tests in which the Pitting Factor was greater than 1.2. In cases where the Pitting Factor was less than 1.2, such as for Trials 27, 57, and 66, additional analysis was not performed as pitting was observed on the electrodes and the predicted result was a failure. However, a determination of the pass/fail status was not always able to be determined using this method, as crevice corrosion persisted as a result of the aggressive conditions created locally at the carbon steel/acrylic interface. Figures 3-3 and 3-4 provide examples of cases where a determination of the pass/fail could and could not be made, respectively. Figure 3-3 shows output data of a Modified ASTM G192 test in which the artifact of crevice corrosion was not present, leading to repassivation of the system (observed by the measured current being less than the passive current). Because the protection or repassivation potential at which this occurred was more than 200 mV higher than the OCP, this test could be determined as a pass. This was the case for Trials 17, 91, and 94. Figure 3-4 shows the results of a Modified ASTM G192 test when crevice corrosion did affect the electrode. This was the case for trials 19, 25, 28, 33, 36, and 88. The presence of spikes in the current magnitude at each potentiostatic step in addition to the current not decreasing below the passive current density are indicative of localized corrosion taking place, which in all cases was the result of crevice corrosion.

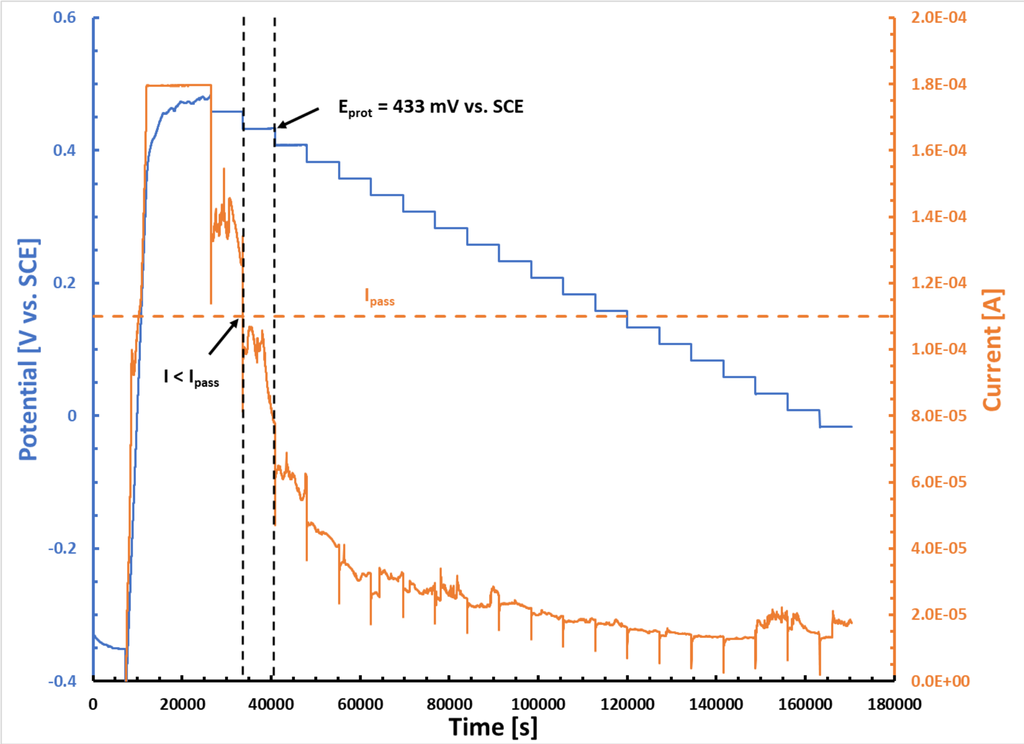

Figure 3-3: Example of ASTM G192 Results that allowed for Determination of Pass/Fail Status. Results of Trial 91 Modified ASTM G192 test are shown.

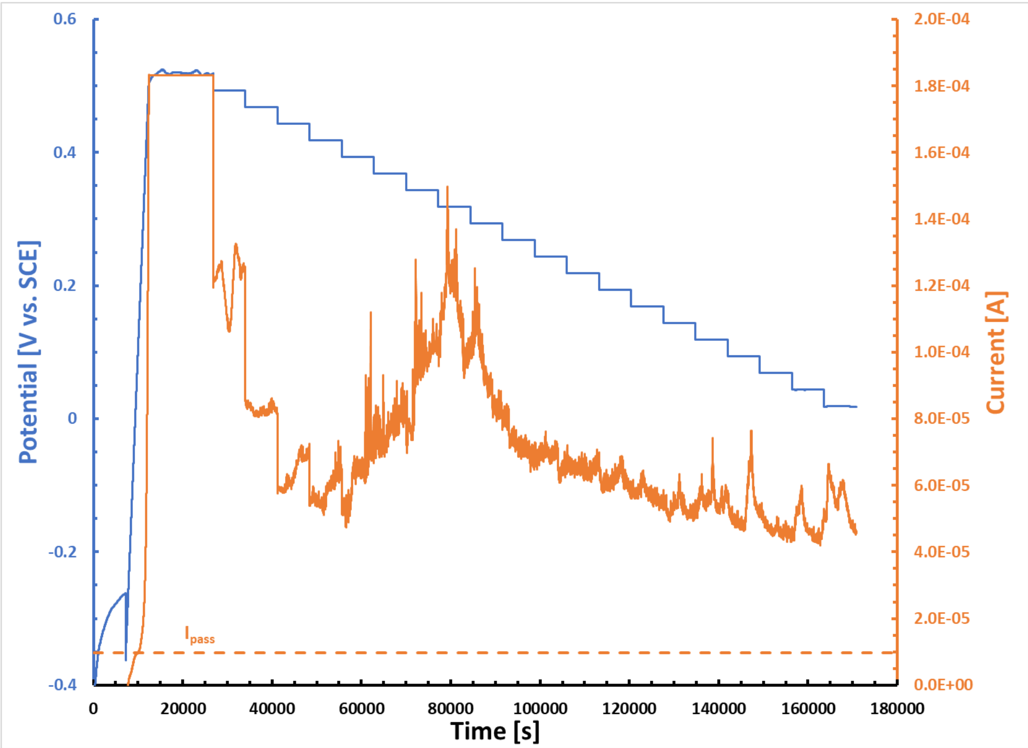

Figure 3-4: Example of ASTM G192 Results that were Affected by Crevice Corrosion. Results from Trial 25 Modified ASTM G192 test are shown.

With the pass/fail status of these tests still undetermined after CPP of the mounted electrodes and Modified G192 testing, a third testing strategy was implemented to clarify the pitting susceptibility of these trials. This final test method consisted of conducting CPP experiments with bullet electrodes. The shape of the bullet electrode and absence of any mount results in a condition that is free from any crevices that were an artifact of experimental design. An example comparing the CPP curves generated using a mounted square electrode and a bullet electrode is presented in Figure 3-5. The CPP test conducted with the mounted square electrode displayed a positive hysteresis and attack emanating from the metal/acrylic interface. Both of these features were absent in the test conducted with the bullet electrode. The CPP test resulted in a negative hysteresis and the electrode was free from any localized corrosion (pitting or crevice). This was the case for all of the aforementioned trials affected by crevice corrosion, and all were determined to be passes with the bullet electrode configuration.

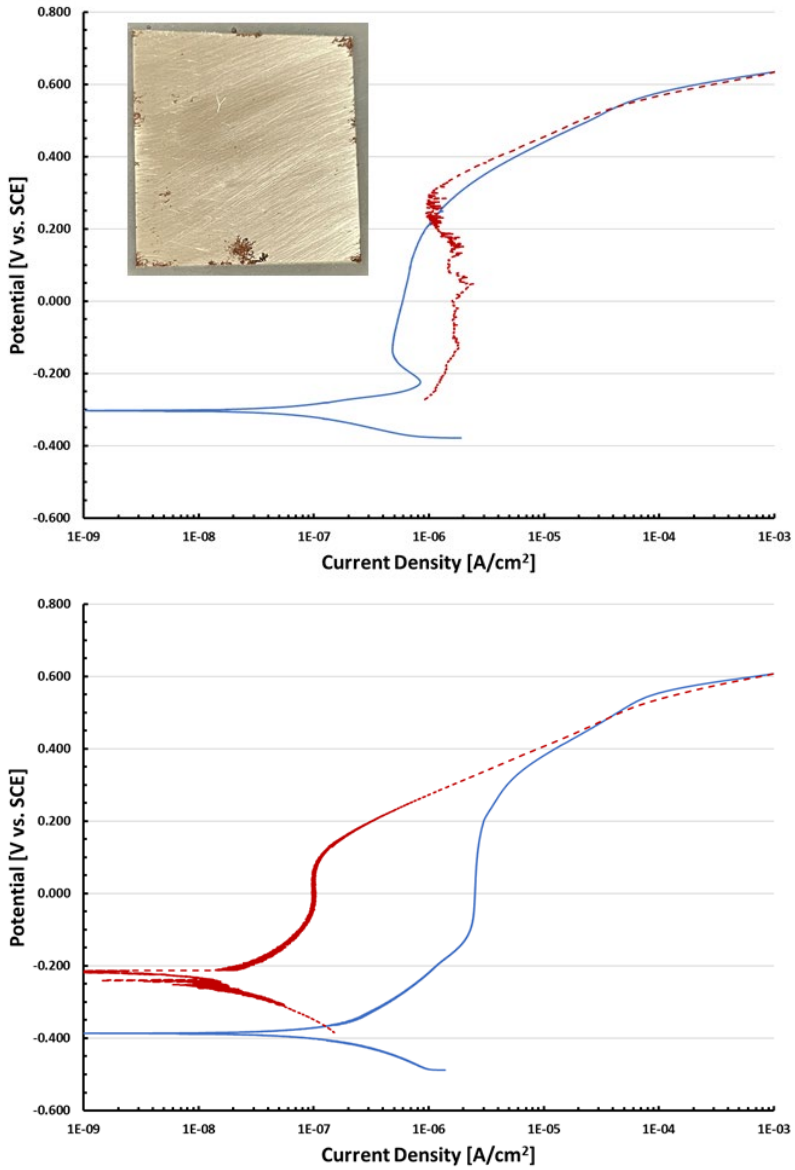

Figure 3-5: Comparison of CPP Curves Generated Using a Mounted Square Electrode (top) and a Bullet Electrode (bottom).

With the issues involving crevice corrosion resolved, the results of the 105 trials were analyzed to determine the effect of inhibiting and aggressive species on the pitting susceptibility. In all trials, no failures were recorded with a PF greater than 1.2, indicating validity of the PF methodology for prediction of pitting susceptibility throughout the chemistry envelope tested. Figure 3-6 illustrates the effect of nitrate concentration on pitting susceptibility. The nitrate concentration had no effect on trials with a PF of greater than 1.2, as all such trials were determined to be passes. However, an effect of nitrate on the pitting susceptibility was observed in trials with a PF of less than 1.2. In all such cases, trials with a nitrate concentration of greater than 1 M resulted in failures due to positive hysteresis and the presence of pits. On the contrary, in more dilute solutions with nitrate concentration less than 1 M, several trials did not display pitting susceptibility despite being predicted fails based on the PF methodology. These results suggested a lower likelihood for pitting to occur at lower nitrate concentrations when a failure is predicted by the pitting factor.

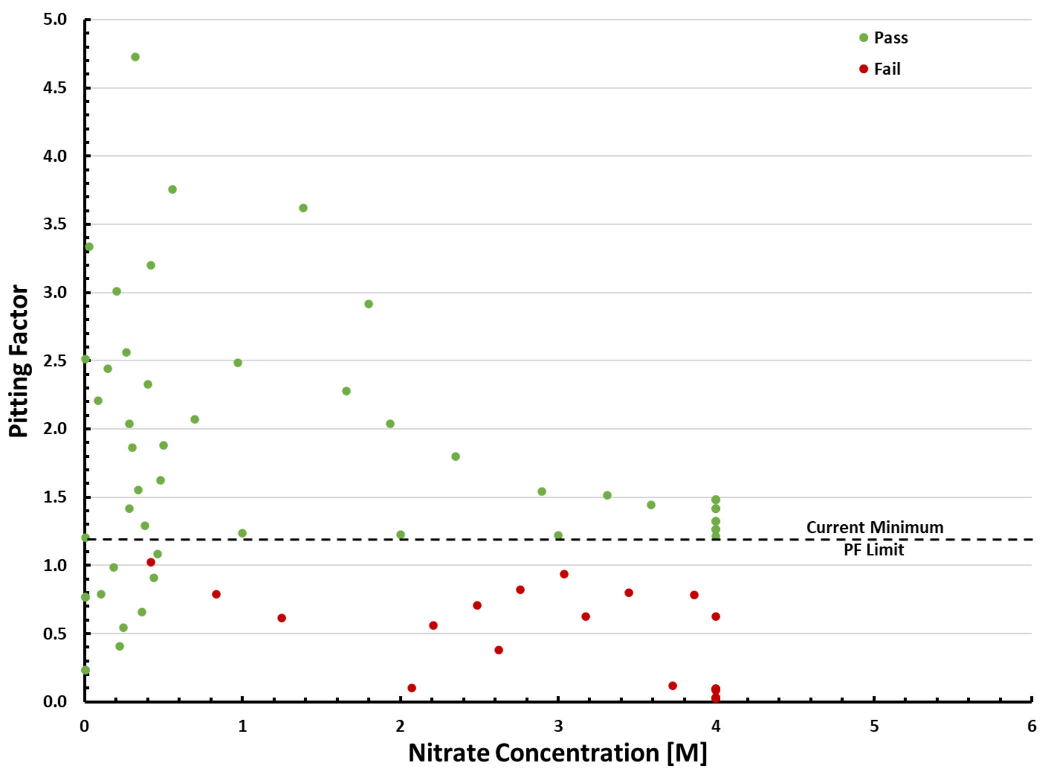

Figure 3-6: Impact of Nitrate Concentration on Pitting Susceptibility.

The effect of nitrite concentration on pitting susceptibility is displayed in Figure 3-7. Again, the trials with PF of greater than 1.2 did not display any effect of nitrite on pitting susceptibility. It is noteworthy, however, that a lower limit in which nitrite is needed for inhibition of pitting corrosion was not observed. Even in the cases with no nitrite present and PFs near the threshold of 1.2, i.e., the only species providing inhibition is hydroxide, all tests resulted in a pass across the full range of nitrate concentrations tested. This result indicated that a minimum nitrite requirement across the chemistry envelope evaluated did not exist, and effective inhibition of pitting corrosion could be achieved within the chemistry envelope tested with sufficient hydroxide to achieve a PF of 1.2. In trials with a PF of less than 1.2, several passing conditions were observed, however, these were distributed relatively evenly across the range of nitrite concentrations tested and no definitive effect on pitting susceptibility could be determined.

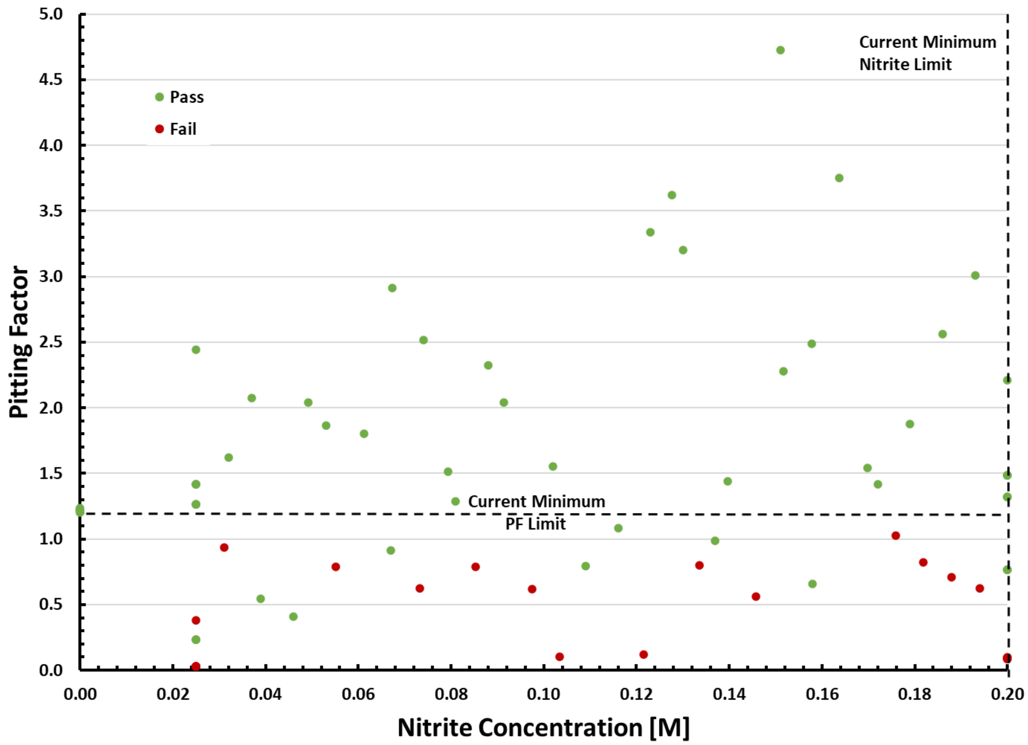

Figure 3-7: Impact of Nitrite Concentration on Pitting Susceptibility.

The effect of hydroxide and chloride concentrations on pitting susceptibility were also evaluated. These results are presented in Figures 3-8 and 3-9 for hydroxide and chloride, respectively. As was discussed previously, the trials with PF greater than 1.2 provide no indication of an effect of either of these two species on pitting susceptibility. Regarding hydroxide concentration (Figure 3-8), there appeared to be an increased likelihood for a passing condition with a PF of less than 1.2 in trials with less than 0.1 M hydroxide. This appeared counterintuitive, as hydroxide is an inhibiting species. However, this result was more indicative of the effect of nitrate concentration and the ratio of nitrite to nitrate in these trials than the hydroxide concentration. As mentioned previously, the likelihood for a passing condition with a PF of less than 1.2 increased markedly with nitrate concentrations less than 1 M. With lower nitrate concentrations, the concentrations of inhibiting species must also be considerably low for the PF to be less than 1.2. Therefore, the increase in the presence of passing conditions at PFs less than 1.2 and hydroxide concentrations less than 0.1 M was attributed to the effect of nitrate concentrations and the ratio of nitrite to nitrate on pitting susceptibility. As pertains to chloride (Figure 3-9), several instances of passing conditions with a PF of less than 1.2 were noted, however, these instances were distributed evenly throughout range of chloride concentrations tested. This indicated that within the chemistry envelope evaluated, chloride concentrations did not appreciably affect pitting susceptibility.

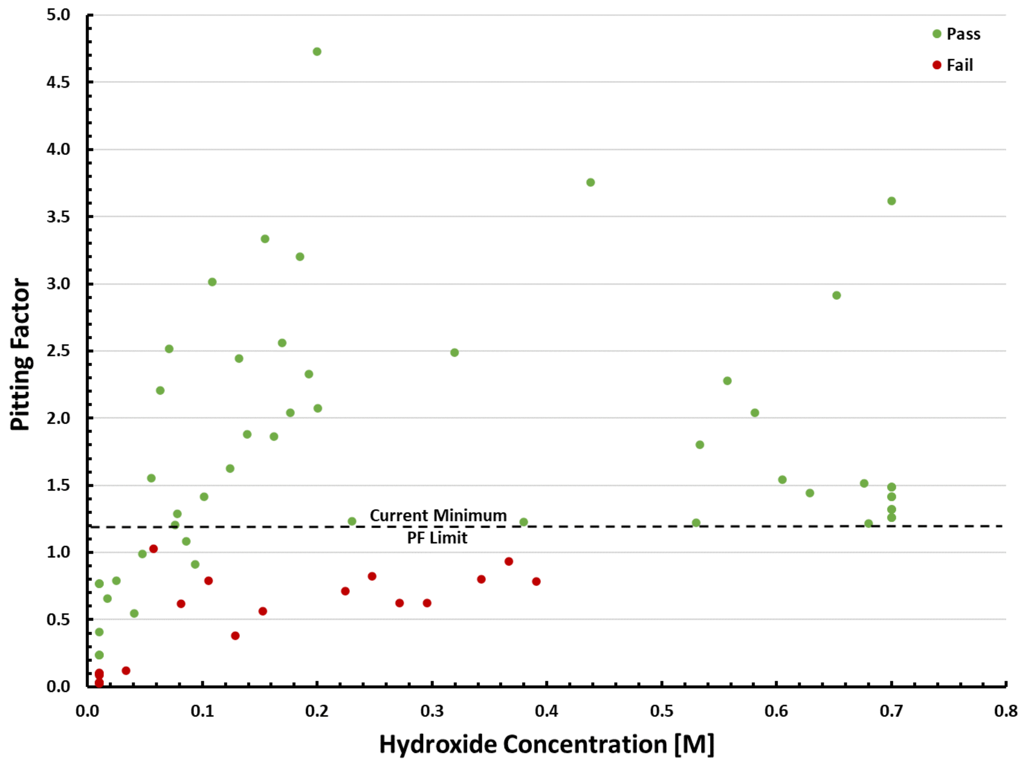

Figure 3-8: Impact of Hydroxide Concentration on Pitting Susceptibility.

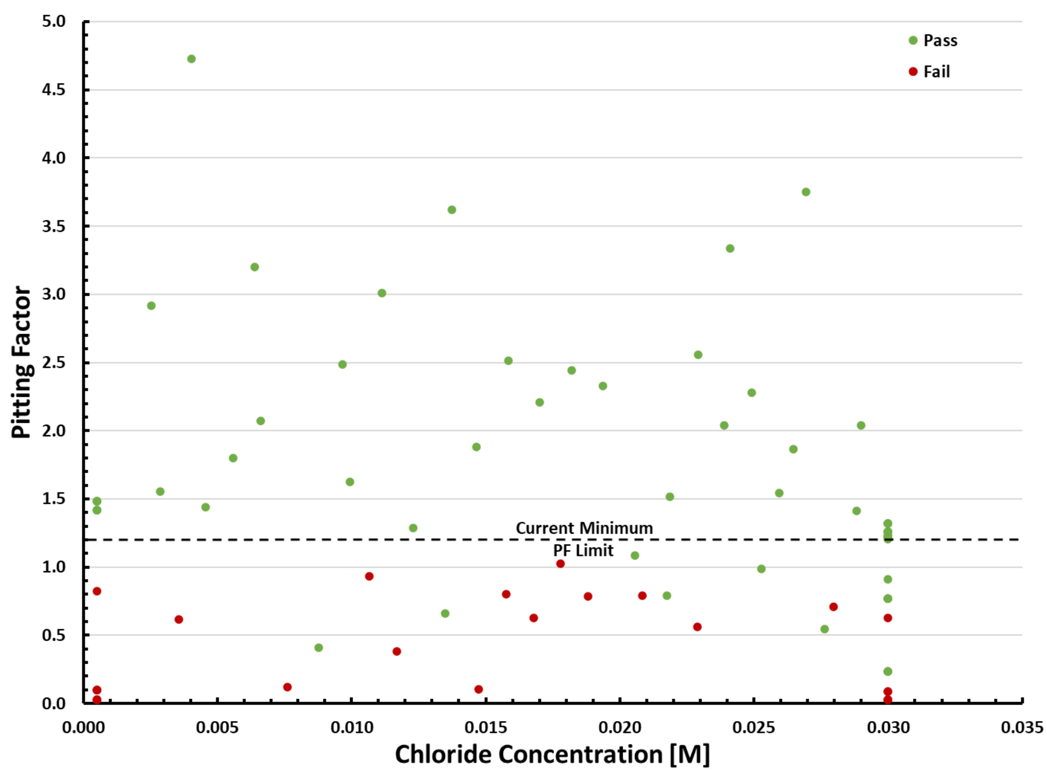

Figure 3-9: Impact of Chloride Concentration on Pitting Susceptibility.

Lastly, the effect of temperature on pitting susceptibility was evaluated. These results can be found in Figure 3-10. With PFs of less than 1.2, passing conditions appeared to be evenly distributed amongst the two temperatures at which tests were conducted, with slightly more occurring at 30 °C. Pitting susceptibility appeared to decrease to some extent with decreasing temperatures, however, this effect was not very pronounced over the temperature and chemistry ranges tested. A more pronounced trend, with significantly higher proportion of passes with pitting factor less than 1.2 occurring at 75 °C than at temperatures of 30 °C or less, was observed in previous work [5]. However, no such correlation was observed at temperatures less than 50 °C in this work.

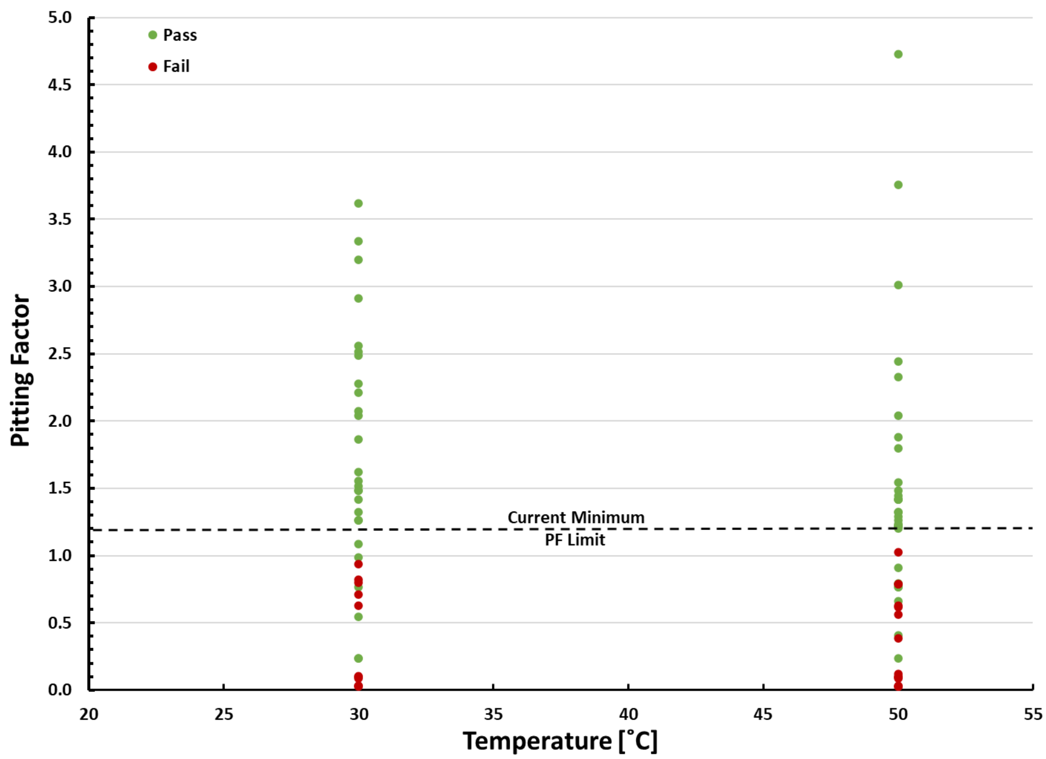

Figure 3-10: Impact of Temperature on Pitting Susceptibility.

4.0 Conclusions

A statistically designed test matrix was developed to evaluate the use of the Pitting Factor methodology in more dilute chemistries and those with chloride concentrations more indicative of SRS tank chemistries. In addition, the need for minimum nitrite requirement for the inhibition of pitting corrosion was assessed. Cyclic potentiodynamic polarization and Modified ASTM G192 test methods were successfully used to assess pitting susceptibility of A537 carbon steel in these environments. The PF was shown to accurately predict pitting susceptibility throughout the chemistry envelope evaluated. In addition, it was shown that hydroxide alone could effectively mitigate pitting corrosion in tank conditions with chloride concentrations observed at SRS up to 4 M nitrate. Based upon these findings, the control limits found in Table 4-1 are proposed.

Table 4-1: Chemistry Envelope Evaluated and Proposed Control Limits.

Chemistry Envelope Tested	
Nitrate [M]	0.008 – 4
Chloride [M]	0.0005 – 0.03
Hydroxide [M]	0.01 – 0.7
Nitrite [M]	0.0 – 0.2
Proposed Control Limits	
Minimum pH	12
Minimum Pitting Factor	1.2
Minimum Nitrite [M]	0
Maximum Temperature [°C]	50

A pH minimum of 12 is proposed to effectively mitigate localized corrosion and to ensure passivity of the carbon steel, ensuring that localized corrosion, not general corrosion, is the primary degradation mechanism [13]. The PF minimum of 1.2 is maintained as no instances of pitting were observed above this threshold. The minimum nitrite limit has been removed, as no instances of pitting were observed above the PF of 1.2 throughout the chemistry envelope evaluated. In addition, a maximum temperature limit of 50 °C is proposed to ensure that pitting corrosion, not SCC, is the primary degradation mechanism. At temperatures in excess of 50 °C, SCC, which is temperature dependent, becomes an issue. At these elevated temperatures, a minimum nitrite/nitrate ratio would be required to inhibit SCC.

Tables 4-2 and 4-3 show minimum hydroxide concentration that would be required for compliant waste tank chemistries using the proposed control limits and the current limits from the Corrosion Control Program [1]. These calculations assume the maximum chloride concentration of 0.03 M and no nitrite being present. For the values presented in the two tables, the amount of hydroxide required could be further reduced by accounting for the amount of nitrite already present in a given waste stream. These two tables show that the amount of hydroxide required for inhibition of pitting corrosion is drastically decreased using the proposed limits based on the Pitting Factor methodology. This would ultimately result in less hydroxide additions being required to maintain compliance with the corrosion control limits.

Table 4-2: Amount of Hydroxide Necessary for Compliance Using Proposed Control Limits.

With New Proposed Control Limits	
Assuming	
$[Cl^-]$	0.03 M
$[NO_2^-]$	0 M
Amount of Hydroxide Necessary for Compliance	
$[NO_3^-]$ [M]	**$[OH^-]$ [M]**
4	0.68
3	0.53
2	0.38
1	0.23
0.008	0.076

Table 4-3: Amount of Hydroxide Necessary for Compliance Using Current Corrosion Control Program.

Required Under Current Corrosion Control Program	
Assuming	
$[Cl^-]$	0.03 M
$[NO_2^-]$	0 M
Amount of Hydroxide Necessary for Compliance	
$[NO_3^-]$ [M]	**$[OH^-]$ [M]**
4	1.1
3	1.1
2	0.8
1	0.4
0.008	1

5.0 Recommendations, Path Forward or Future Work

In many cases, a simple correlation between a given aggressive or inhibiting species' concentration and the Pitting Factor does not completely account for susceptibility to pitting corrosion. In actuality, the interplay of multiple variables governs this susceptibility. Future work will evaluate other factors that may influence susceptibility to pitting corrosion, such as the nitrite/nitrate ratio for a given test. In addition, the amount, and not just the ratios of inhibiting and aggressive species can affect susceptibility to pitting corrosion. These relationships will be evaluated in the Final Report and a statistical analysis will be performed to determine if the coefficients used previously in the Pitting Factor equation would need to be adjusted over the compositional range tested in this work.

Pitting corrosion is not the only form of localized corrosion that may be detrimental to waste tank integrity. Stress corrosion cracking can also affect low carbon steel exposed to waste tank chemistries in tanks experiencing temperatures in excess of 50 °C. The Pitting Factor methodology has also been used as a predictive metric for the presence of stress corrosion cracking. However, other metrics, such as the ratio of nitrite to nitrate in the waste must also be considered. Tests are being conducted to evaluate the use of the Pitting Factor methodology, along with a nitrite/nitrate ratio minimum, for the prediction of stress corrosion cracking at temperatures up to 75 °C. This work will likely further refine the proposed control limits for tank temperatures between 50 °C and 75 °C to address susceptibility to both pitting corrosion and stress corrosion cracking.

6.0 References

1. K.B. Martin, "CSTF Corrosion Control Program: Program Description Document", WSRC-TR-2002-00327, Rev. 9, December 16, 2015.
2. B. J. Wiersma, J. I. Mickalonis "Determination of Corrosion Inhibitor Criteria for Type III/IIIA Tanks During Salt Dissolution Operations", WSRC-STI-2006-00029, Rev. 0, September 2007.
3. K. M. Counts, B. J. Wiersma, J. I. Mickalonis, "Determination of Corrosion Inhibitor Criteria for Type III/IIIA Tanks During Salt Dissolution Operations-Interim Report", WSRC-STI-2007-00552, Rev. 0, December 2007.
4. B. L. Garcia-Diaz, J. I. Mickalonis, B. J. Wiersma, "Determination of Corrosion Inhibitor Criteria for Type III/IIIA Tanks During Salt Dissolution Operations-Summary Document", SRNL-STI-2009-00600, Rev. 0, October 2009.
5. J. T. Boerstler, "Refinement of Salt Dissolution Inhibitor Requirements – Interim Report", SRNL-STI-2021-00116, Rev. 0, March 2021.
6. B. J. Wiersma, R. E. Fuentes, L. M. Stock, "Chemistry Envelope for Pitting and Stress Corrosion Cracking Mitigation", SRNL-STI-2019-00217, Rev. 0, September 2019.
7. K. B. Martin, "Task Technical Request for Refinement of Pitting Factor Basis in Support of Corrosion Control Program Implementation", X-TTR-H-00127, Rev. 0, December 21.
8. J. T. Boerstler, "Task Technical and Quality Assurance Plan for the Refinement of Pitting Factor Basis in Support of Corrosion Control Program Implementation", SRNL-RP-2022-00106, Rev. 0, March 2022.
9. T. M. Martin, "Outcomes from the August 2013 Expert Panel Oversight Committee Meeting", RPP-ASMT-56781, Rev. 0, February 2014.
10. ASTM G61-86, "Standard Test Method for Conducting Cyclic Potentiodynamic Polarization Measurements for Localized Corrosion Susceptibility of Iron-, Nickel-, or Cobalt-Based Alloys", June 2018.
11. Evans, Kenneth & Chawla, S & Sherer, K & Gerst, J & Beavers, J & Boomer, K, "The Use of ASTM G192 (Tsujikawa-Hisamatsu Electrochemical Method) to Evaluate the Susceptibility of Hanford Tank Steels to Pitting Corrosion", *Corrosion,* 2016.
12. Evan, Kenneth, "Standard Operating Procedure for Performing G192 Tests for WRPS Projects", SOP-052, Rev. 0, August 2016.
13. C. S. Brossia and G. A. Cragnolino, "Effect of Environmental Variables on Localized Corrosion of Carbon Steel", *Corrosion*, Vol. 56, No. 5, 2000.

Appendix A. Cyclic potentiodynamic polarization curves for each screening trial

The following pages contain the cyclic potentiodynamic polarization curves and Modified ASTM G192 data (where applicable) for each screening trial. For CPP curves, the blue line indicates the forward scan, and the red dashed line indicates the reverse scan.

Trial 1

Mounted Electrode

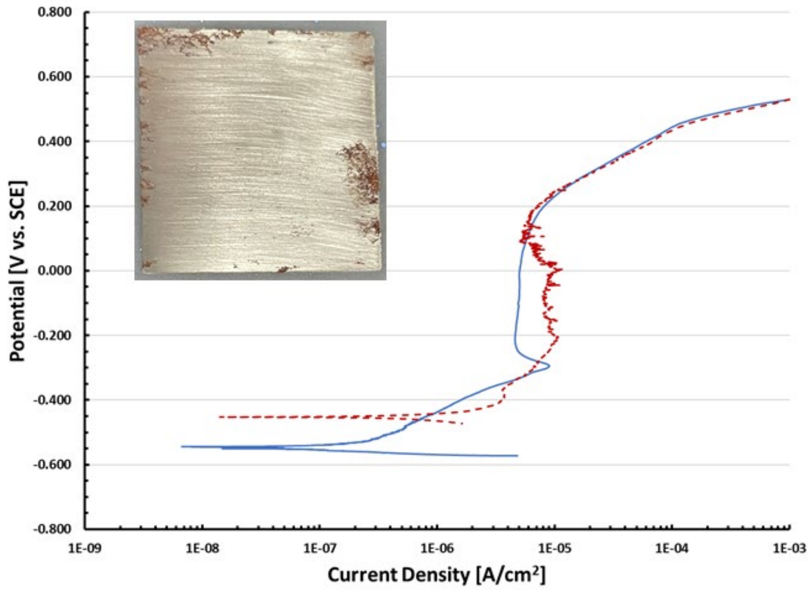

Bullet Electrode

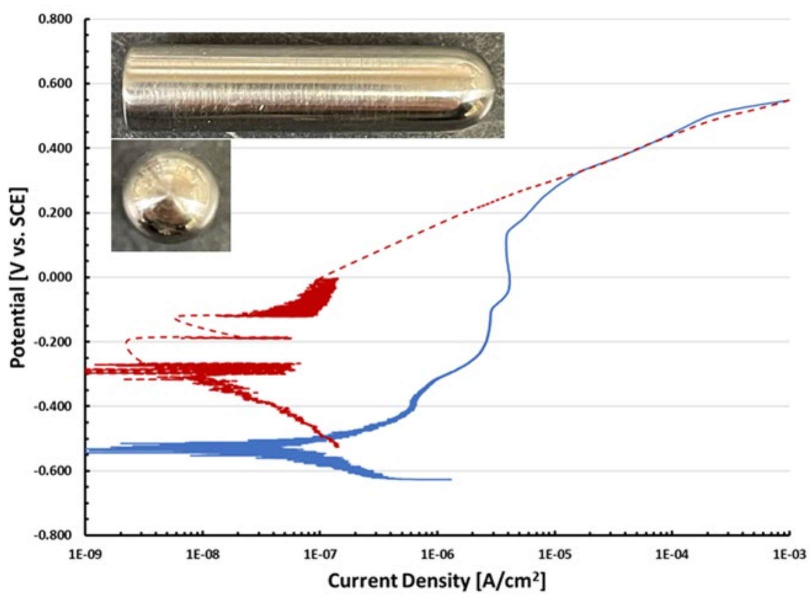

Trial 2

Mounted Electrode

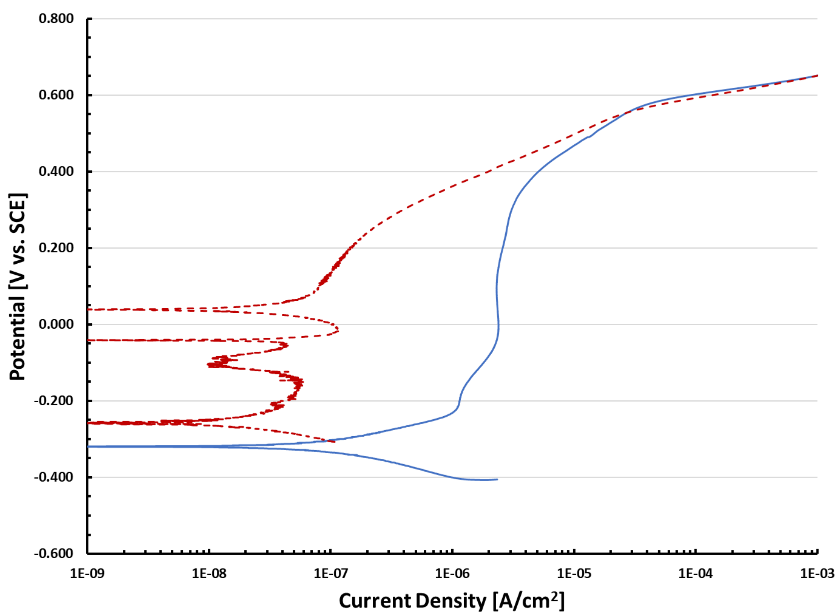

Trial 3

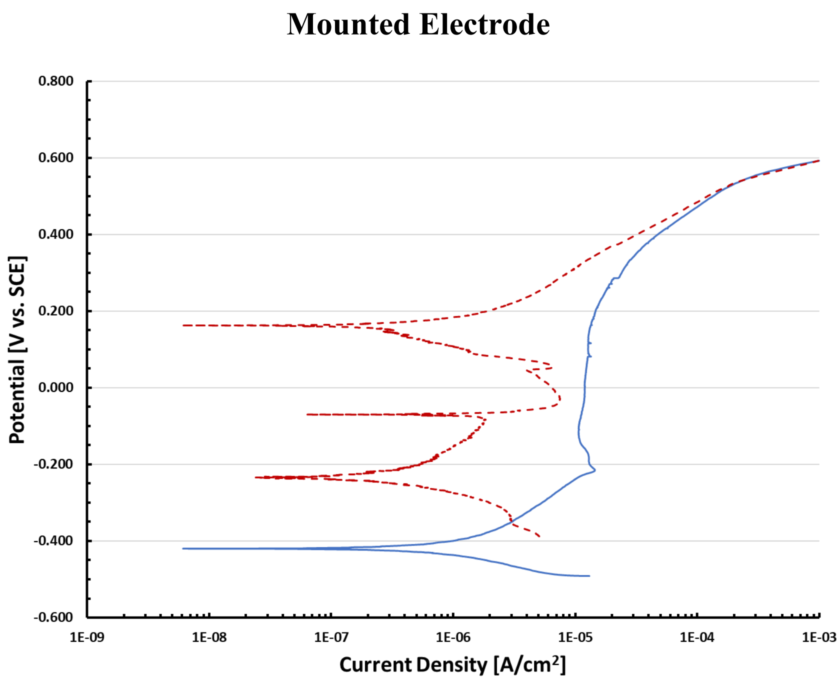
Mounted Electrode
0.800
0.600
0.400
0.200
0.000
-0.200
-0.400
-0.600
Potential [V vs. SCE]
1E-09
1E-08
1E-07
1E-06
1E-05
1E-04
1E-03
Current Density [A/cm²]

Trial 4

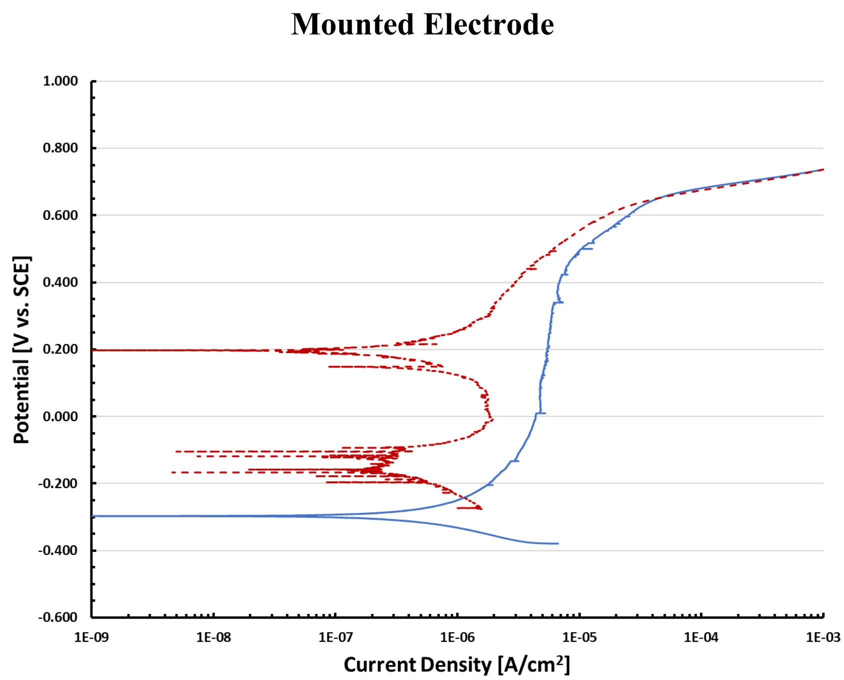
Mounted Electrode
1.000
0.800
0.600
0.400
0.200
0.000
-0.200
-0.400
-0.600
Potential [V vs. SCE]
1E-09
1E-08
1E-07
1E-06
1E-05
1E-04
1E-03
Current Density [A/cm²]

Trial 5

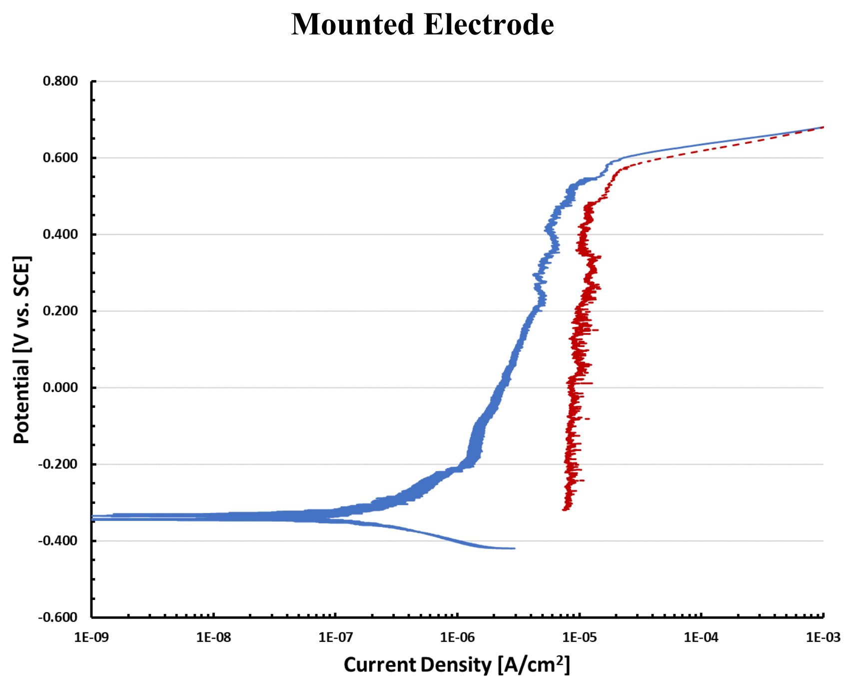
Mounted Electrode
0.800
0.600
0.400
0.200
0.000
-0.200
-0.400
-0.600
Potential [V vs. SCE]
1E-09
1E-08
1E-07
1E-06
1E-05
1E-04
1E-03
Current Density [A/cm²]

Trial 6

Mounted Electrode

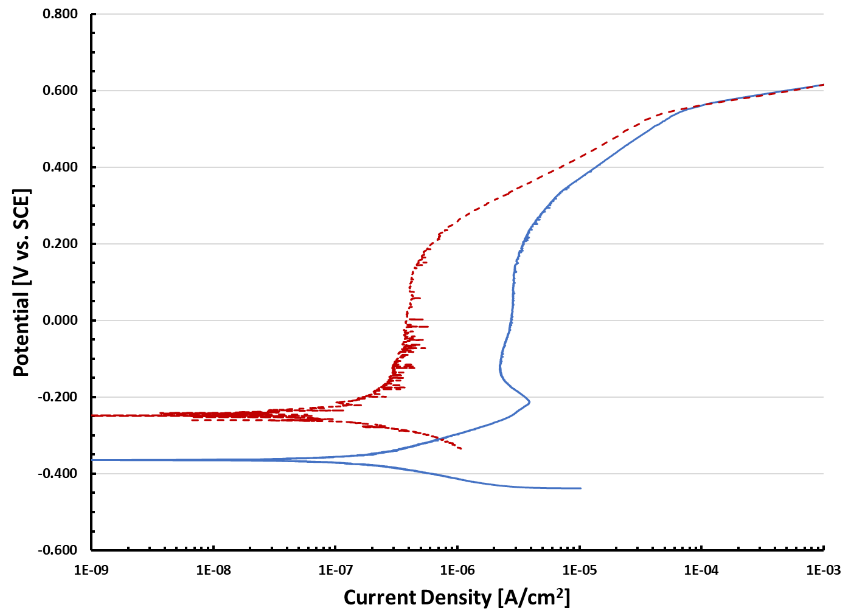

Trial 7

Mounted Electrode

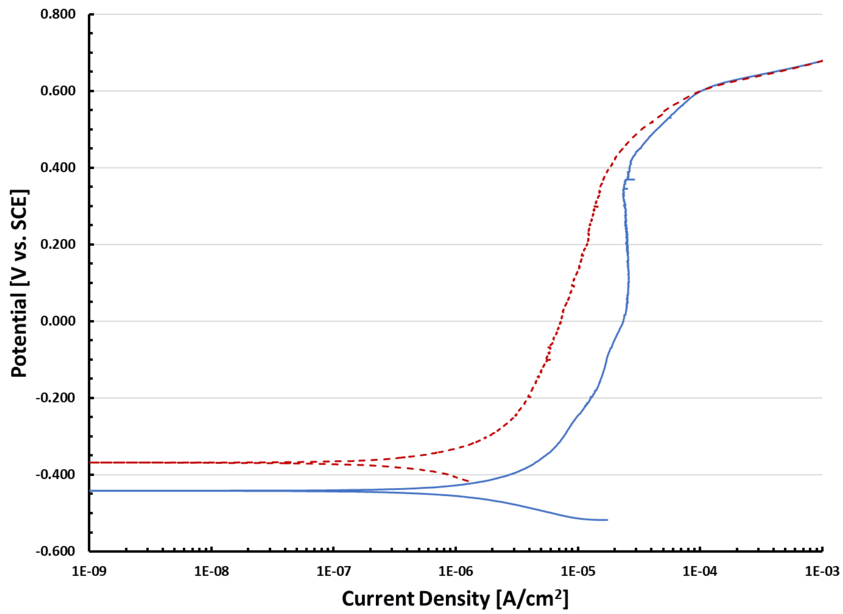

Trial 8

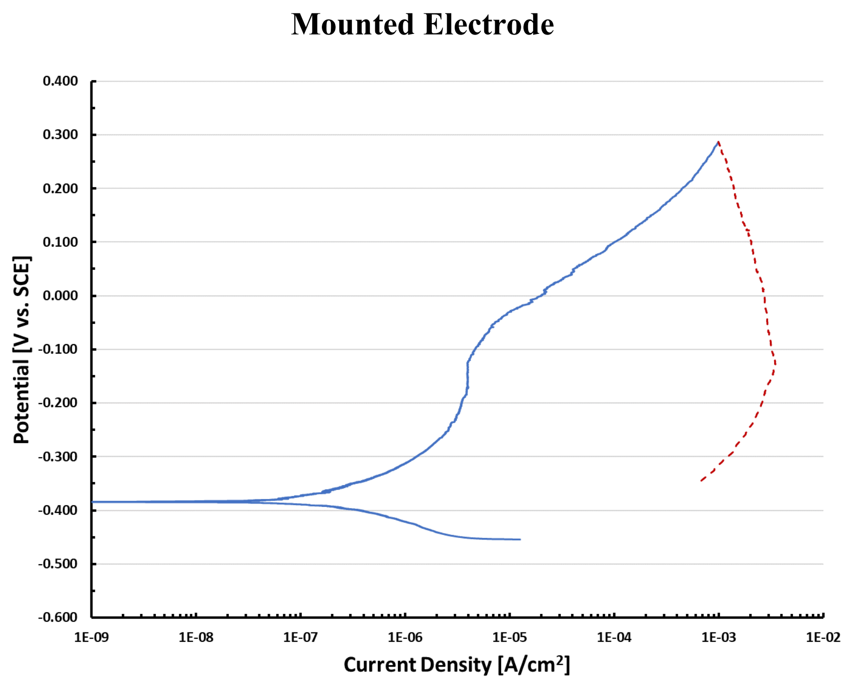
Mounted Electrode
0.400
0.300
0.200
0.100
0.000
-0.100
-0.200
-0.300
-0.400
-0.500
-0.600
Potential [V vs. SCE]
1E-09
1E-08
1E-07
1E-06
1E-05
1E-04
1E-03
1E-02
Current Density [A/cm²]

Trial 9

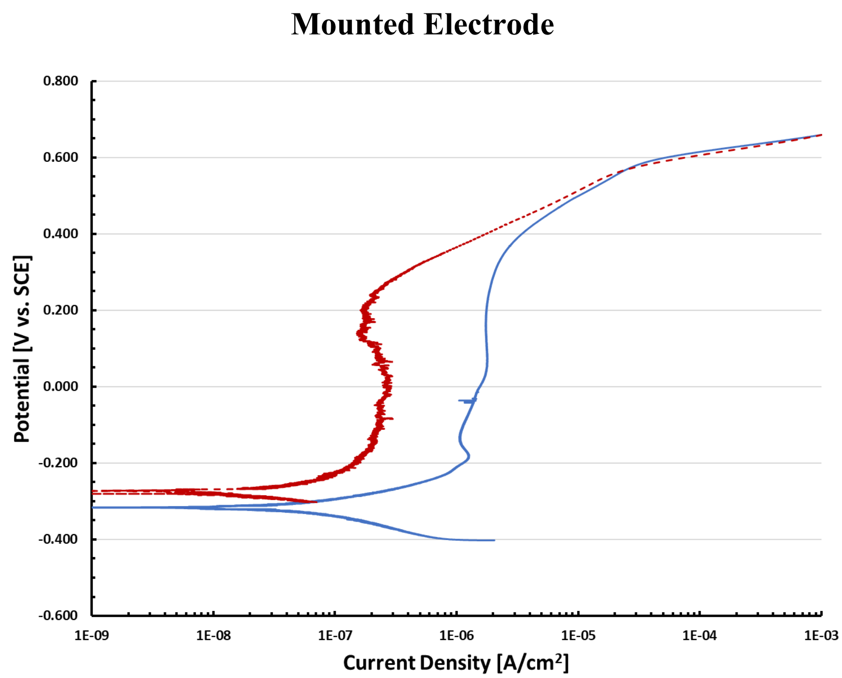
Mounted Electrode
0.800
0.600
0.400
0.200
0.000
-0.200
-0.400
-0.600
Potential [V vs. SCE]
1E-09
1E-08
1E-07
1E-06
1E-05
1E-04
1E-03
Current Density [A/cm2]

Trial 10

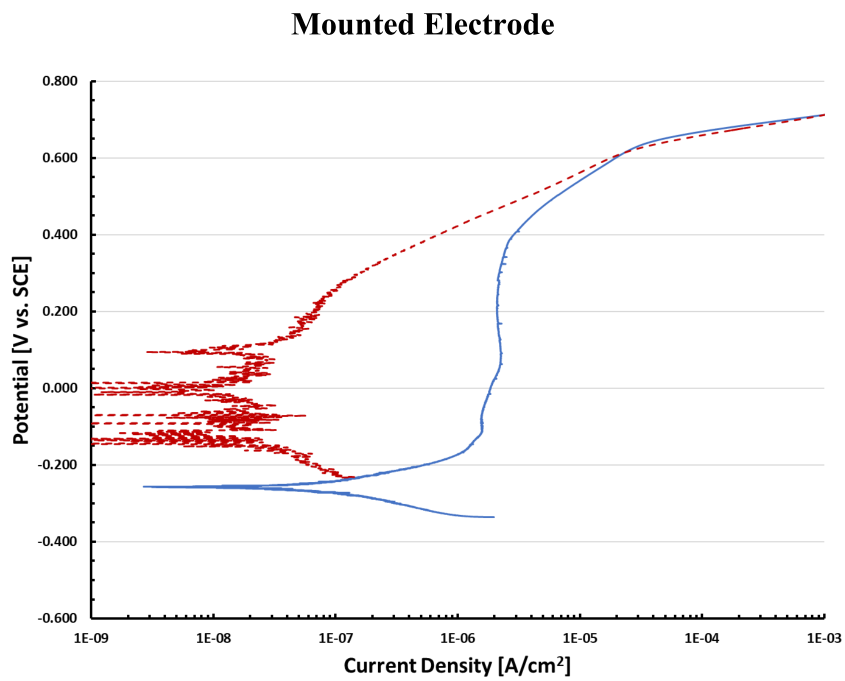
Mounted Electrode
0.800
0.600
0.400
0.200
0.000
-0.200
-0.400
-0.600
Potential [V vs. SCE]
1E-09
1E-08
1E-07
1E-06
1E-05
1E-04
1E-03
Current Density [A/cm²]

Trial 11

Mounted Electrode

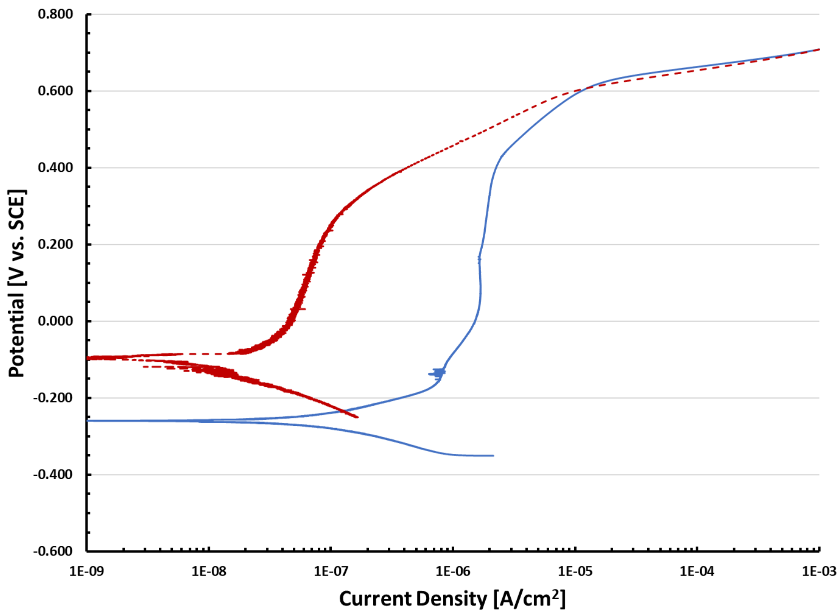

Trial 12

Mounted Electrode

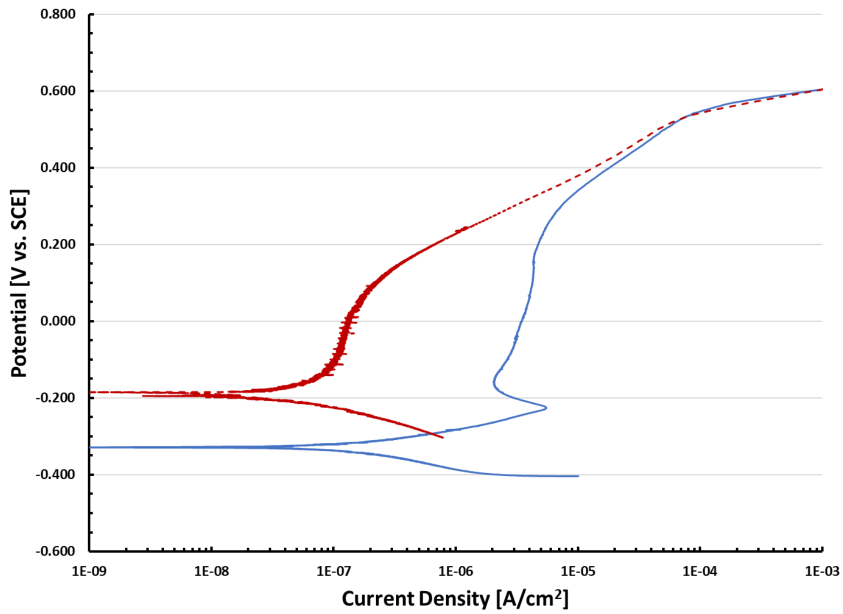

Trial 13

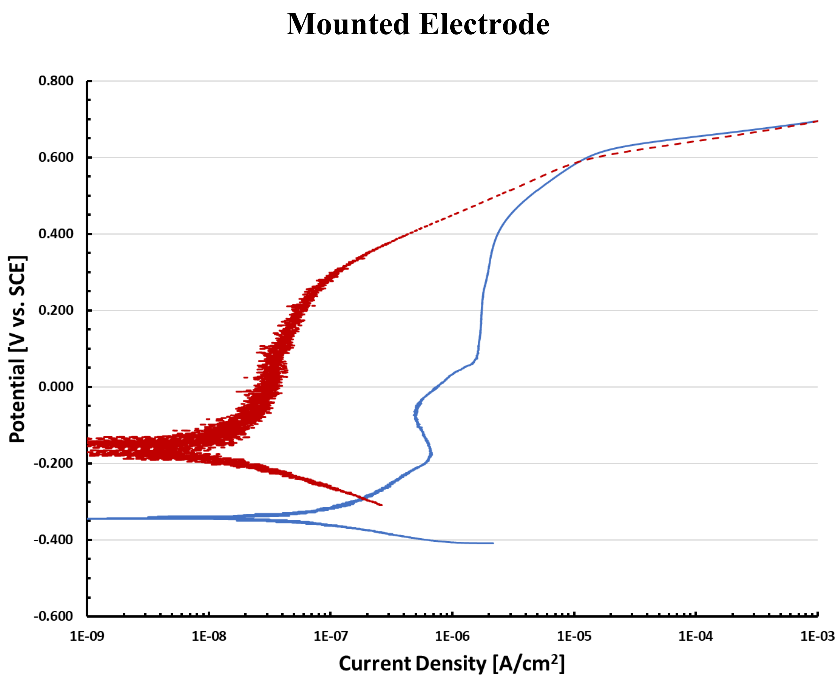
Mounted Electrode
0.800
0.600
0.400
0.200
0.000
-0.200
-0.400
-0.600
Potential [V vs. SCE]
1E-09
1E-08
1E-07
1E-06
1E-05
1E-04
1E-03
Current Density [A/cm2]

Trial 14

Mounted Electrode

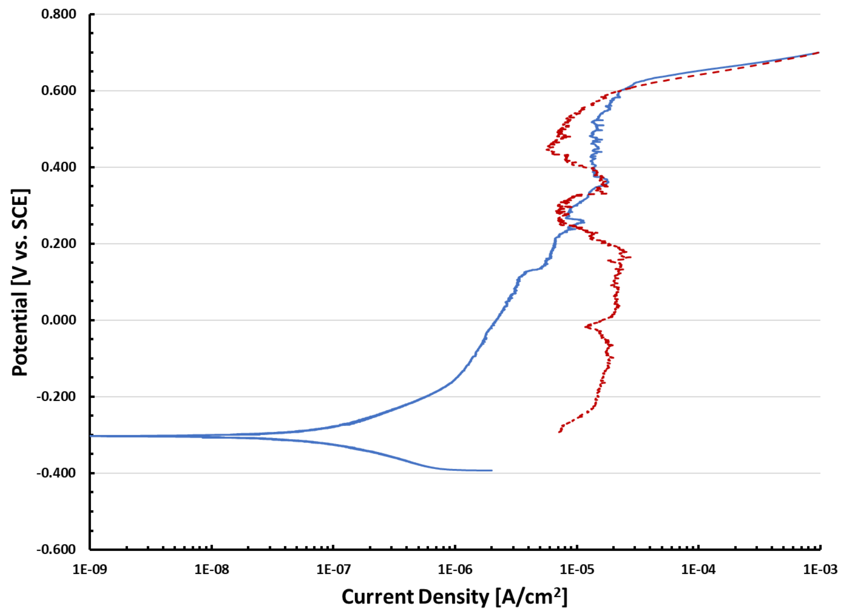

Trial 15

Mounted Electrode

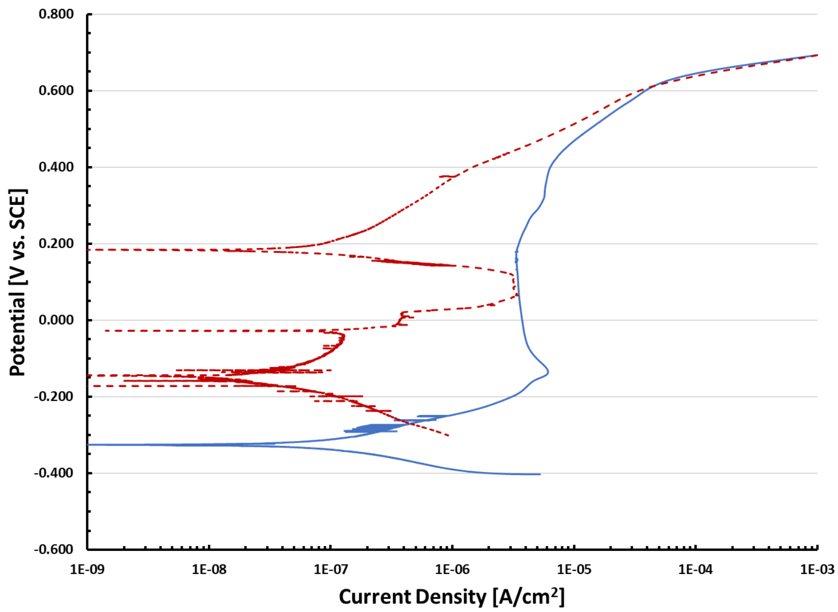

Trial 16

Mounted Electrode

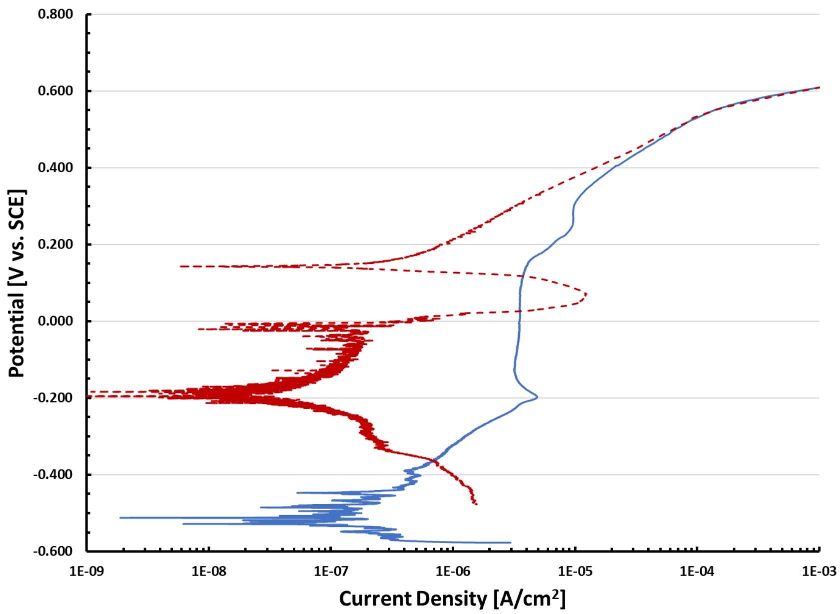

Trial 17

Mounted Electrode

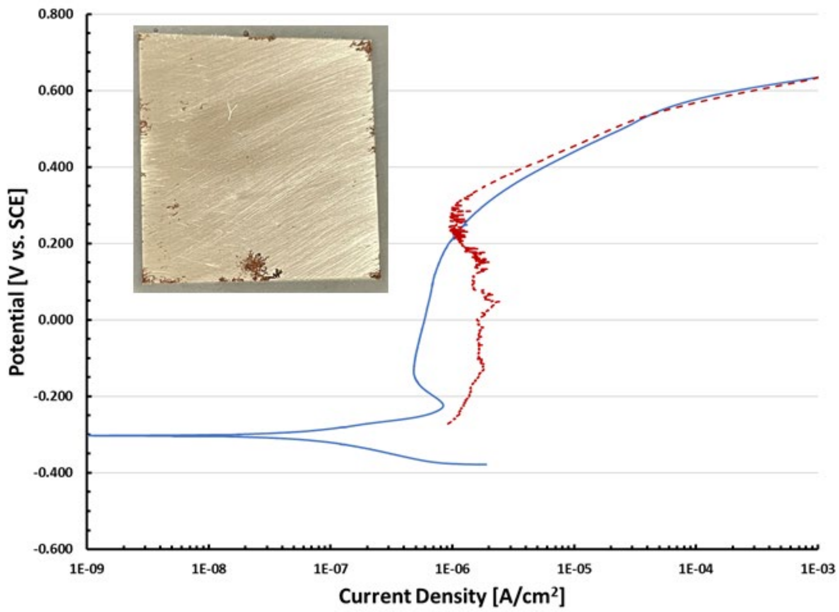

Bullet Electrode

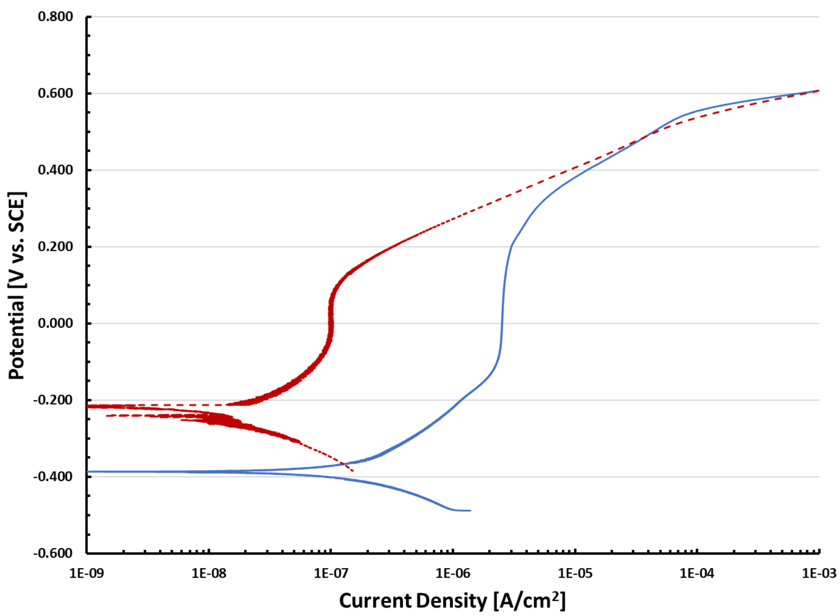

Trial 17 (Continued)

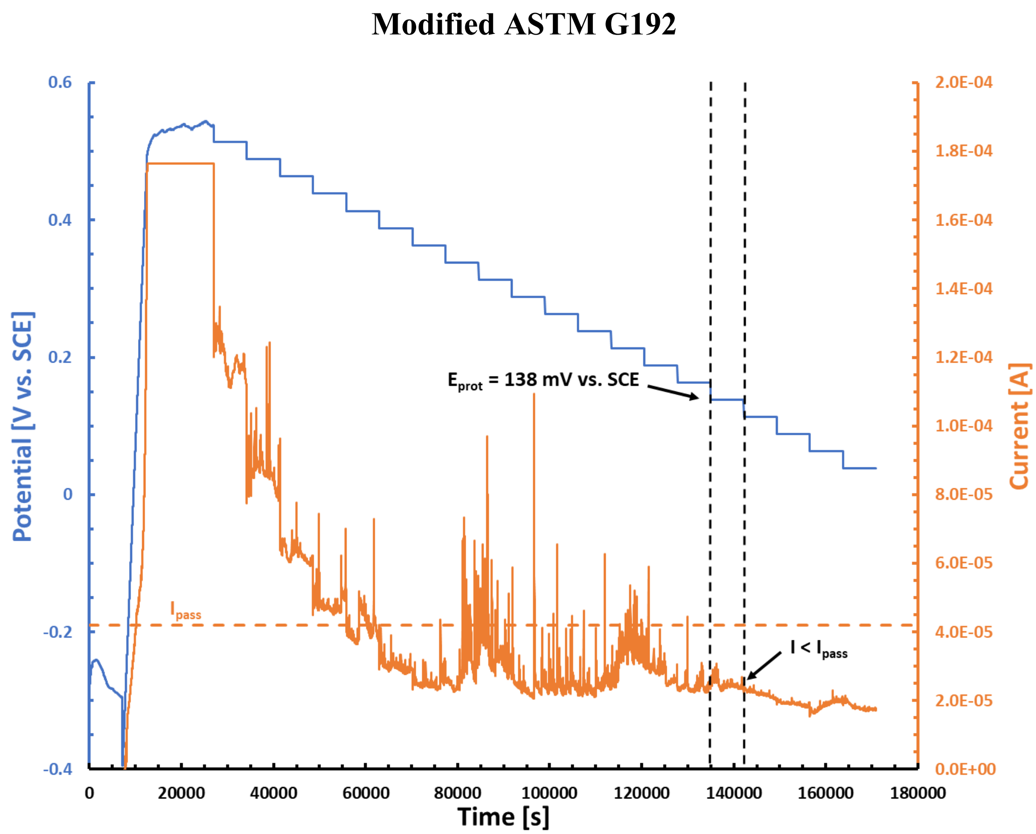

Trial 18

Mounted Electrode

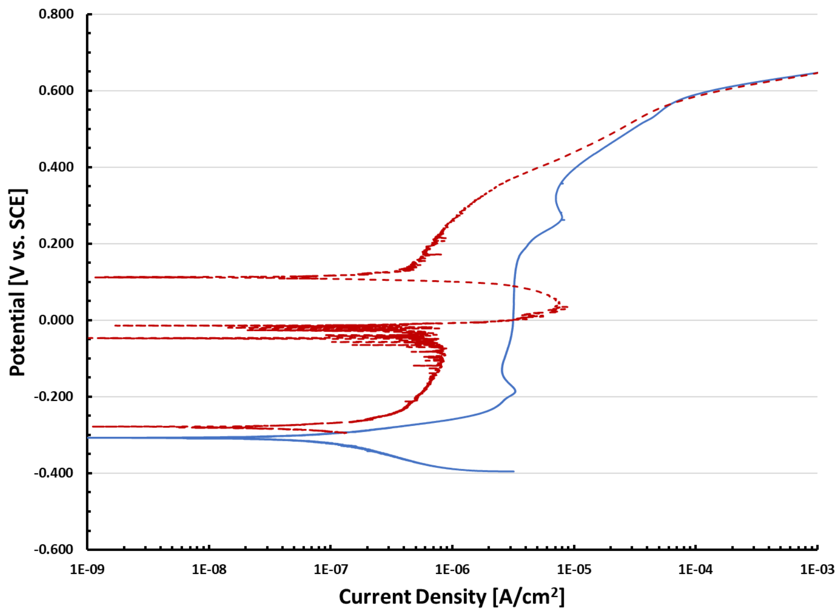

Trial 19

Mounted Electrode

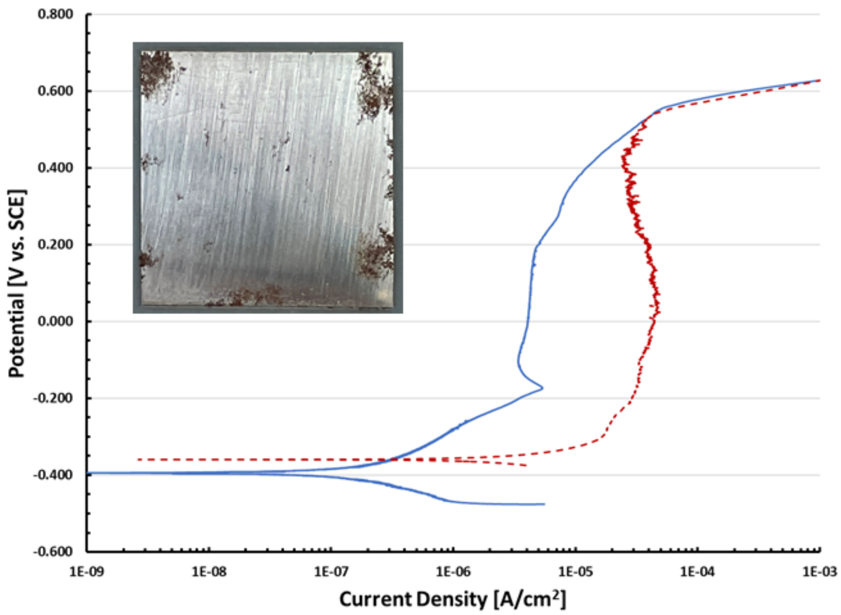

Bullet Electrode

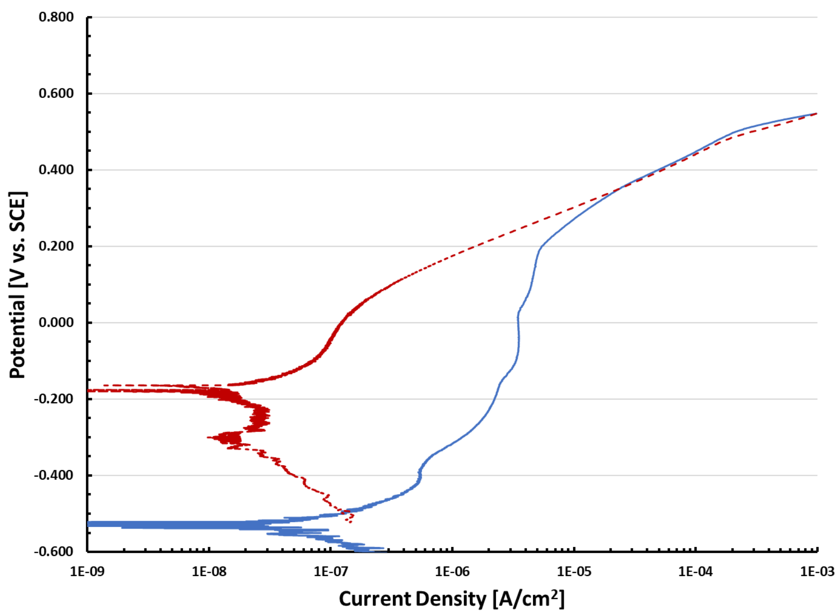

Trial 19 (Continued)

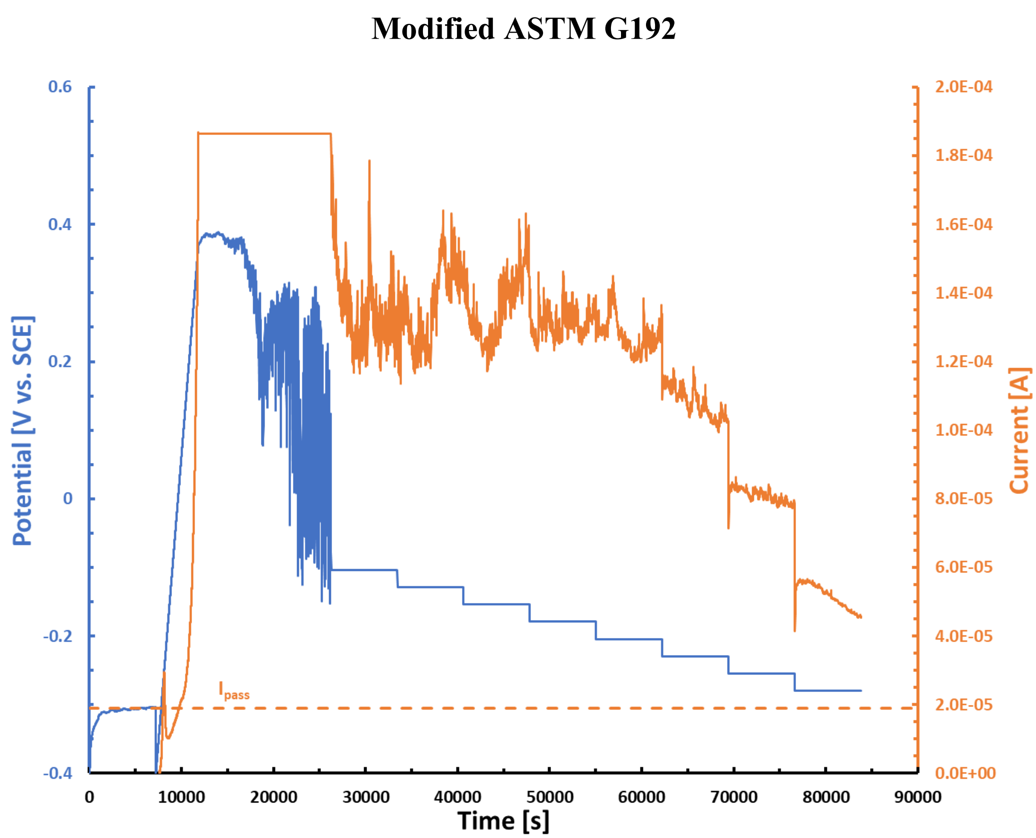

Trial 20

Mounted Electrode

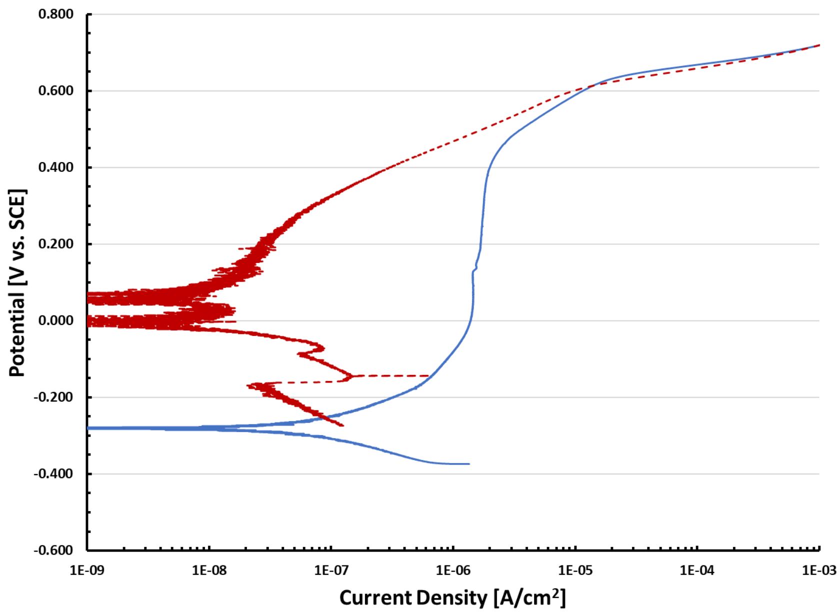

Trial 21

Mounted Electrode

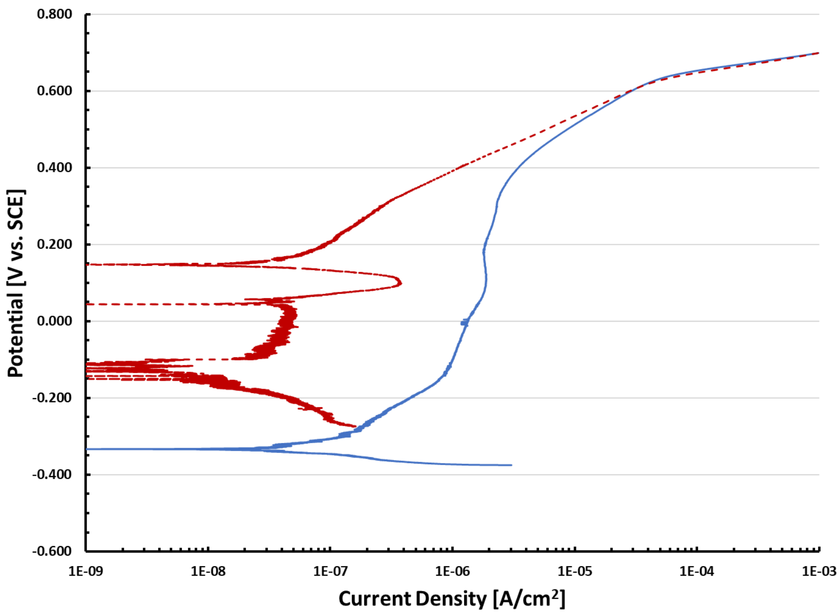

Trial 22

Mounted Electrode

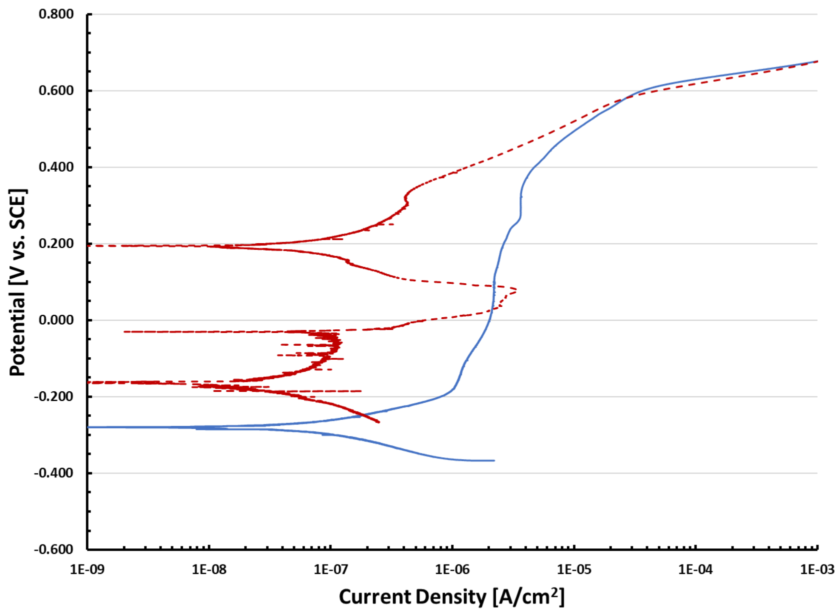

Trial 23

Mounted Electrode

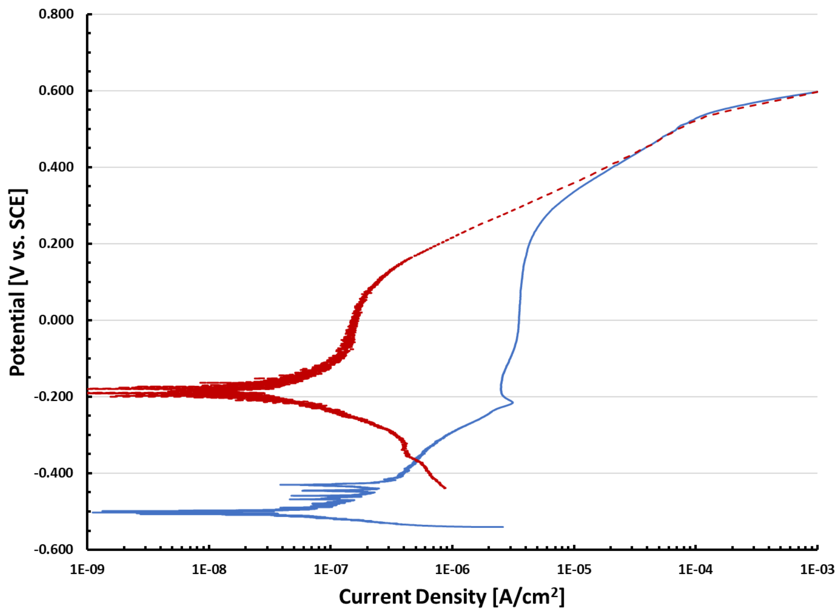

Trial 24

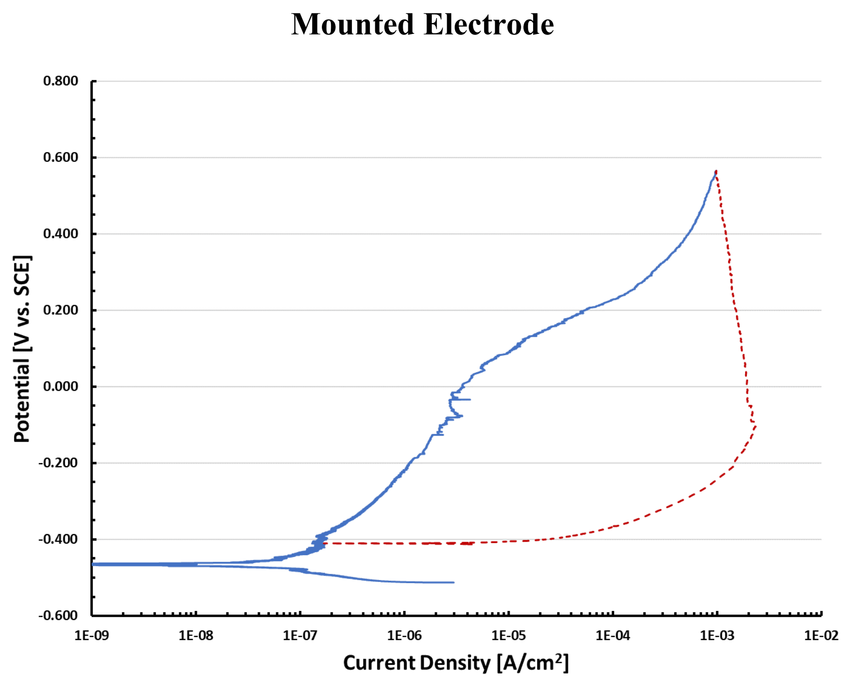
Mounted Electrode
0.800
0.600
0.400
0.200
0.000
-0.200
-0.400
-0.600
Potential [V vs. SCE]
1E-09
1E-08
1E-07
1E-06
1E-05
1E-04
1E-03
1E-02
Current Density [A/cm²]

Trial 25

Mounted Electrode

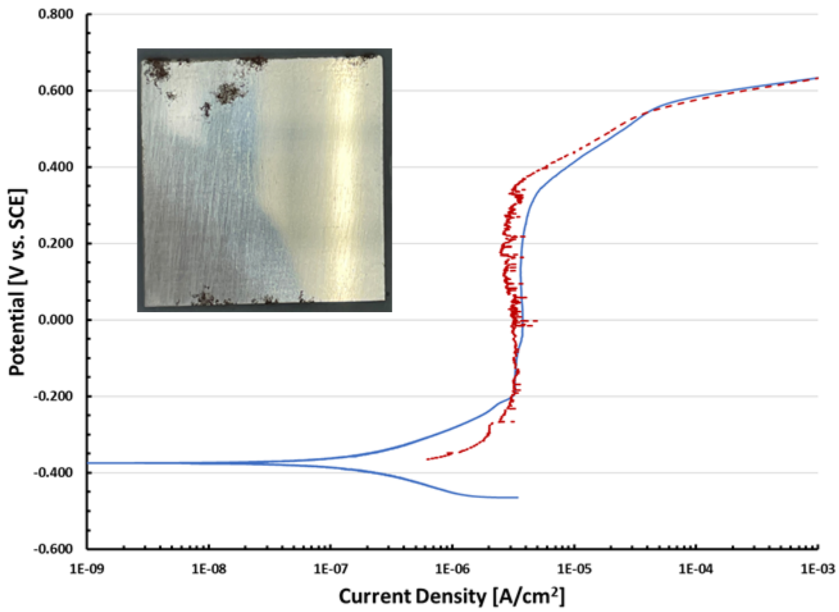

Bullet Electrode

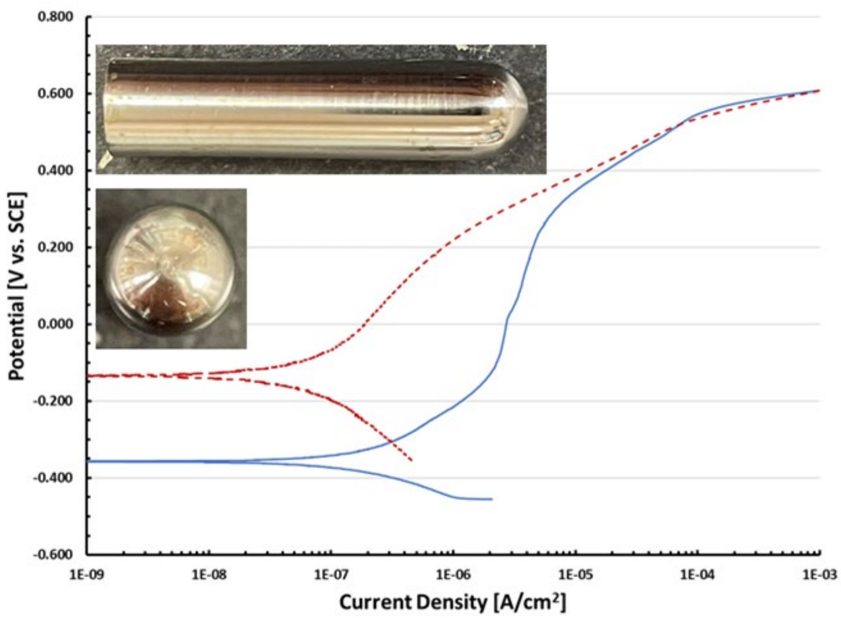

Trial 25 (Continued)

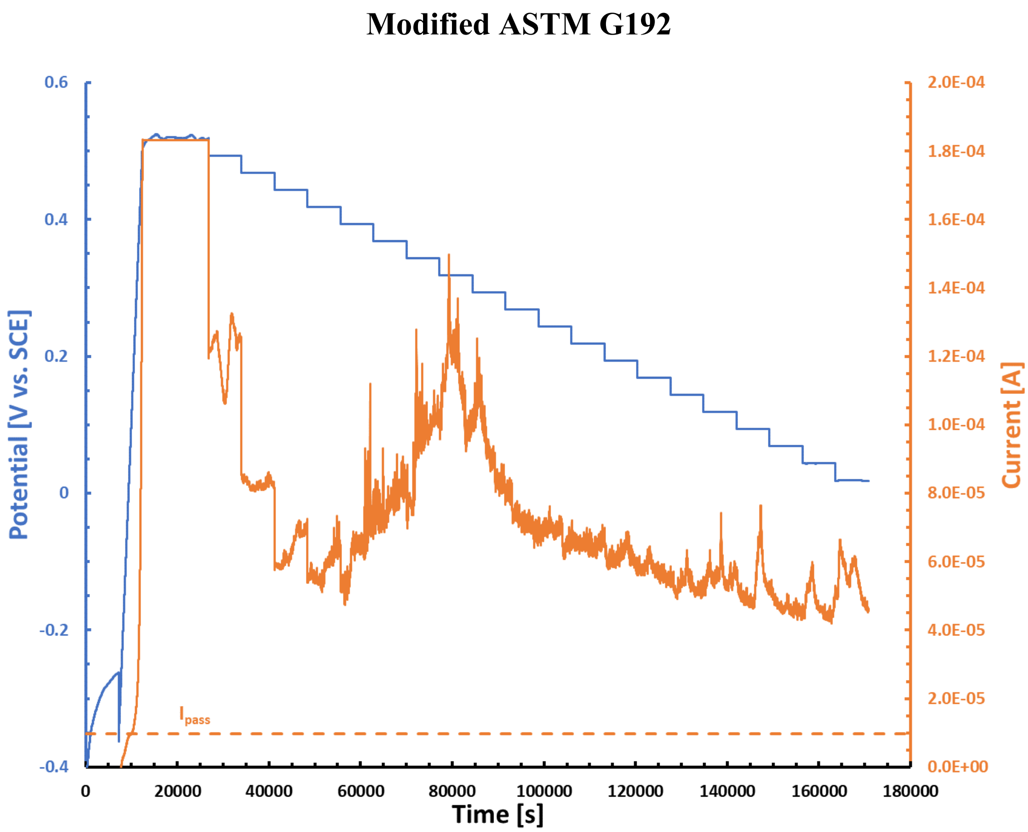

Trial 26

Mounted Electrode

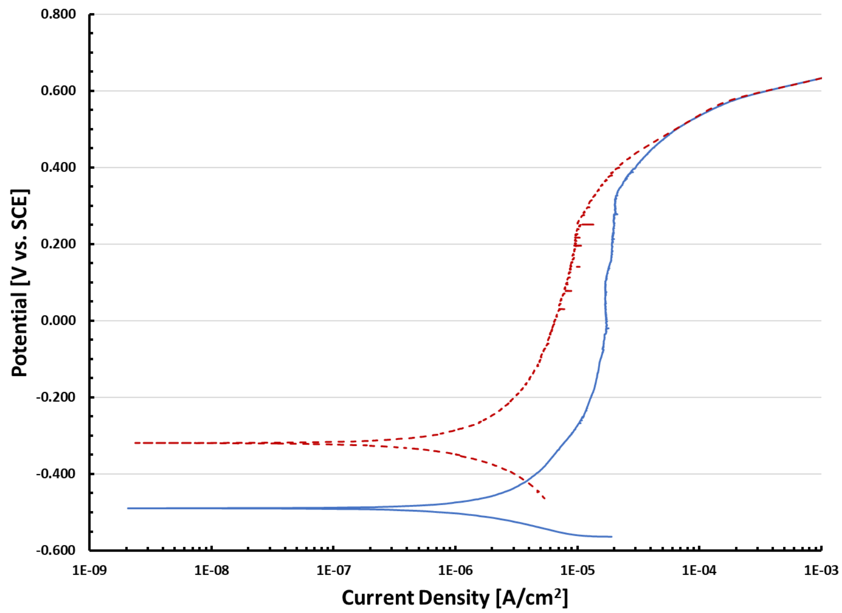

Trial 27

Mounted Electrode

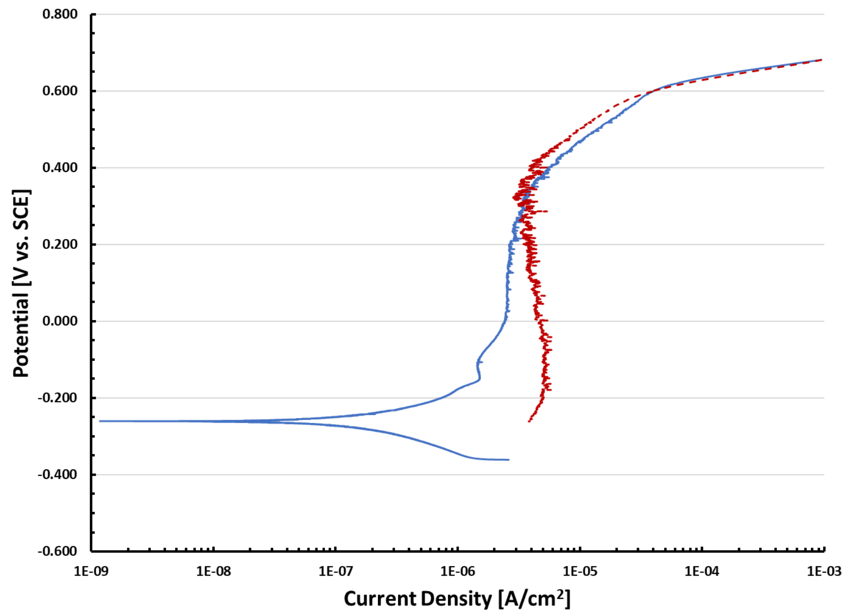

Trial 28

Mounted Electrode

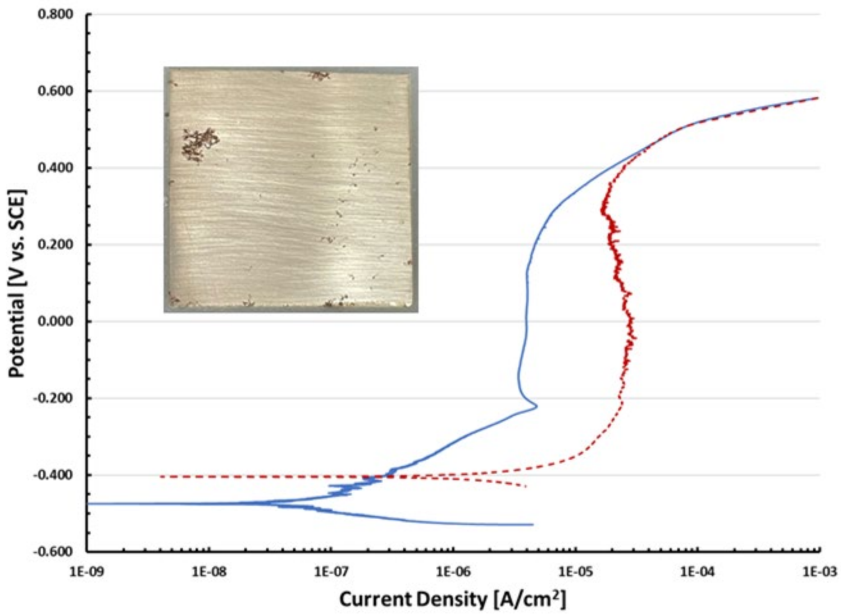

Bullet Electrode

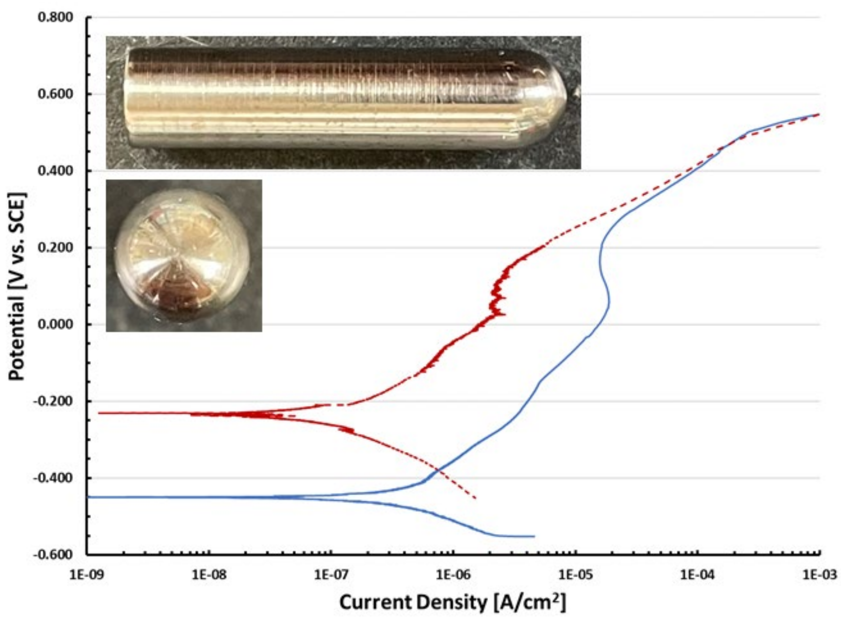

Trial 28 (Continued)

Modified ASTM G192

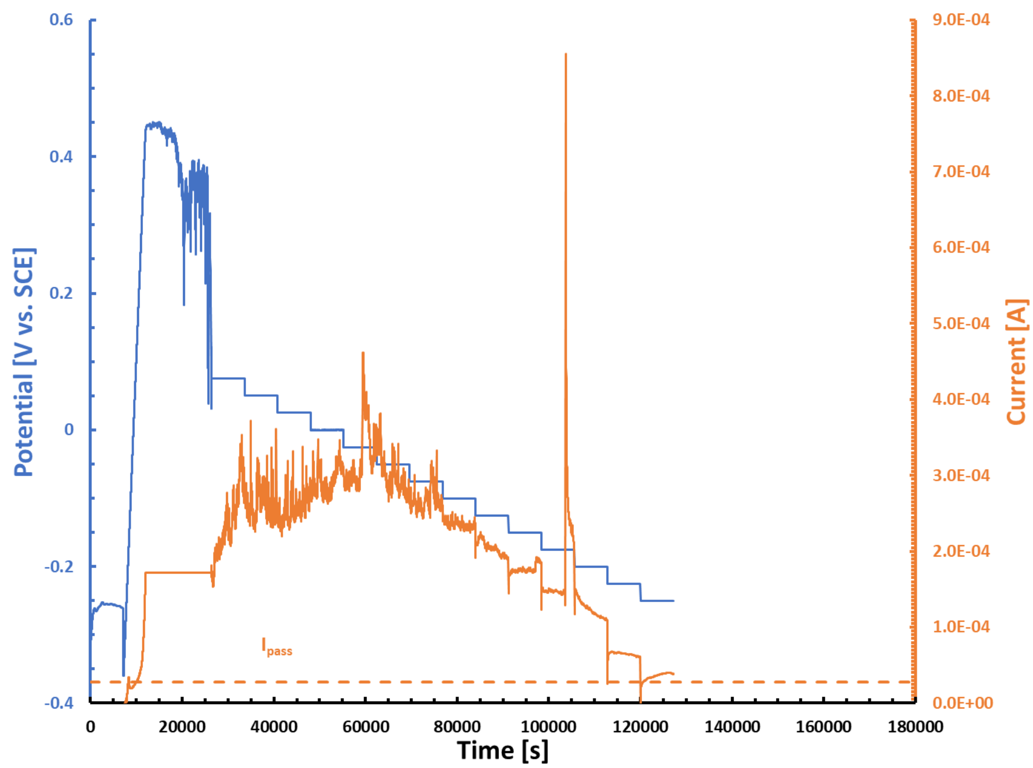

Trial 29

Mounted Electrode

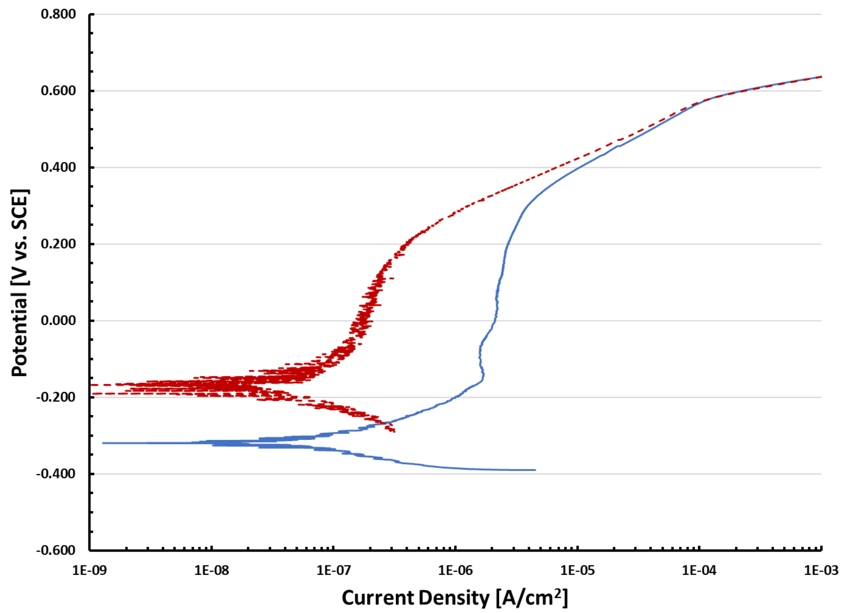

Trial 30

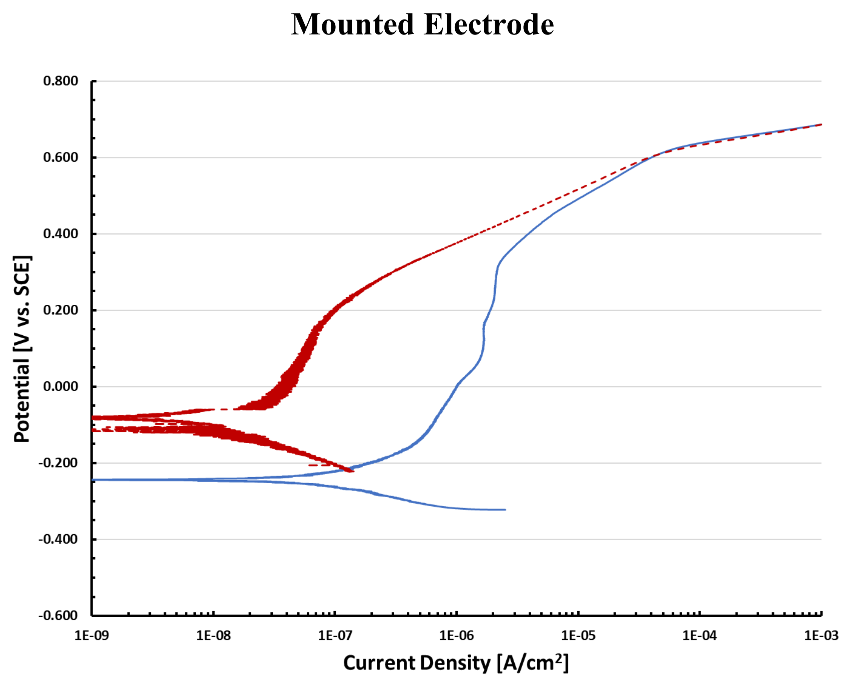
Mounted Electrode
0.800
0.600
0.400
0.200
0.000
-0.200
-0.400
-0.600
Potential [V vs. SCE]
1E-09
1E-08
1E-07
1E-06
1E-05
1E-04
1E-03
Current Density [A/cm²]

Trial 31

Mounted Electrode

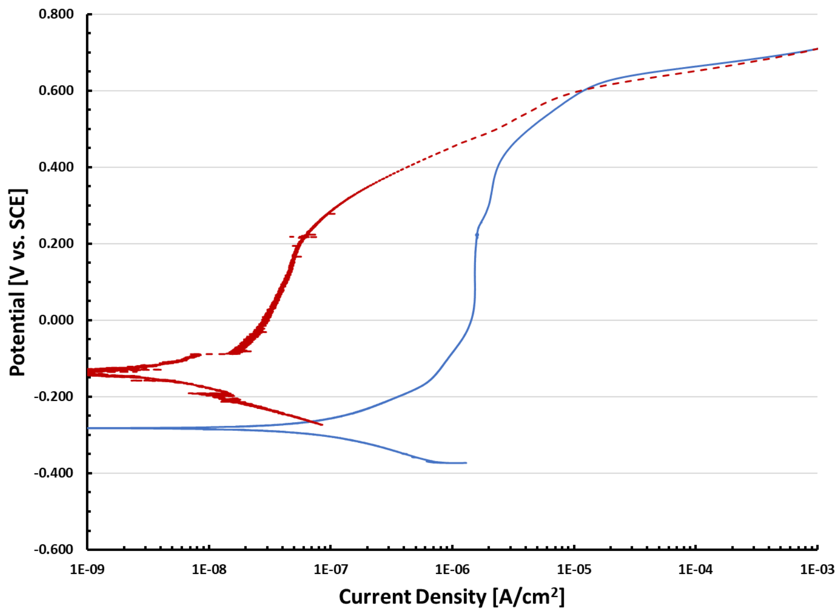

Trial 32

Mounted Electrode

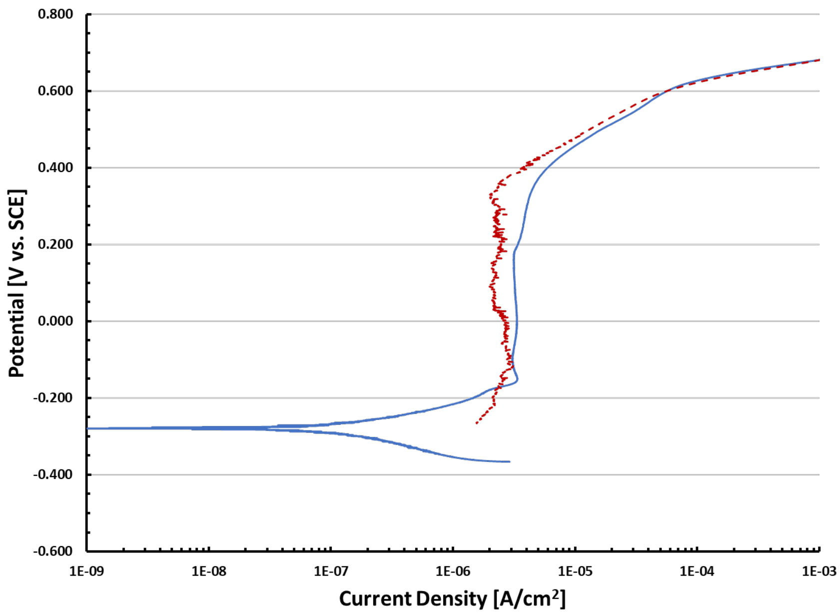

Trial 33

Mounted Electrode

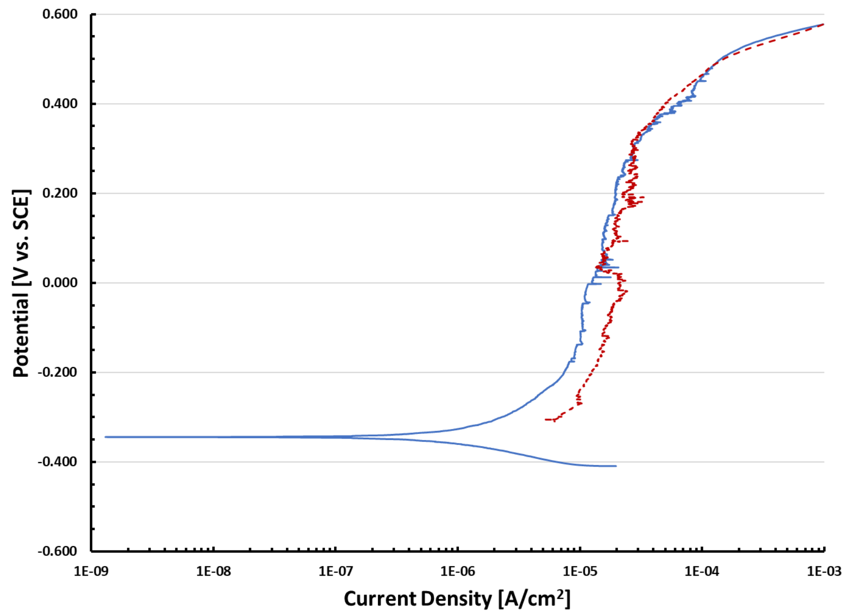

Bullet Electrode

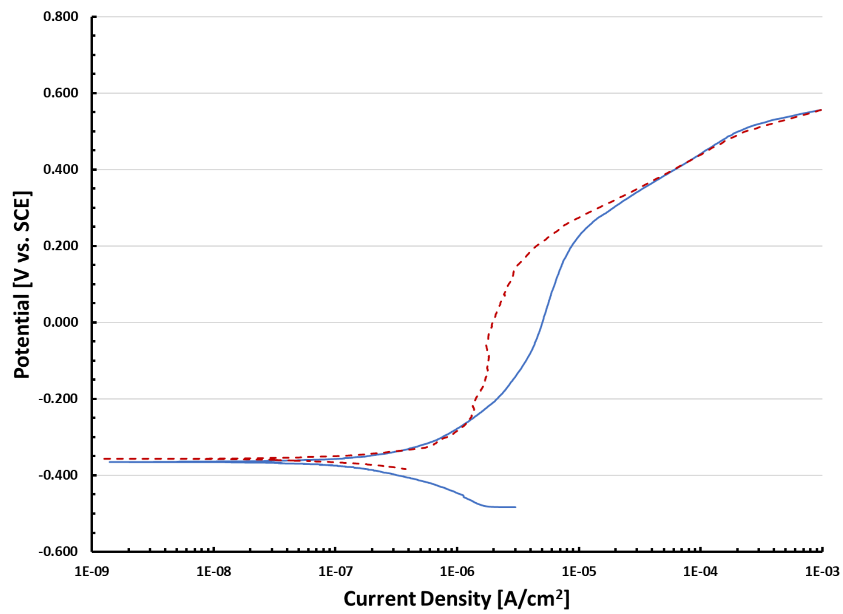

Trial 33 (Continued)

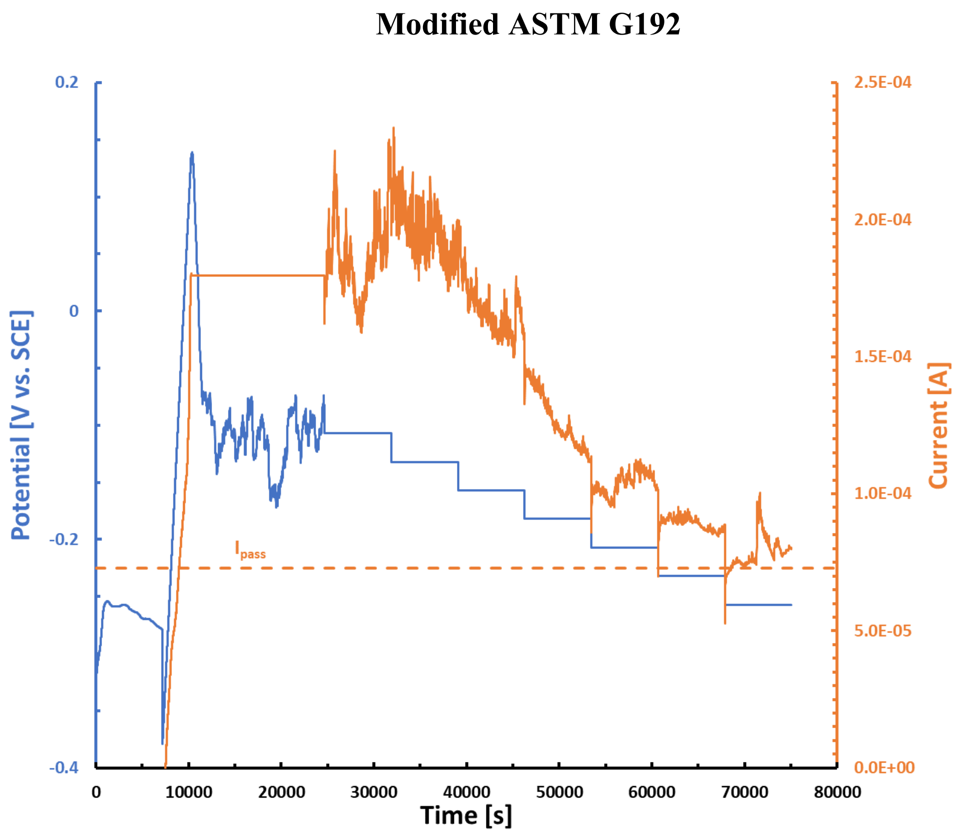

Trial 34

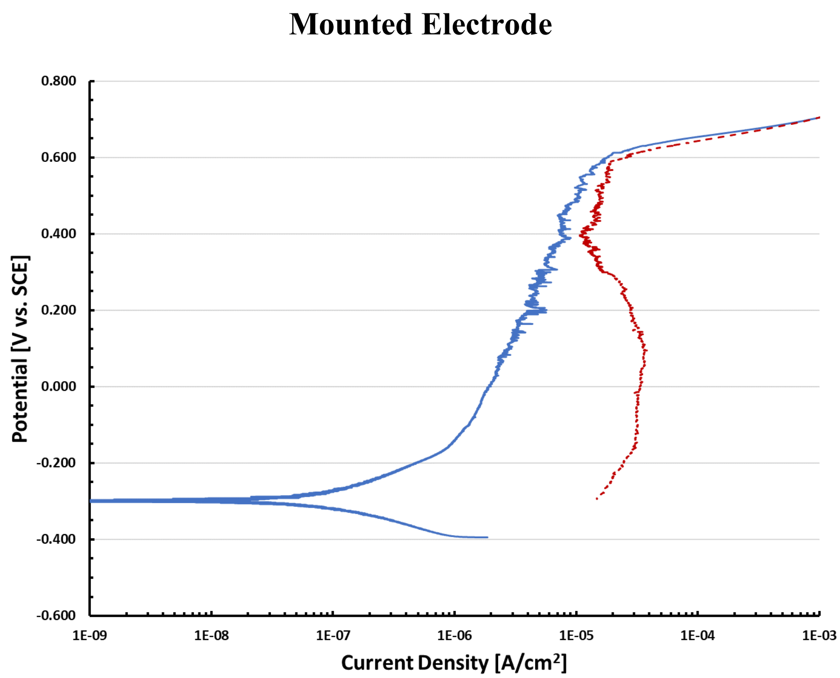
Mounted Electrode
0.800
0.600
0.400
0.200
0.000
-0.200
-0.400
-0.600
Potential [V vs. SCE]
1E-09
1E-08
1E-07
1E-06
1E-05
1E-04
1E-03
Current Density [A/cm²]

Trial 35

Mounted Electrode

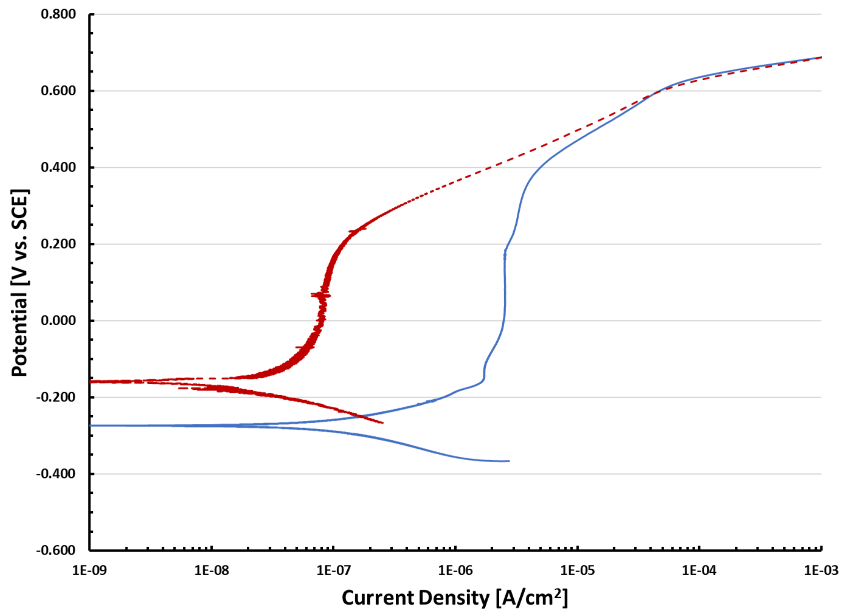

Trial 36

Mounted Electrode

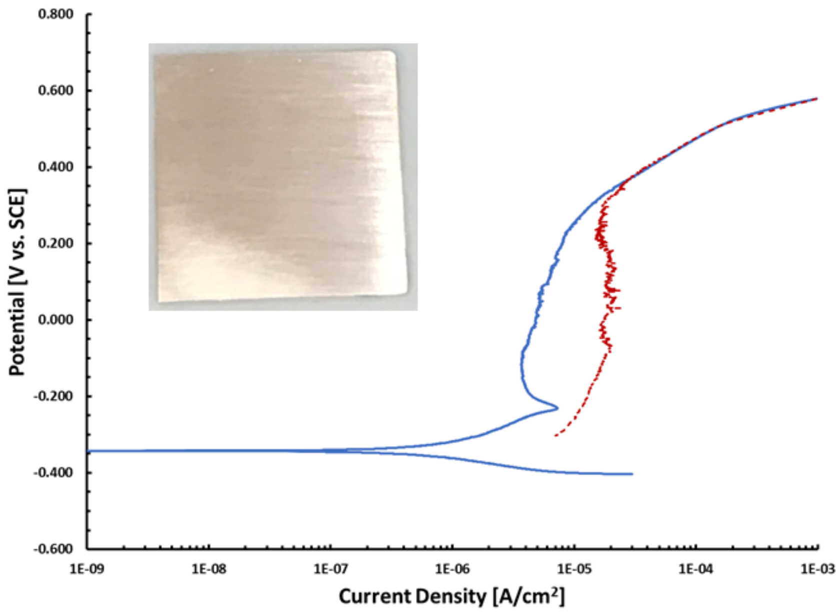

Bullet Electrode

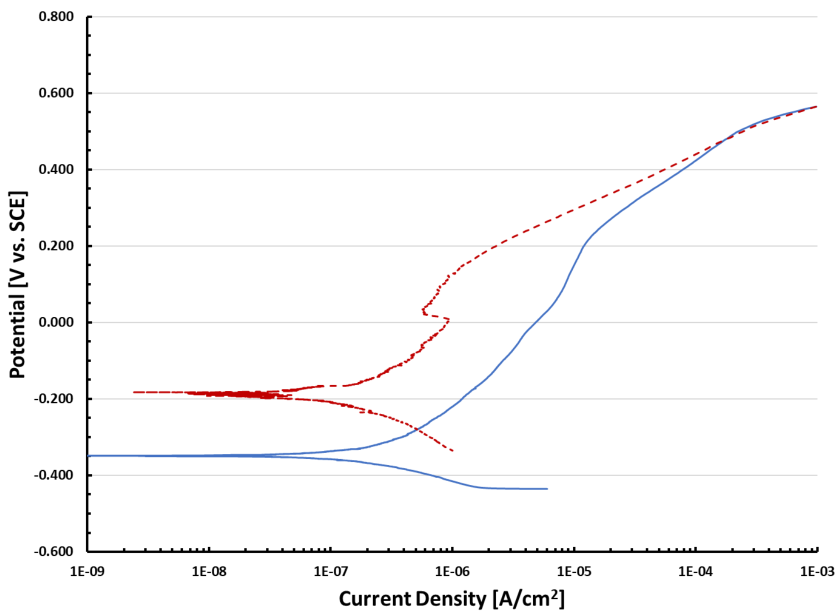

Trial 36 (Continued)

Modified ASTM G192

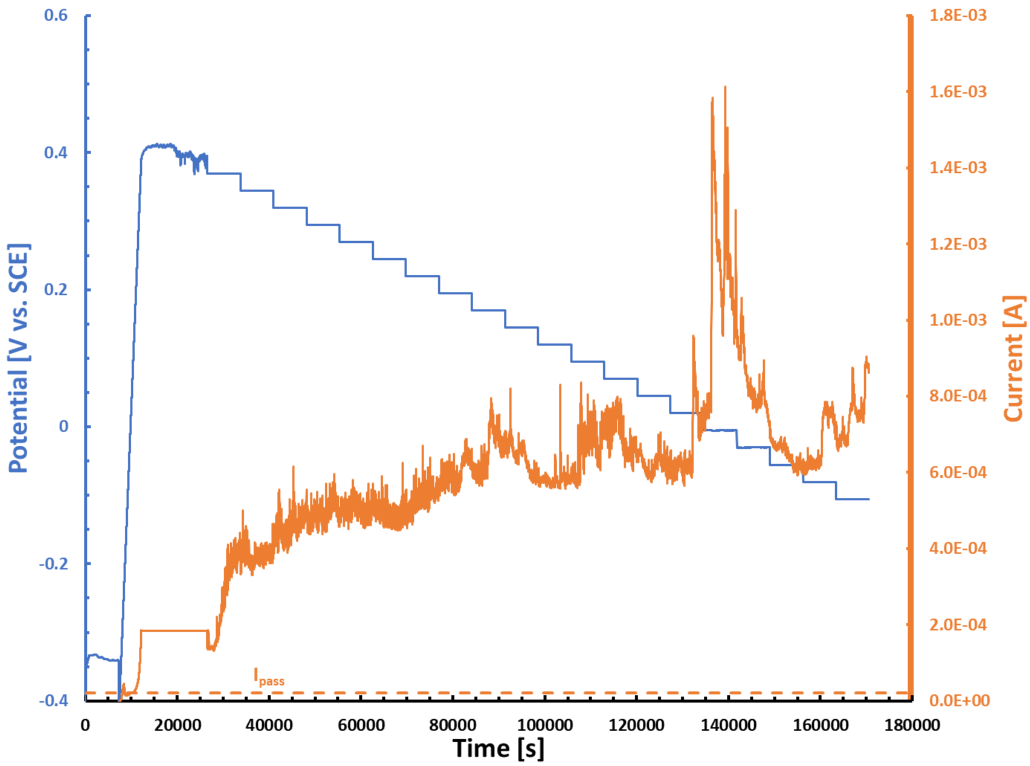

Trial 37

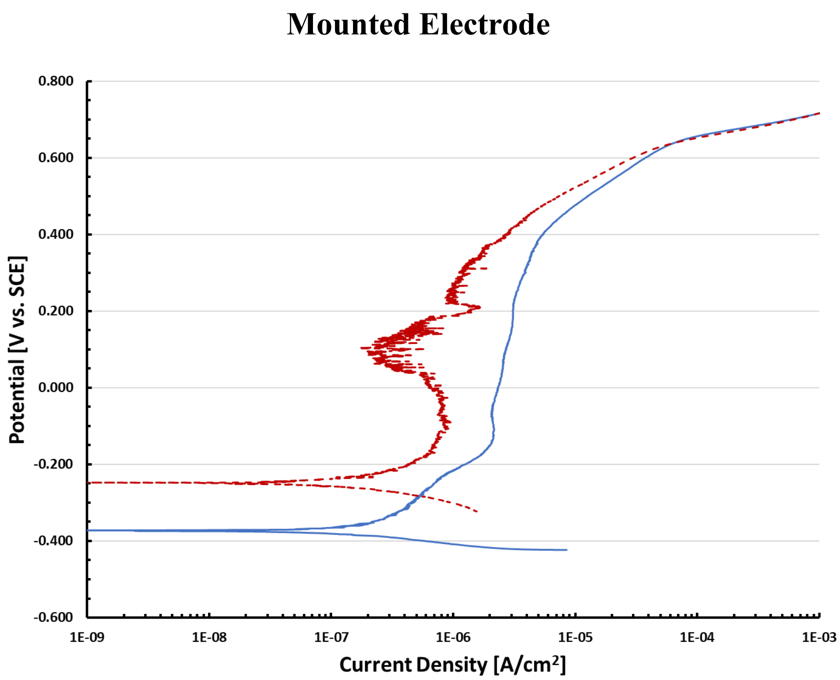
Mounted Electrode
0.800
0.600
0.400
0.200
0.000
-0.200
-0.400
-0.600
Potential [V vs. SCE]
1E-09
1E-08
1E-07
1E-06
1E-05
1E-04
1E-03
Current Density [A/cm2]

Trial 38

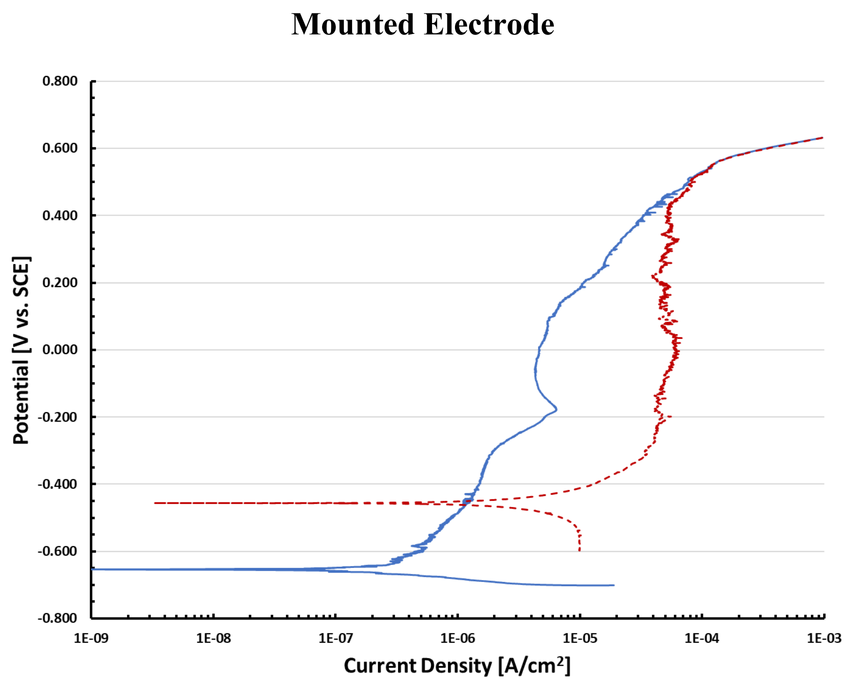
Mounted Electrode
0.800
0.600
0.400
0.200
0.000
-0.200
-0.400
-0.600
-0.800
Potential [V vs. SCE]
1E-09
1E-08
1E-07
1E-06
1E-05
1E-04
1E-03
Current Density [A/cm2]

Trial 39

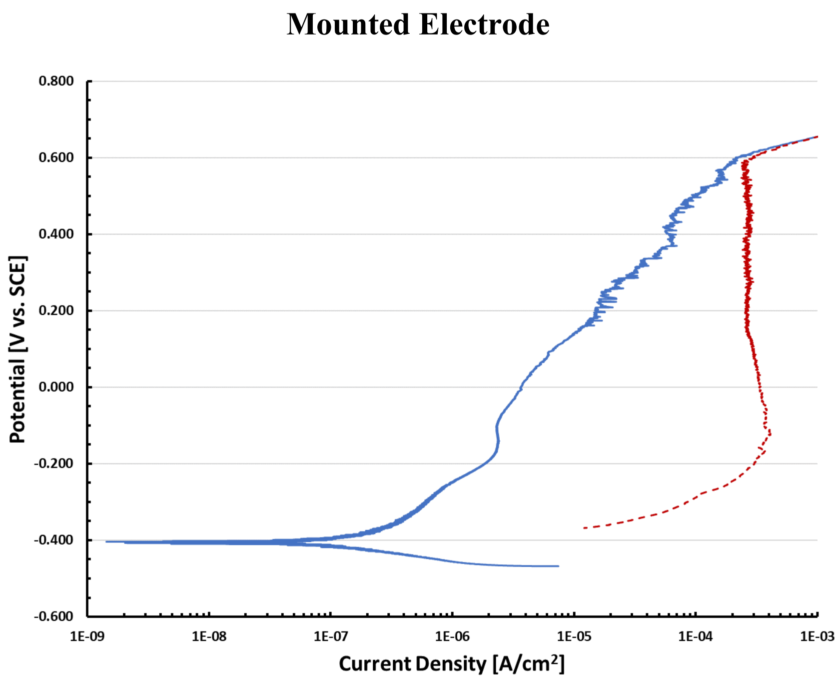
Mounted Electrode
0.800
0.600
0.400
0.200
0.000
-0.200
-0.400
-0.600
Potential [V vs. SCE]
1E-09
1E-08
1E-07
1E-06
1E-05
1E-04
1E-03
Current Density [A/cm2]

Trial 40

Mounted Electrode

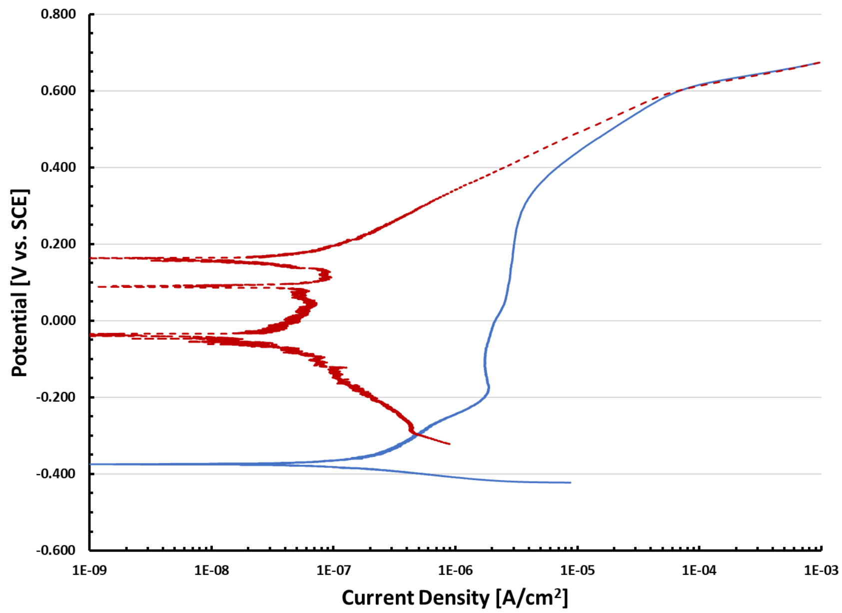

Trial 41

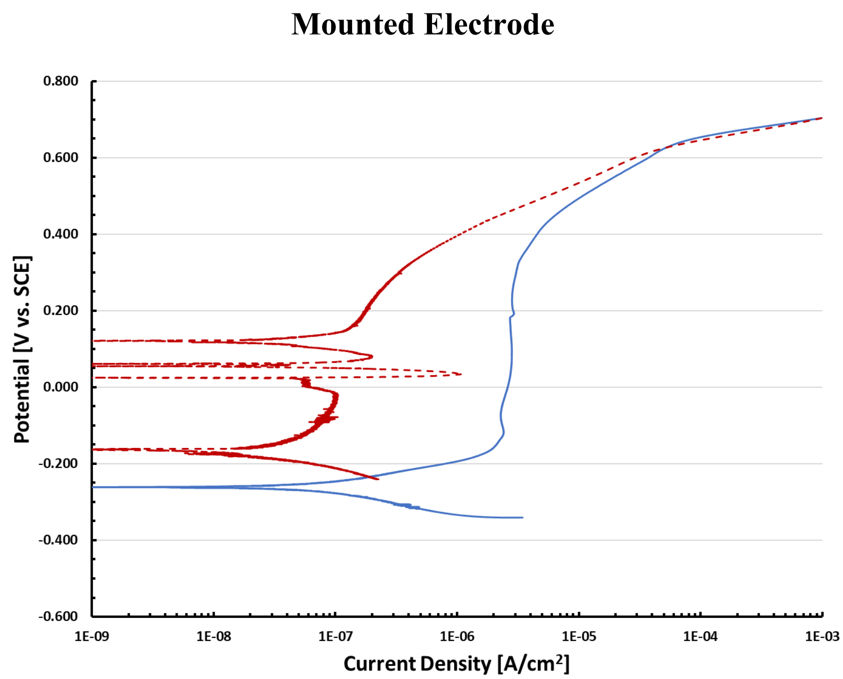
Mounted Electrode
0.800
0.600
0.400
0.200
0.000
-0.200
-0.400
-0.600
Potential [V vs. SCE]
1E-09
1E-08
1E-07
1E-06
1E-05
1E-04
1E-03
Current Density [A/cm²]

Trial 42

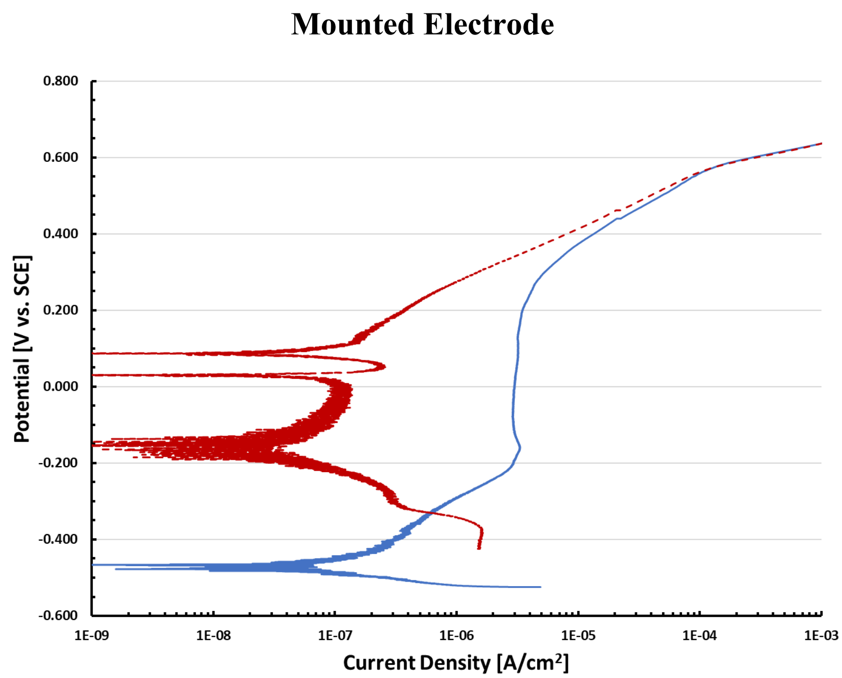
Mounted Electrode
0.800
0.600
0.400
0.200
0.000
-0.200
-0.400
-0.600
Potential [V vs. SCE]
1E-09
1E-08
1E-07
1E-06
1E-05
1E-04
1E-03
Current Density [A/cm2]

Trial 43

Mounted Electrode

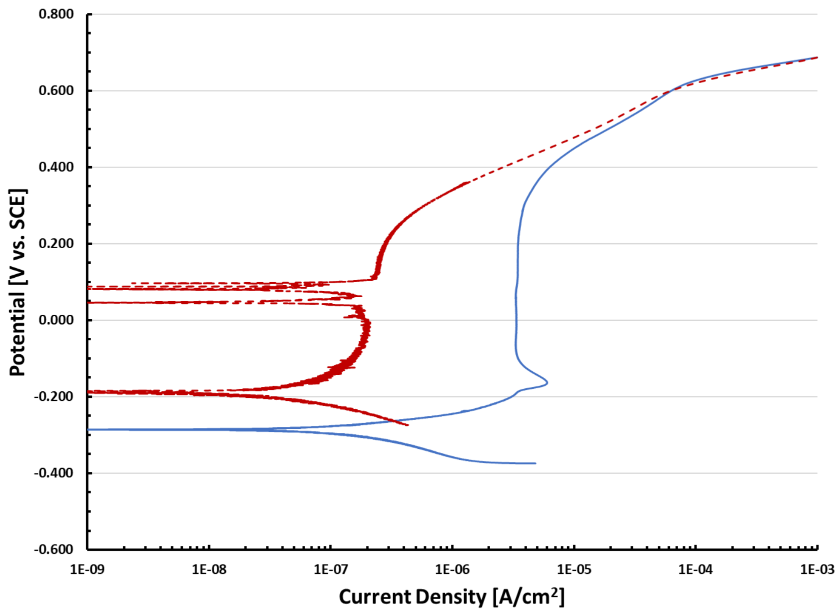

Trial 44

Mounted Electrode

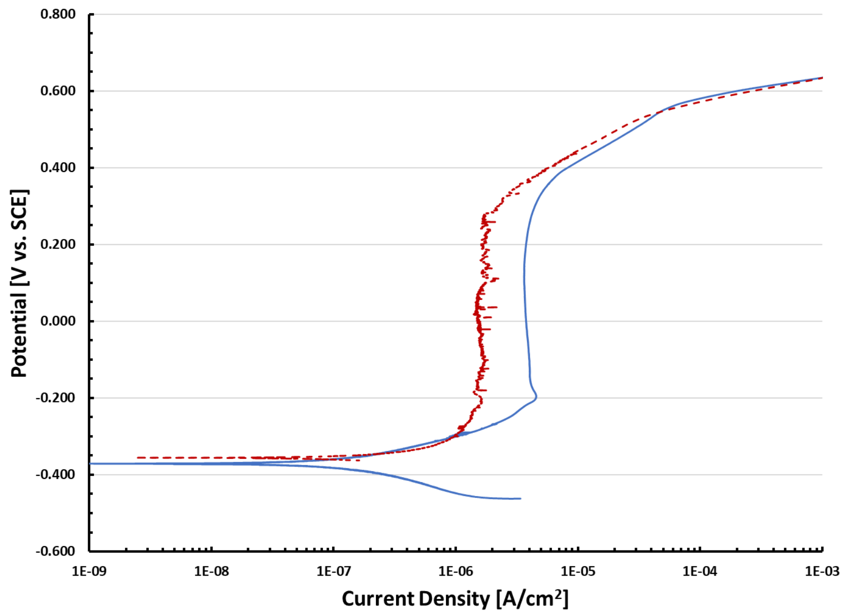

Trial 45

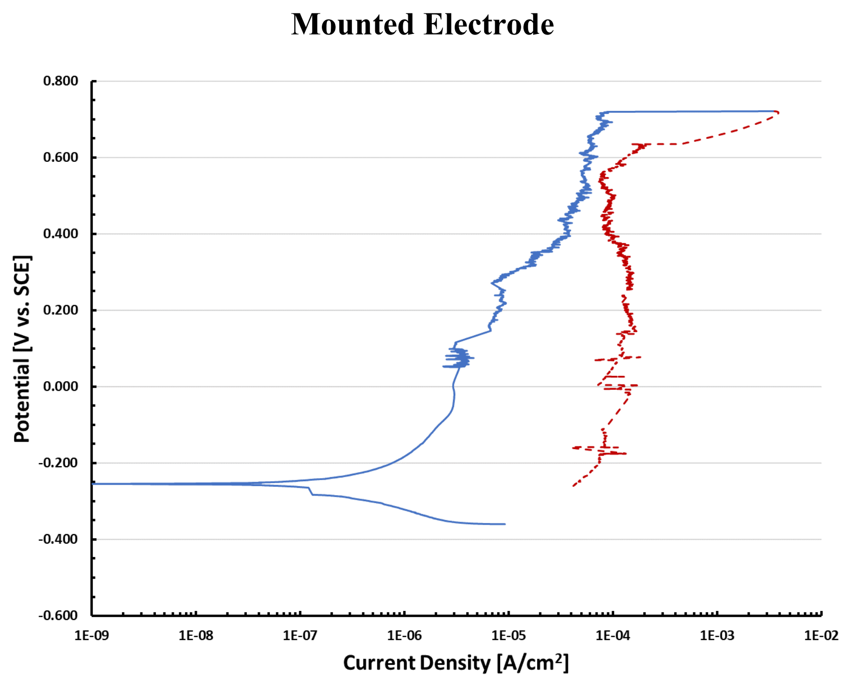
Mounted Electrode
0.800
0.600
0.400
0.200
0.000
-0.200
-0.400
-0.600
Potential [V vs. SCE]
1E-09
1E-08
1E-07
1E-06
1E-05
1E-04
1E-03
1E-02
Current Density [A/cm2]

Trial 46

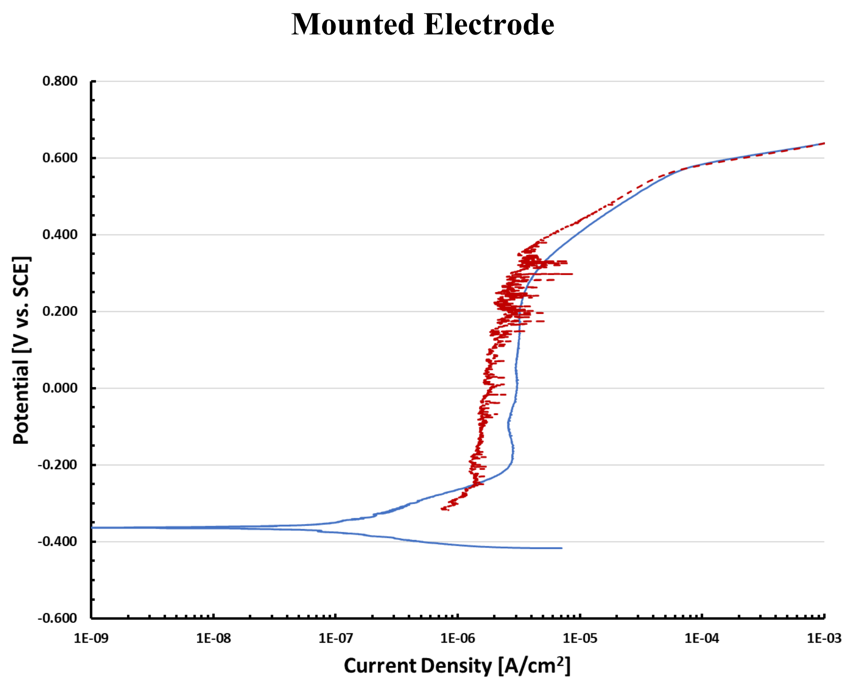
Mounted Electrode
0.800
0.600
0.400
0.200
0.000
-0.200
-0.400
-0.600
Potential [V vs. SCE]
1E-09
1E-08
1E-07
1E-06
1E-05
1E-04
1E-03
Current Density [A/cm²]

Trial 47

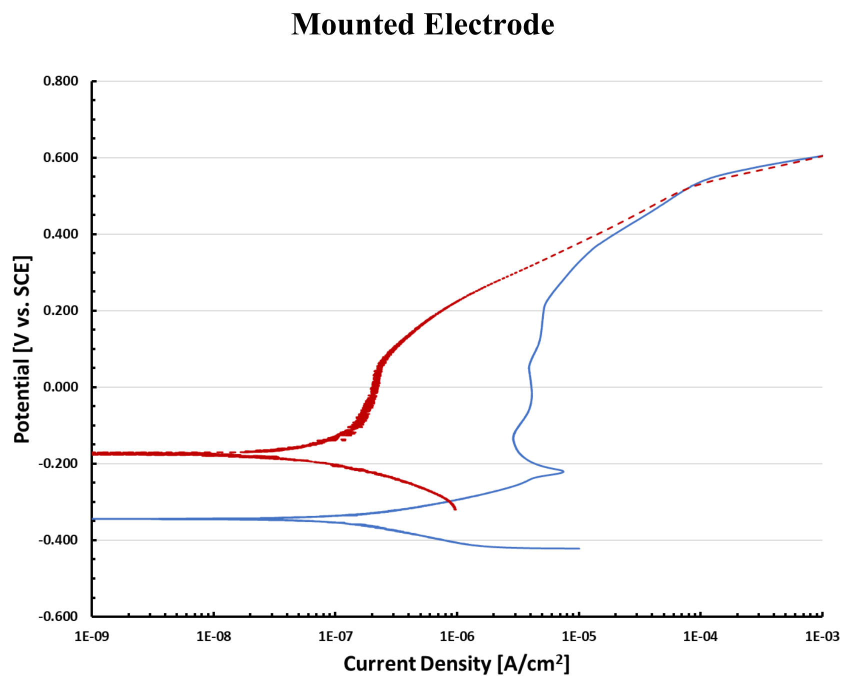
Mounted Electrode
0.800
0.600
0.400
0.200
0.000
-0.200
-0.400
-0.600
Potential [V vs. SCE]
1E-09
1E-08
1E-07
1E-06
1E-05
1E-04
1E-03
Current Density [A/cm²]

Trial 48

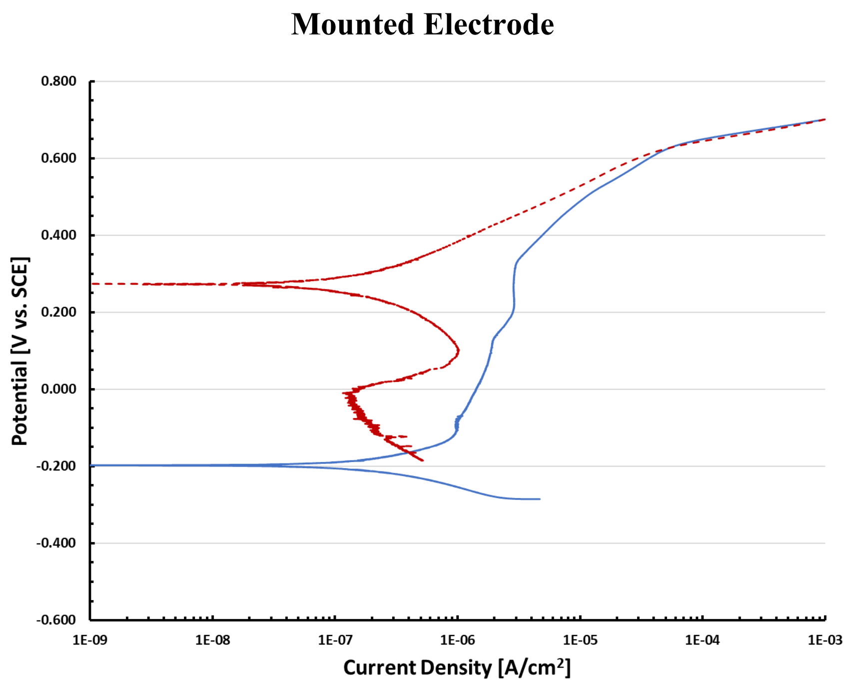
Mounted Electrode
0.800
0.600
0.400
0.200
0.000
-0.200
-0.400
-0.600
Potential [V vs. SCE]
1E-09
1E-08
1E-07
1E-06
1E-05
1E-04
1E-03
Current Density [A/cm²]

Trial 49

Mounted Electrode

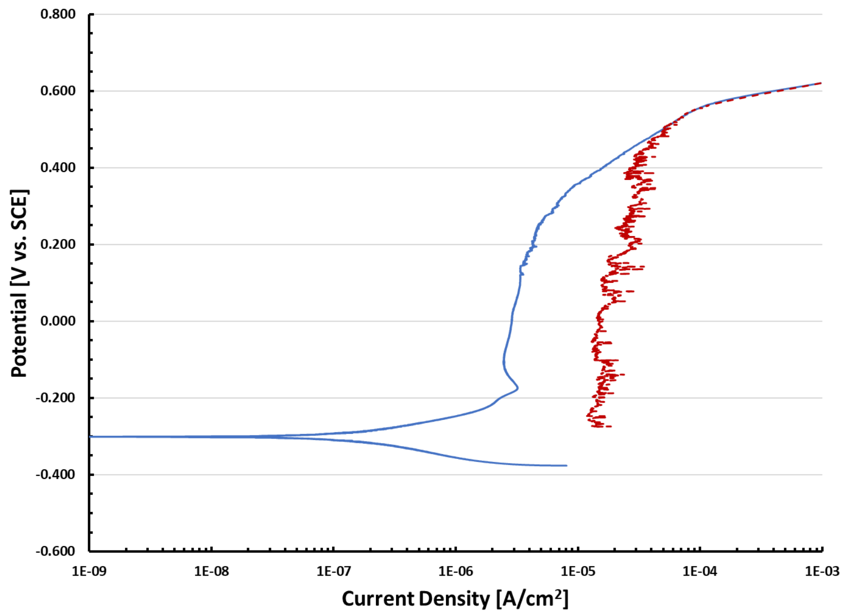

Trial 50

Mounted Electrode

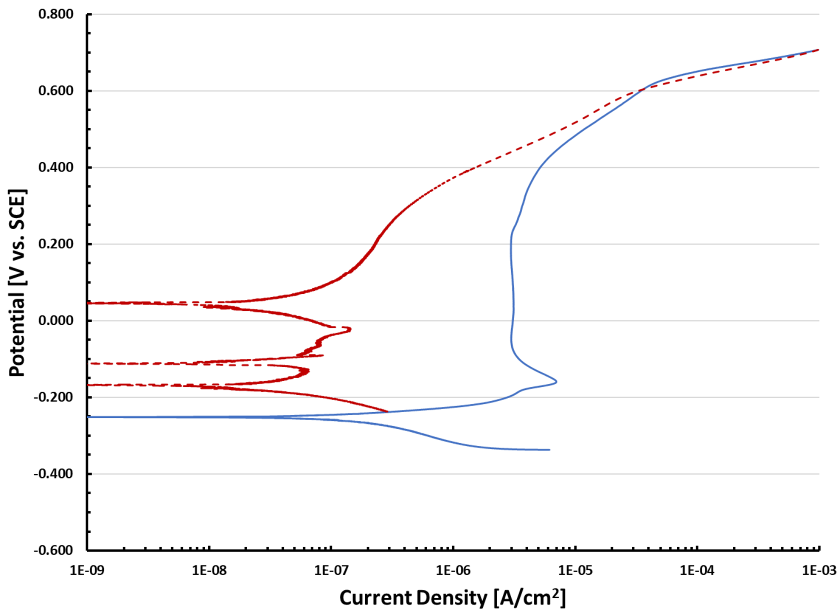

Trial 51

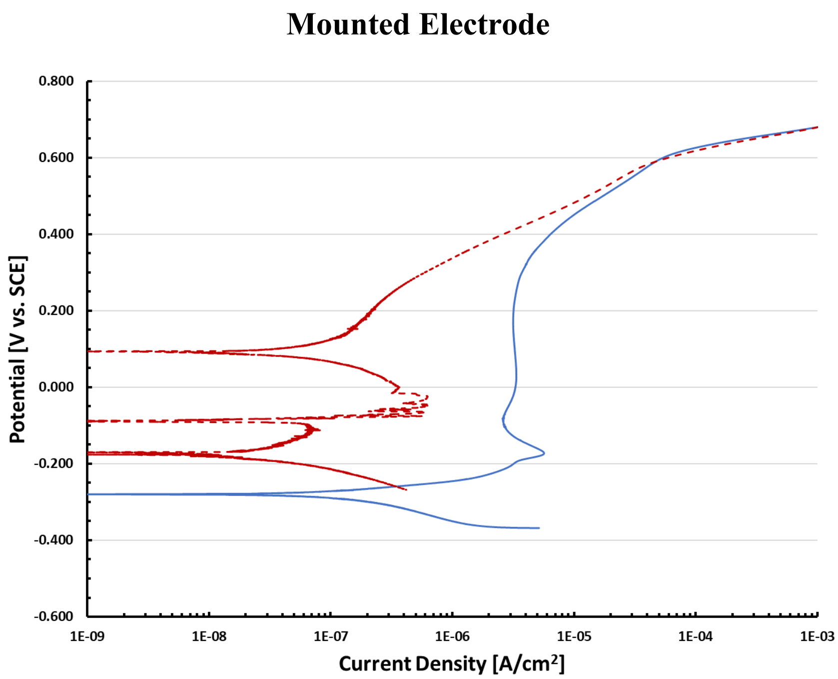
Mounted Electrode
0.800
0.600
0.400
0.200
0.000
-0.200
-0.400
-0.600
Potential [V vs. SCE]
1E-09
1E-08
1E-07
1E-06
1E-05
1E-04
1E-03
Current Density [A/cm²]

Trial 52

Mounted Electrode

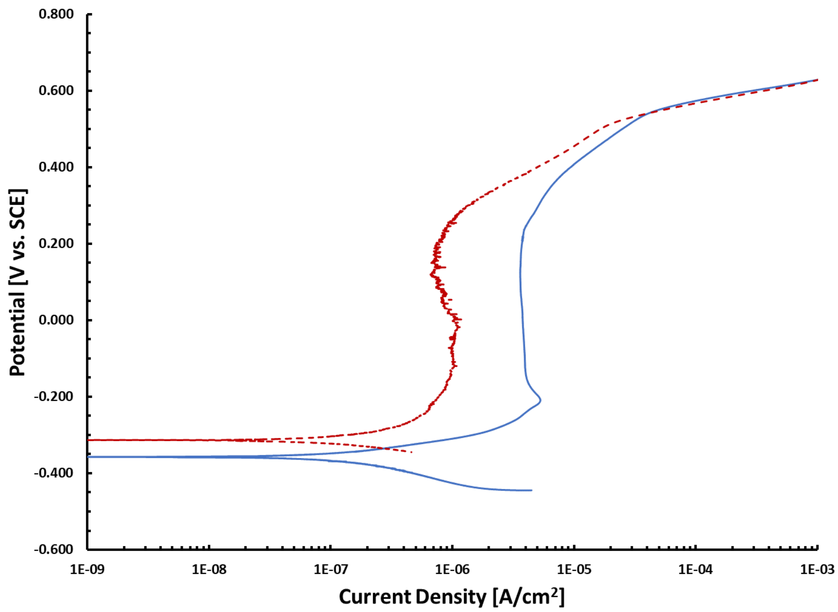

Trial 53

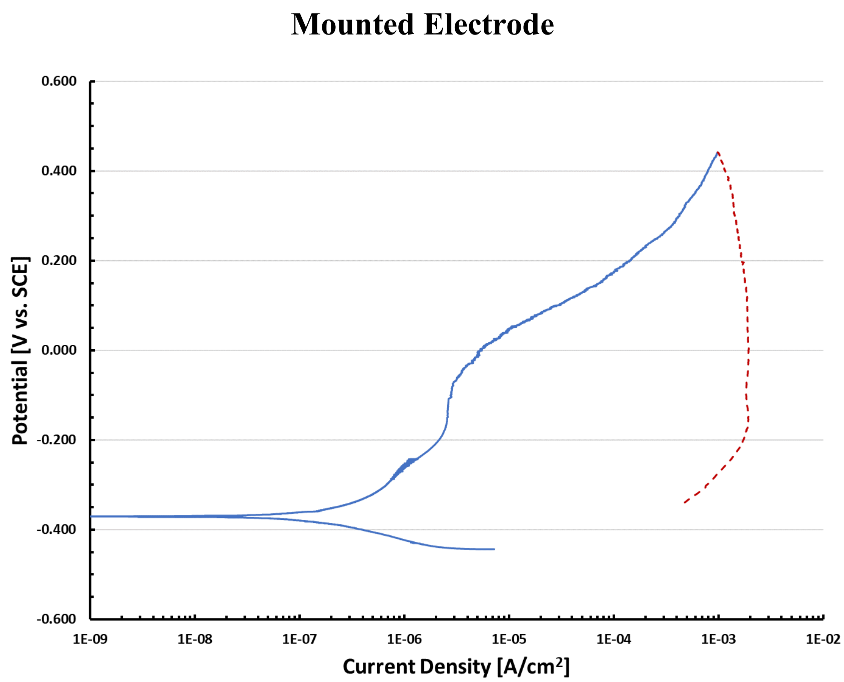
Mounted Electrode
0.600
0.400
0.200
0.000
-0.200
-0.400
-0.600
Potential [V vs. SCE]
1E-09
1E-08
1E-07
1E-06
1E-05
1E-04
1E-03
1E-02
Current Density [A/cm2]

Trial 54

Mounted Electrode

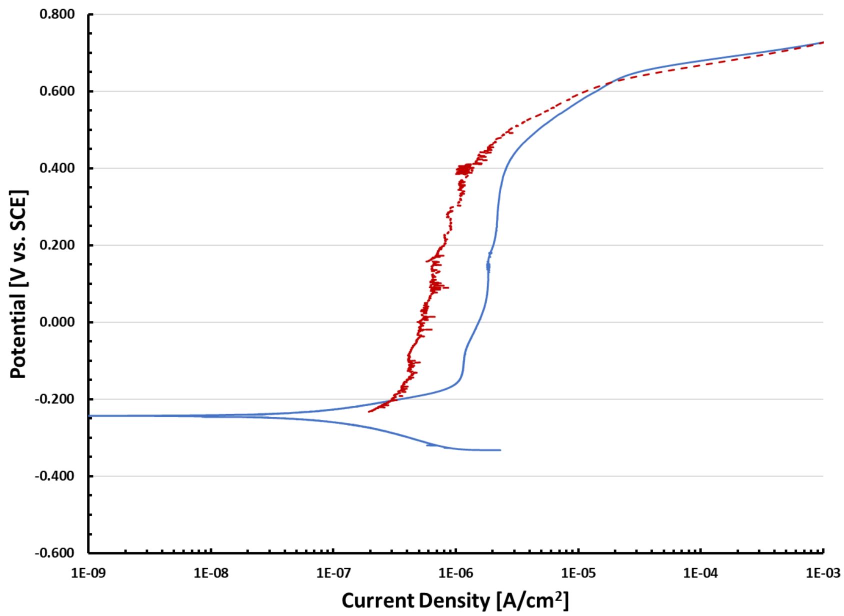

Trial 55

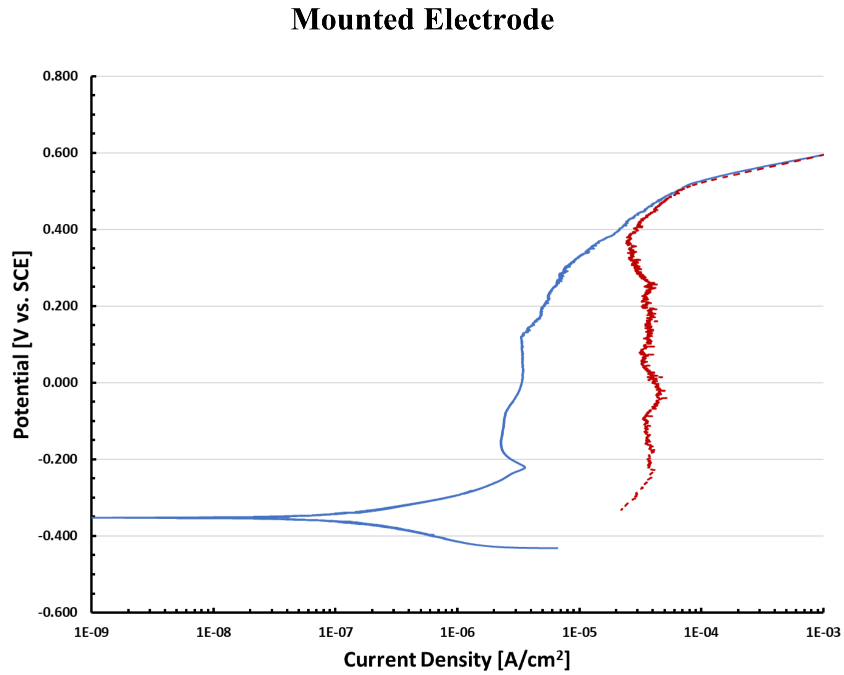
Mounted Electrode
0.800
0.600
0.400
0.200
0.000
-0.200
-0.400
-0.600
Potential [V vs. SCE]
1E-09
1E-08
1E-07
1E-06
1E-05
1E-04
1E-03
Current Density [A/cm²]

Trial 56

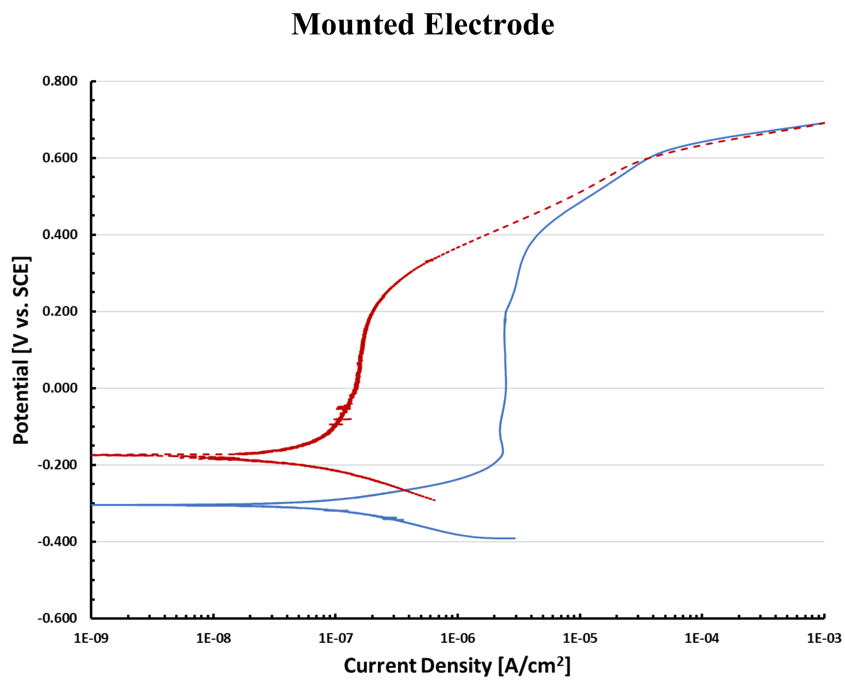
Mounted Electrode
0.800
0.600
0.400
0.200
0.000
-0.200
-0.400
-0.600
Potential [V vs. SCE]
1E-09
1E-08
1E-07
1E-06
1E-05
1E-04
1E-03
Current Density [A/cm2]

Trial 57

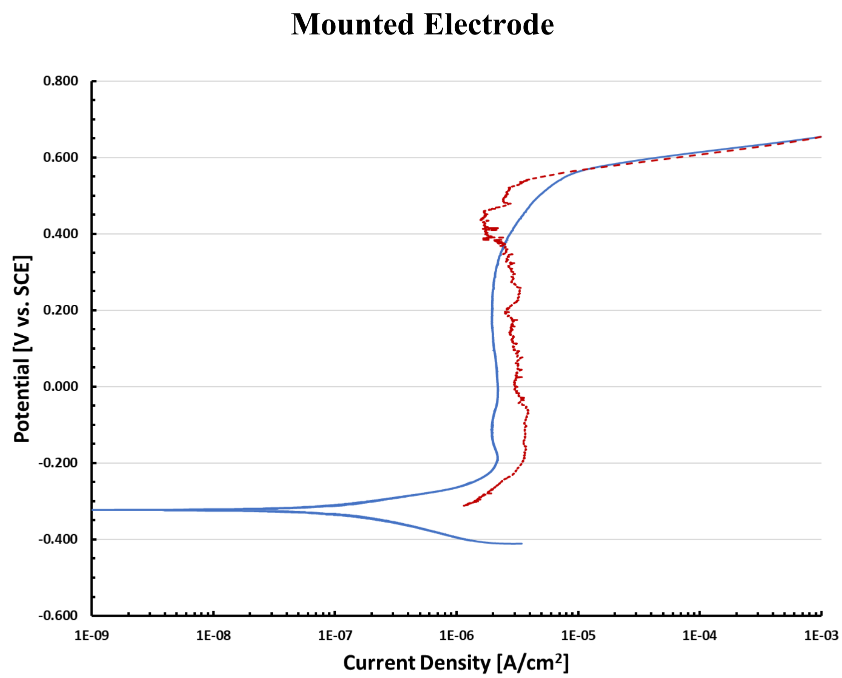
Mounted Electrode
0.800
0.600
0.400
0.200
0.000
-0.200
-0.400
-0.600
Potential [V vs. SCE]
1E-09
1E-08
1E-07
1E-06
1E-05
1E-04
1E-03
Current Density [A/cm2]

Trial 58

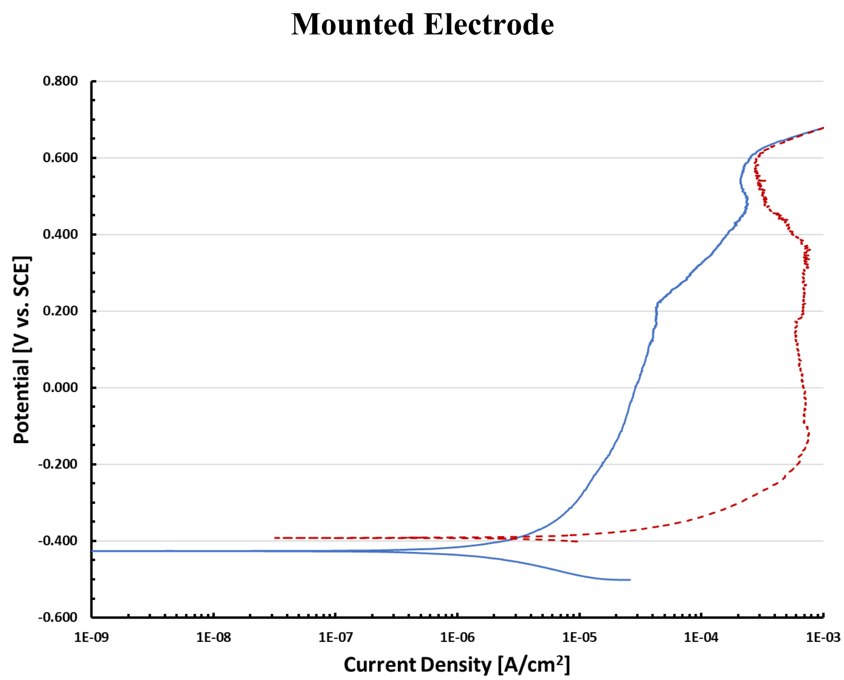
Mounted Electrode
0.800
0.600
0.400
0.200
0.000
-0.200
-0.400
-0.600
Potential [V vs. SCE]
1E-09
1E-08
1E-07
1E-06
1E-05
1E-04
1E-03
Current Density [A/cm²]

Trial 59

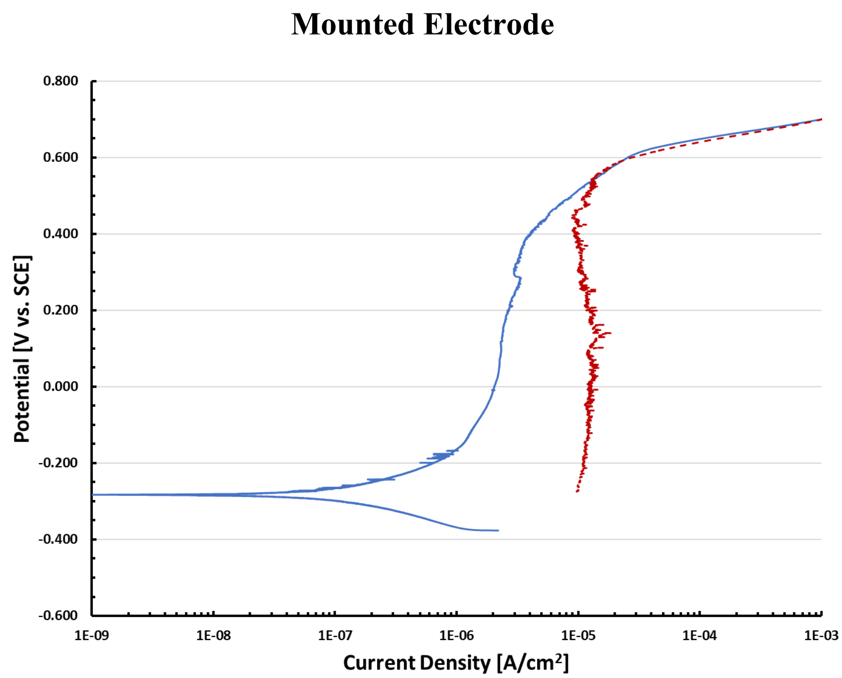
Mounted Electrode
0.800
0.600
0.400
0.200
0.000
-0.200
-0.400
-0.600
Potential [V vs. SCE]
1E-09
1E-08
1E-07
1E-06
1E-05
1E-04
1E-03
Current Density [A/cm2]

Trial 60

Mounted Electrode

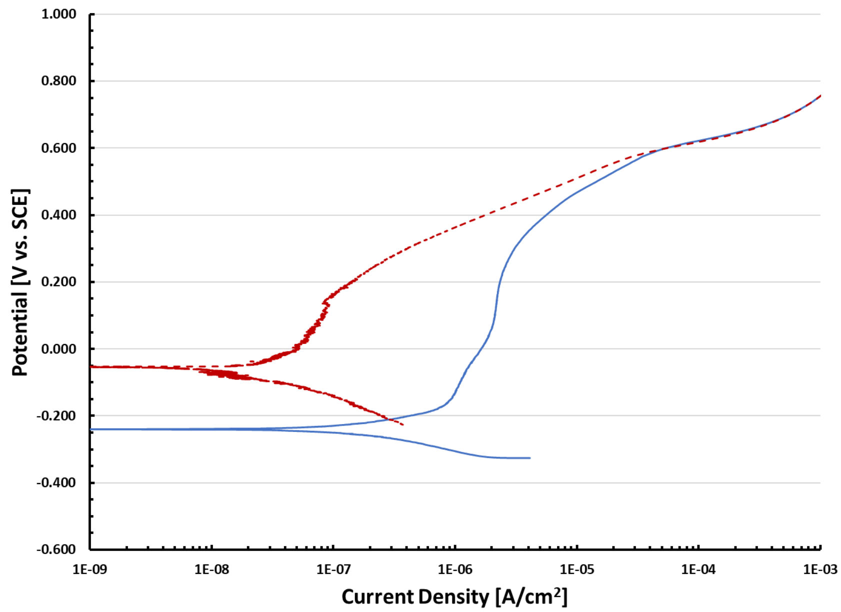

Trial 61

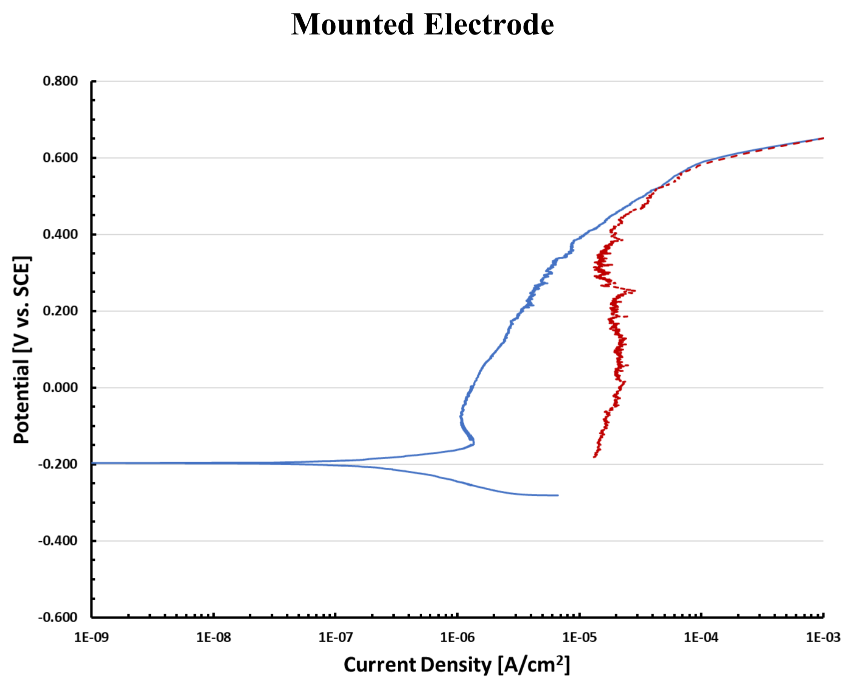
Mounted Electrode
0.800
0.600
0.400
0.200
0.000
-0.200
-0.400
-0.600
Potential [V vs. SCE]
1E-09
1E-08
1E-07
1E-06
1E-05
1E-04
1E-03
Current Density [A/cm²]

Trial 62

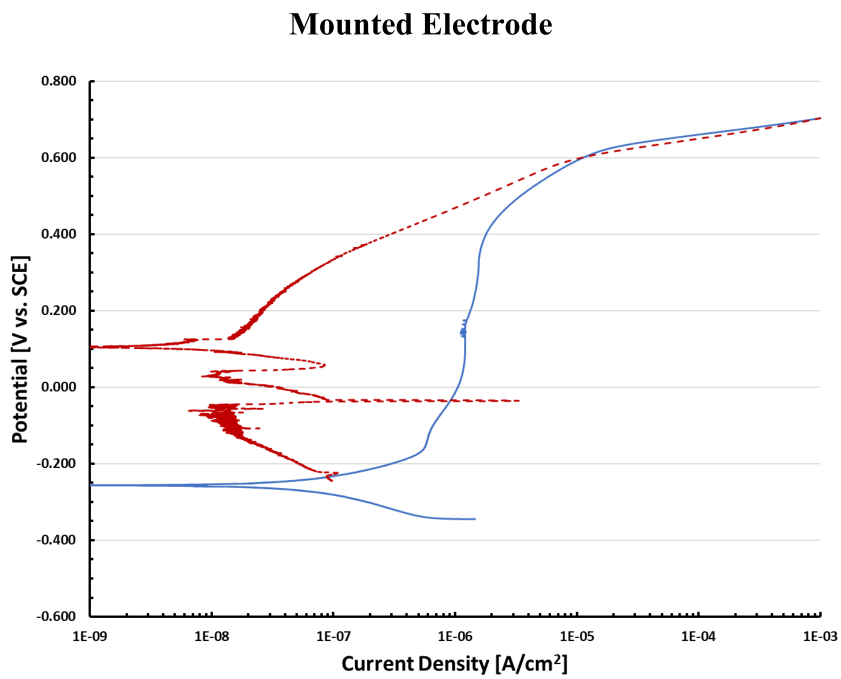
Mounted Electrode
0.800
0.600
0.400
0.200
0.000
-0.200
-0.400
-0.600
Potential [V vs. SCE]
1E-09
1E-08
1E-07
1E-06
1E-05
1E-04
1E-03
Current Density [A/cm^2]

Trial 63

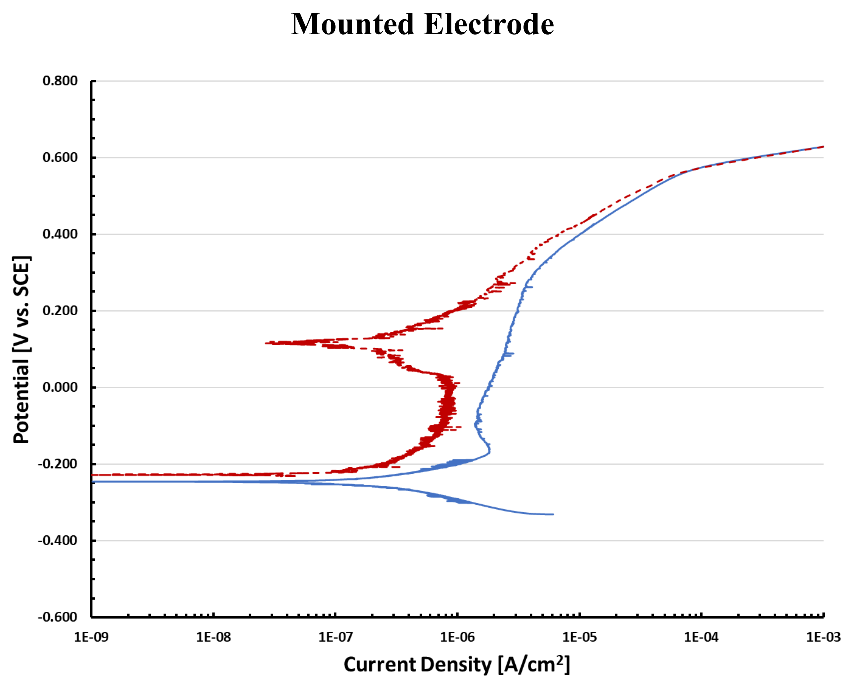
Mounted Electrode
0.800
0.600
0.400
0.200
0.000
-0.200
-0.400
-0.600
Potential [V vs. SCE]
1E-09
1E-08
1E-07
1E-06
1E-05
1E-04
1E-03
Current Density [A/cm²]

Trial 64

Mounted Electrode

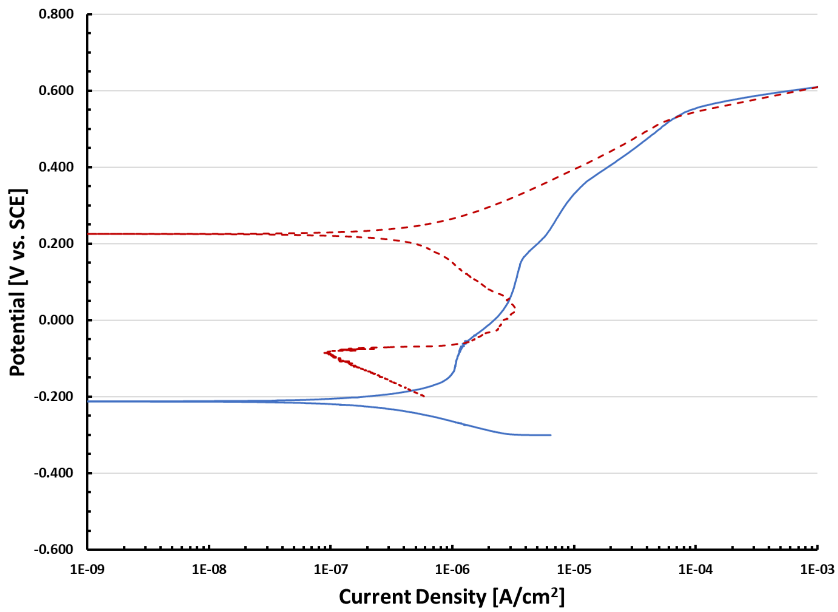

Trial 65

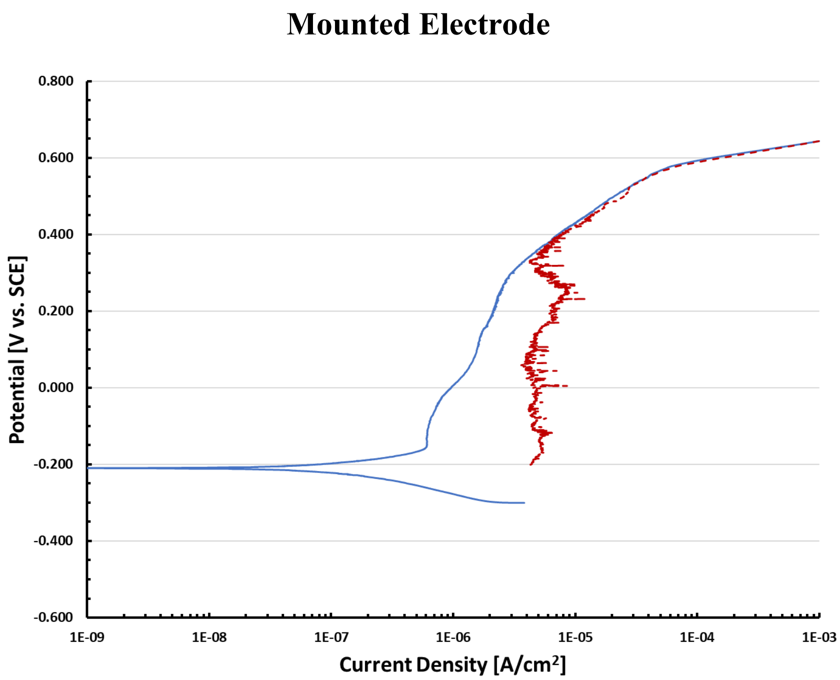
Mounted Electrode
0.800
0.600
0.400
0.200
0.000
-0.200
-0.400
-0.600
Potential [V vs. SCE]
1E-09
1E-08
1E-07
1E-06
1E-05
1E-04
1E-03
Current Density [A/cm2]

Trial 66

Mounted Electrode

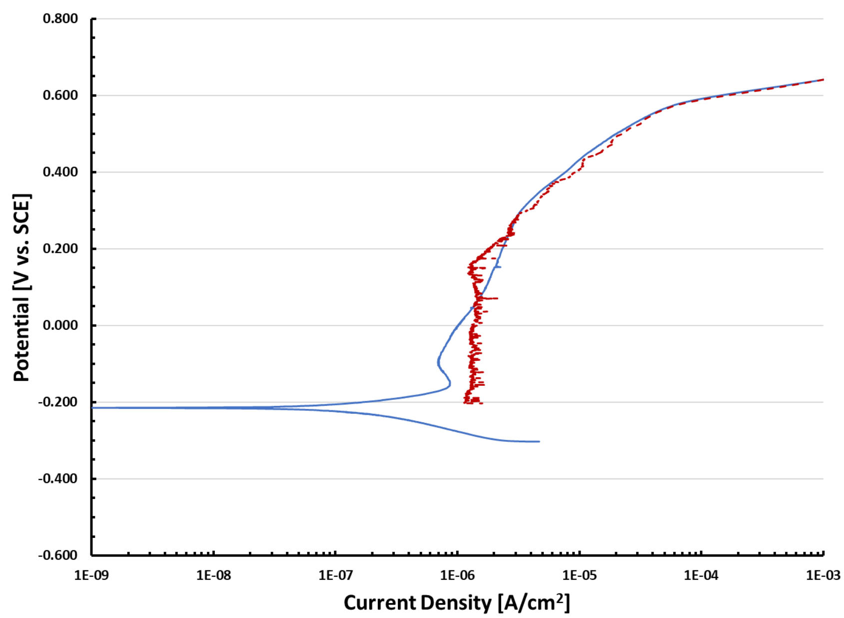

Trial 67

Mounted Electrode

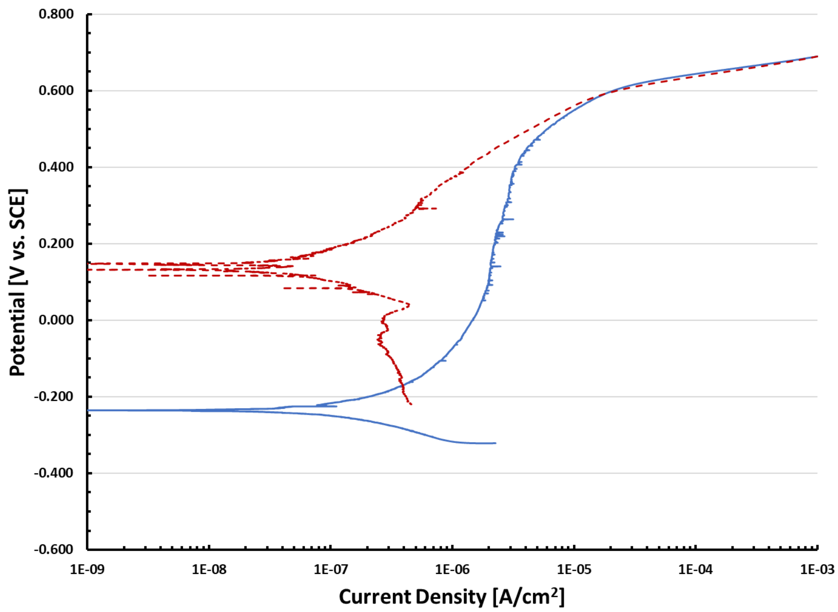

Trial 68

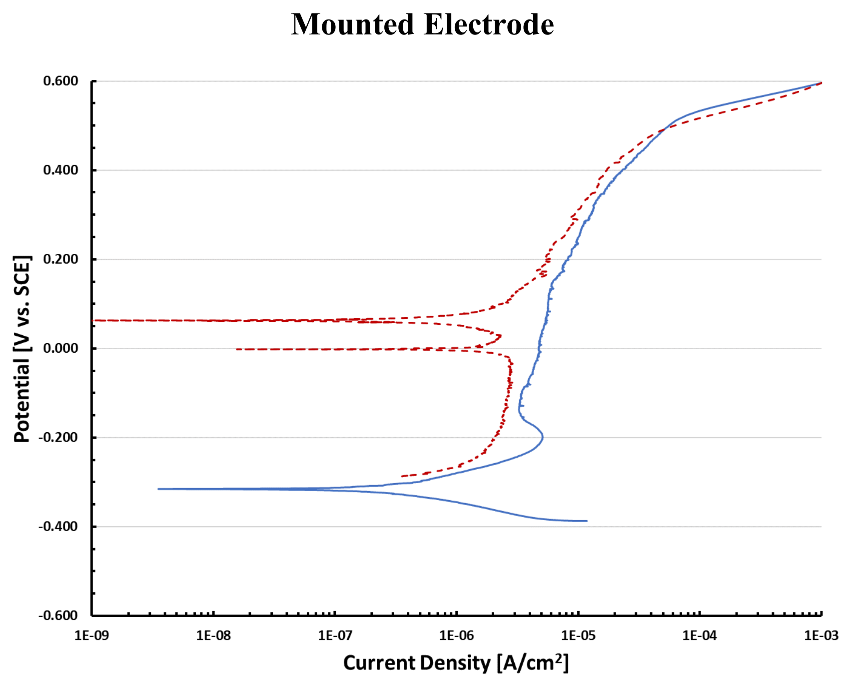
Mounted Electrode
0.600
0.400
0.200
0.000
-0.200
-0.400
-0.600
Potential [V vs. SCE]
1E-09
1E-08
1E-07
1E-06
1E-05
1E-04
1E-03
Current Density [A/cm2]

Trial 69

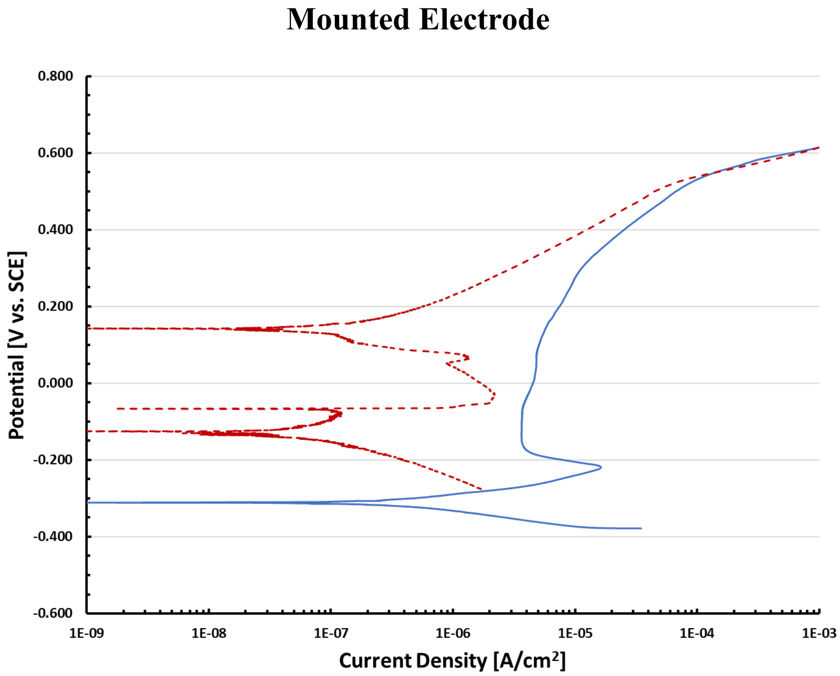
Mounted Electrode
Potential [V vs. SCE]
0.800
0.600
0.400
0.200
0.000
-0.200
-0.400
-0.600
1E-09
1E-08
1E-07
1E-06
1E-05
1E-04
1E-03
Current Density [A/cm²]

Trial 70

Mounted Electrode

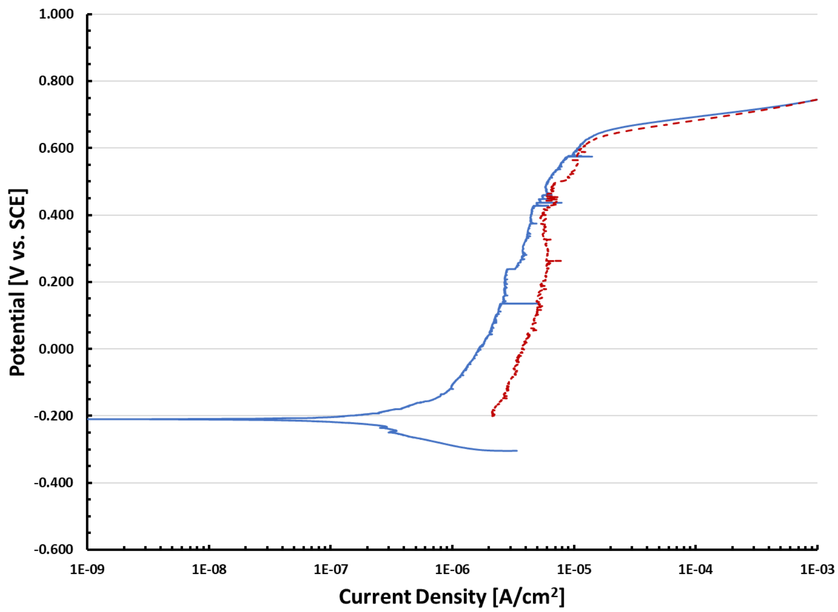

Trial 71

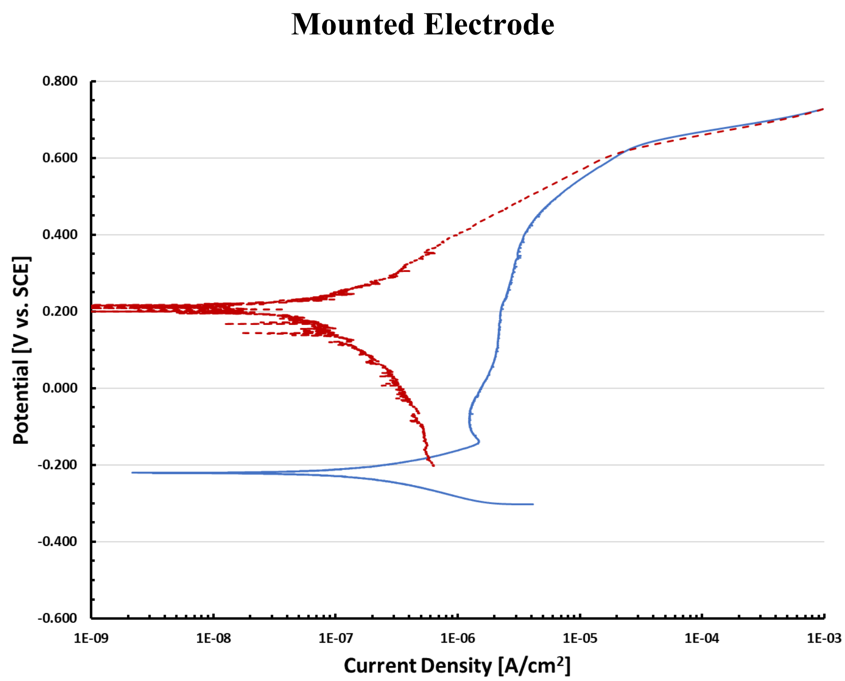
Mounted Electrode
0.800
0.600
0.400
0.200
0.000
-0.200
-0.400
-0.600
Potential [V vs. SCE]
1E-09
1E-08
1E-07
1E-06
1E-05
1E-04
1E-03
Current Density [A/cm²]

Trial 72

Mounted Electrode

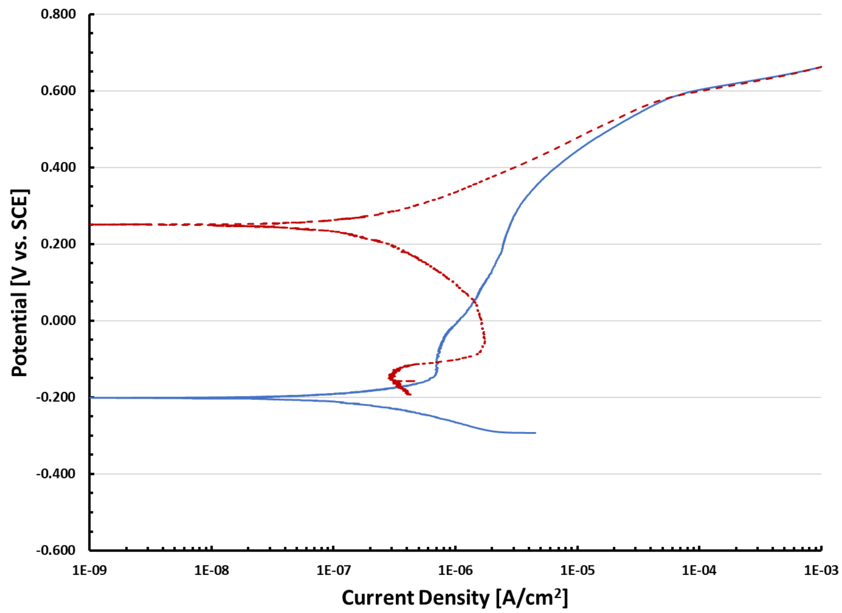

Trial 73

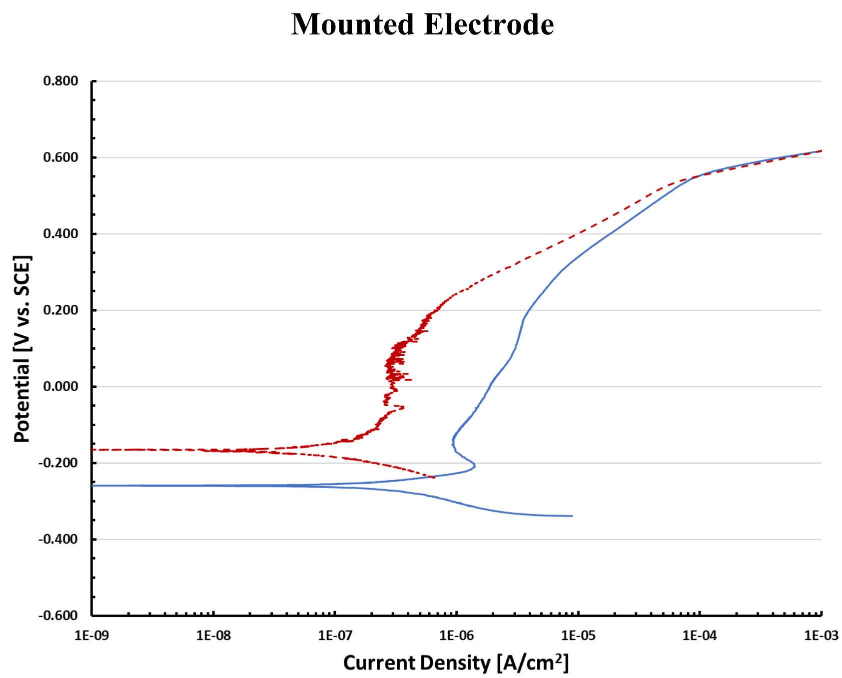
Mounted Electrode
0.800
0.600
0.400
0.200
0.000
-0.200
-0.400
-0.600
Potential [V vs. SCE]
1E-09
1E-08
1E-07
1E-06
1E-05
1E-04
1E-03
Current Density [A/cm2]

Trial 74

Mounted Electrode

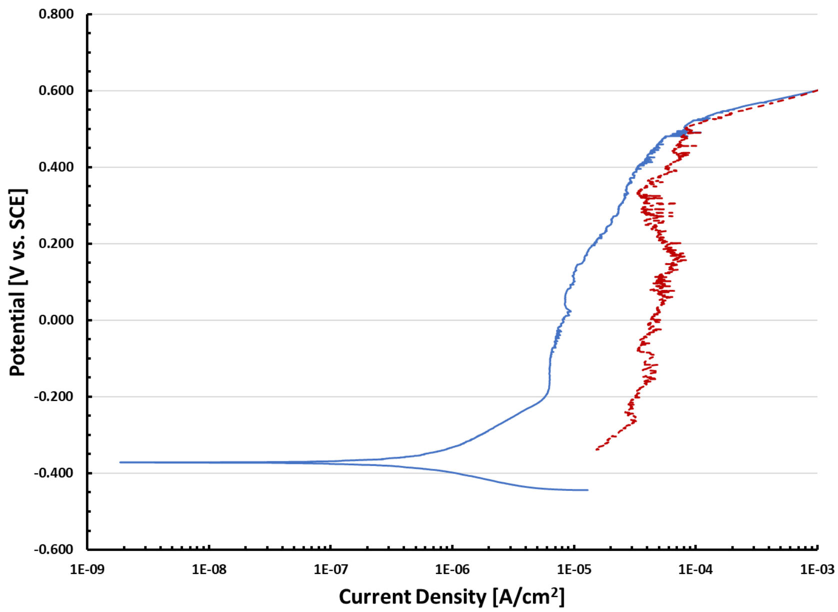

Trial 75

Mounted Electrode

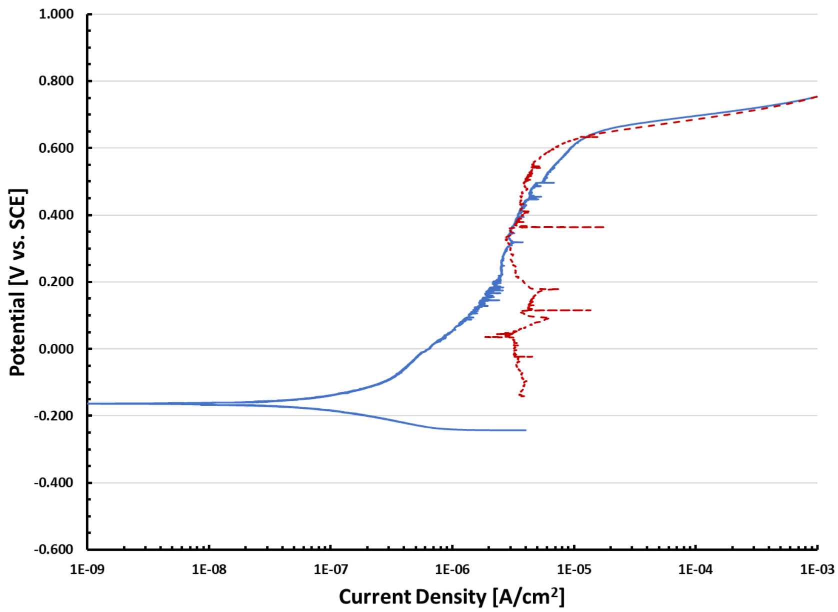

Trial 76

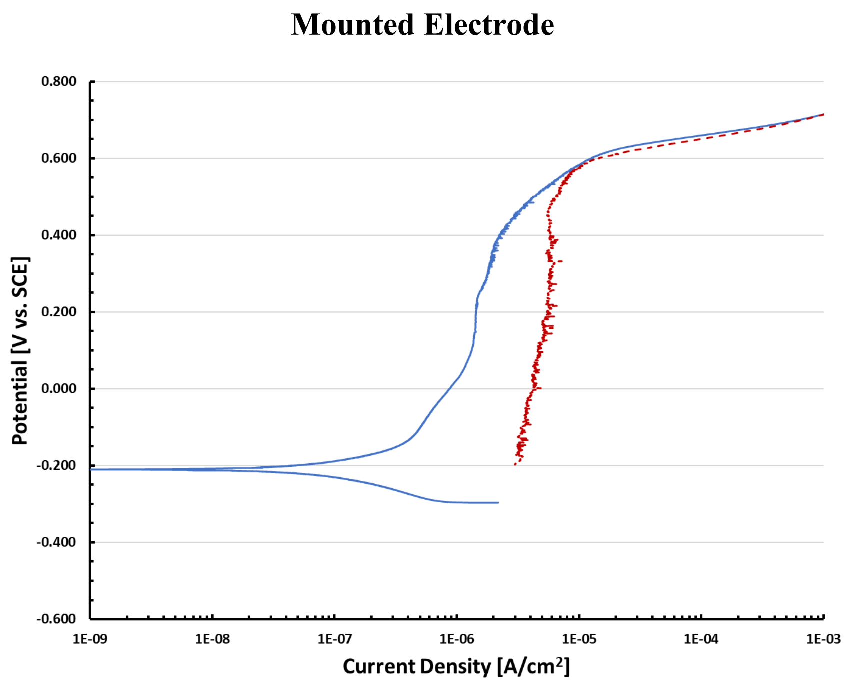
Mounted Electrode
0.800
0.600
0.400
0.200
0.000
-0.200
-0.400
-0.600
Potential [V vs. SCE]
1E-09
1E-08
1E-07
1E-06
1E-05
1E-04
1E-03
Current Density [A/cm2]

Trial 77

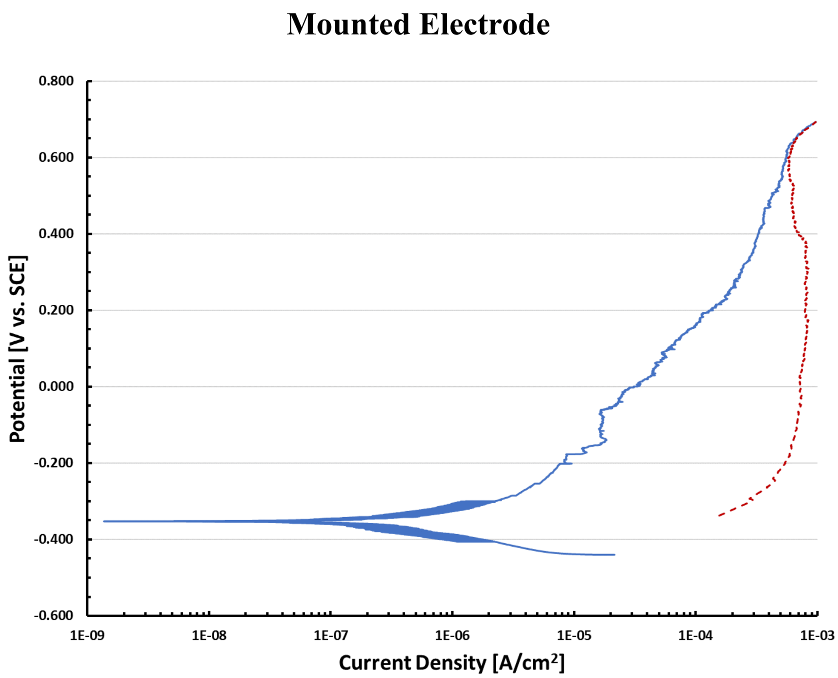
Mounted Electrode
0.800
0.600
0.400
0.200
0.000
-0.200
-0.400
-0.600
Potential [V vs. SCE]
1E-09
1E-08
1E-07
1E-06
1E-05
1E-04
1E-03
Current Density [A/cm2]

Trial 78

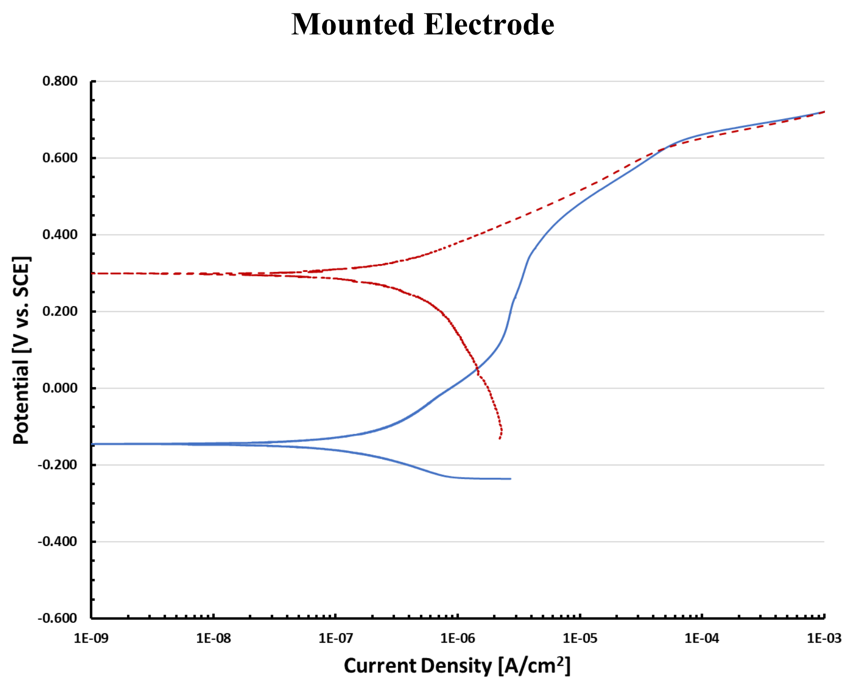
Mounted Electrode
0.800
0.600
0.400
0.200
0.000
-0.200
-0.400
-0.600
Potential [V vs. SCE]
1E-09
1E-08
1E-07
1E-06
1E-05
1E-04
1E-03
Current Density [A/cm²]

Trial 79

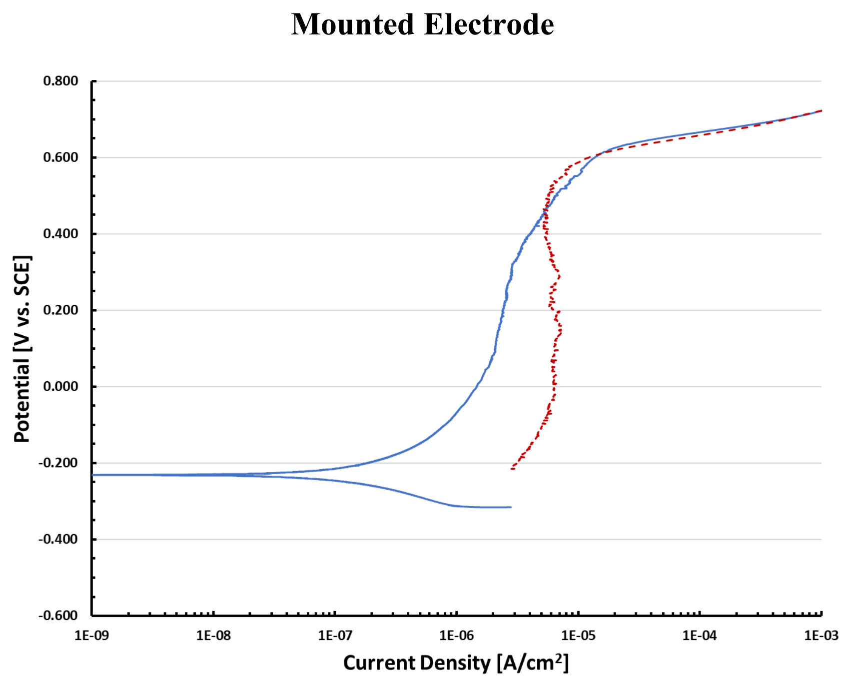
Mounted Electrode
0.800
0.600
0.400
0.200
0.000
-0.200
-0.400
-0.600
Potential [V vs. SCE]
1E-09
1E-08
1E-07
1E-06
1E-05
1E-04
1E-03
Current Density [A/cm2]

Trial 80

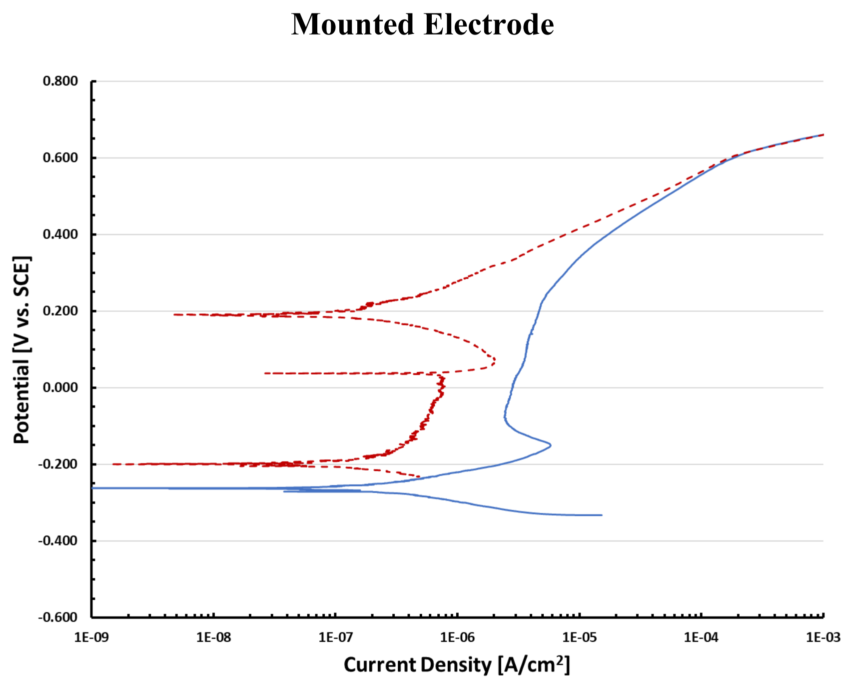
Mounted Electrode
0.800
0.600
0.400
0.200
0.000
-0.200
-0.400
-0.600
Potential [V vs. SCE]
1E-09
1E-08
1E-07
1E-06
1E-05
1E-04
1E-03
Current Density [A/cm²]

Trial 81

Mounted Electrode

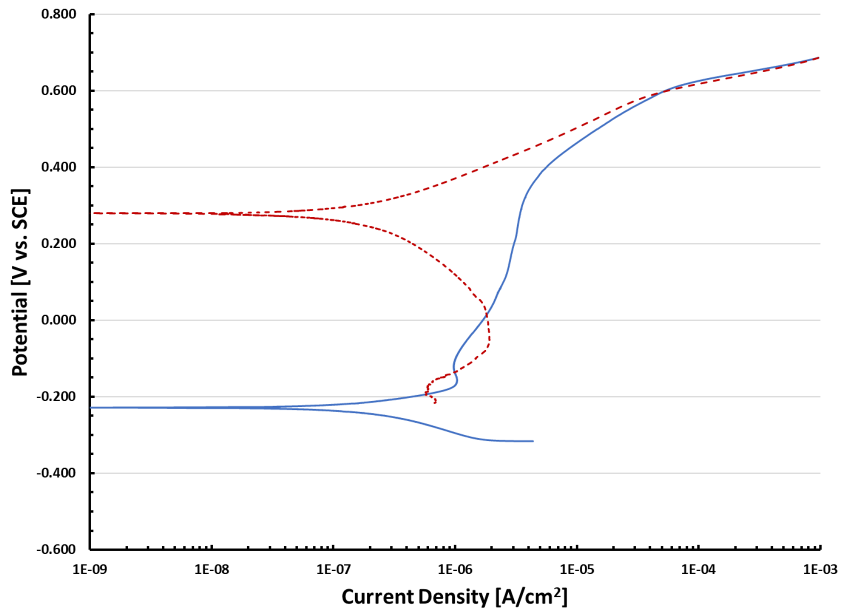

Trial 82

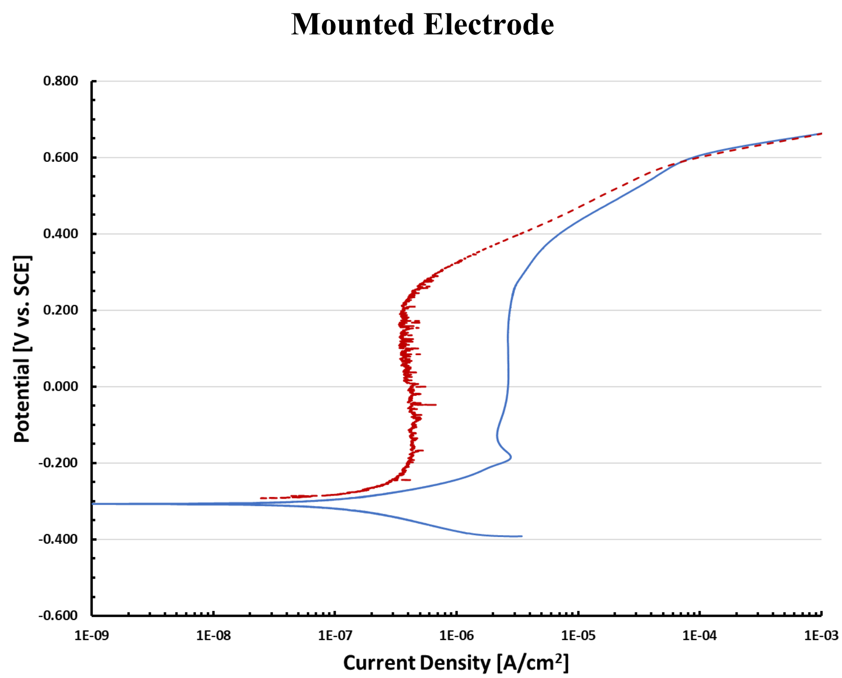
Mounted Electrode
0.800
0.600
0.400
0.200
0.000
-0.200
-0.400
-0.600
Potential [V vs. SCE]
1E-09
1E-08
1E-07
1E-06
1E-05
1E-04
1E-03
Current Density [A/cm2]

Trial 83

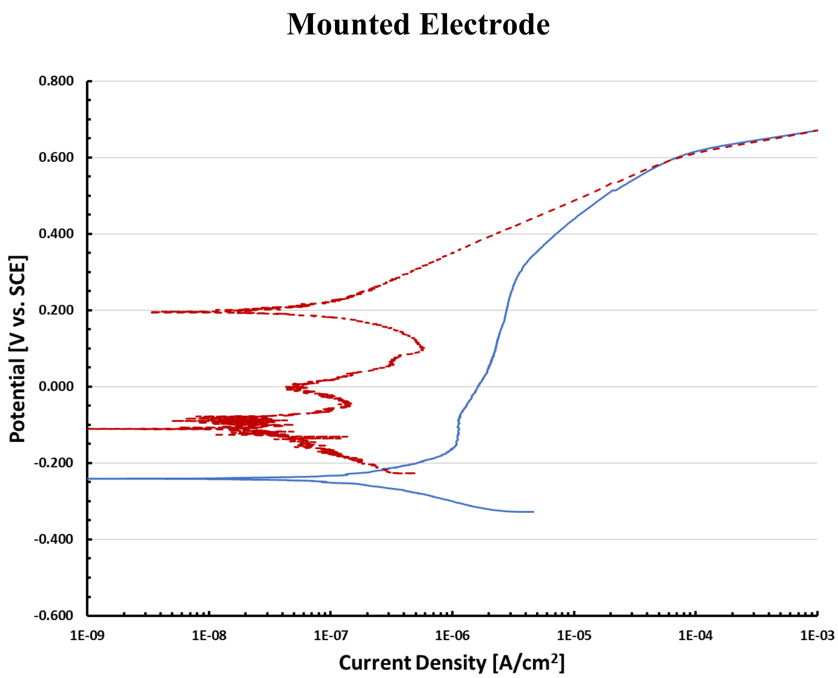
Mounted Electrode
0.800
0.600
0.400
0.200
0.000
-0.200
-0.400
-0.600
Potential [V vs. SCE]
1E-09
1E-08
1E-07
1E-06
1E-05
1E-04
1E-03
Current Density [A/cm2]

Trial 84

Mounted Electrode

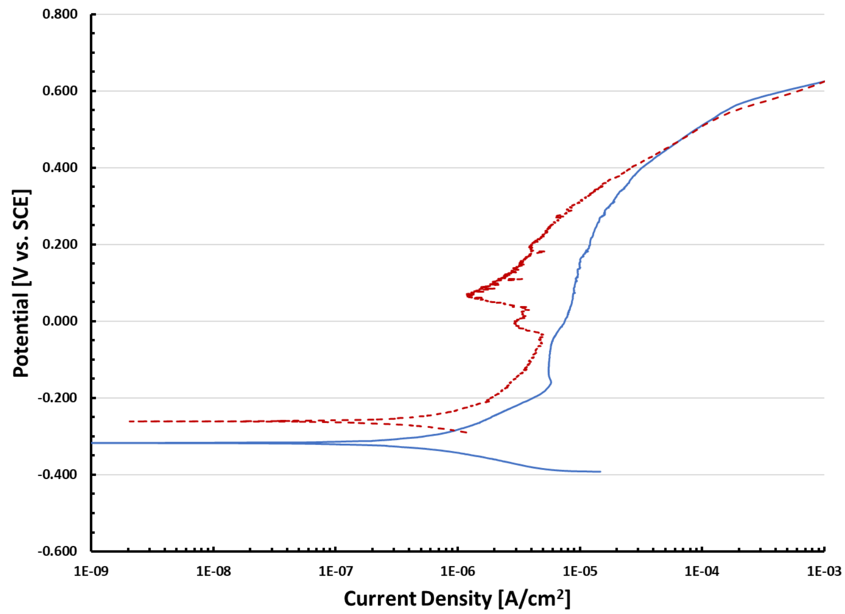

Trial 85

Mounted Electrode

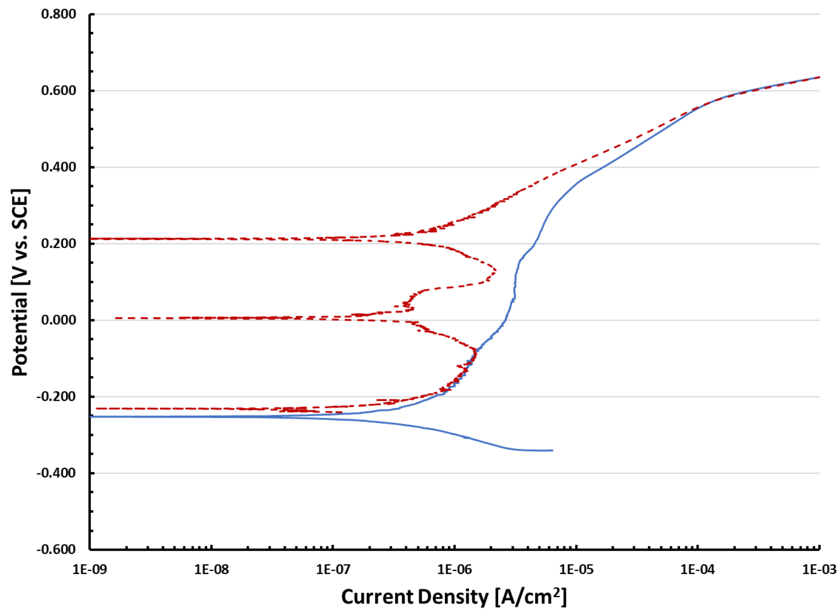

Trial 86

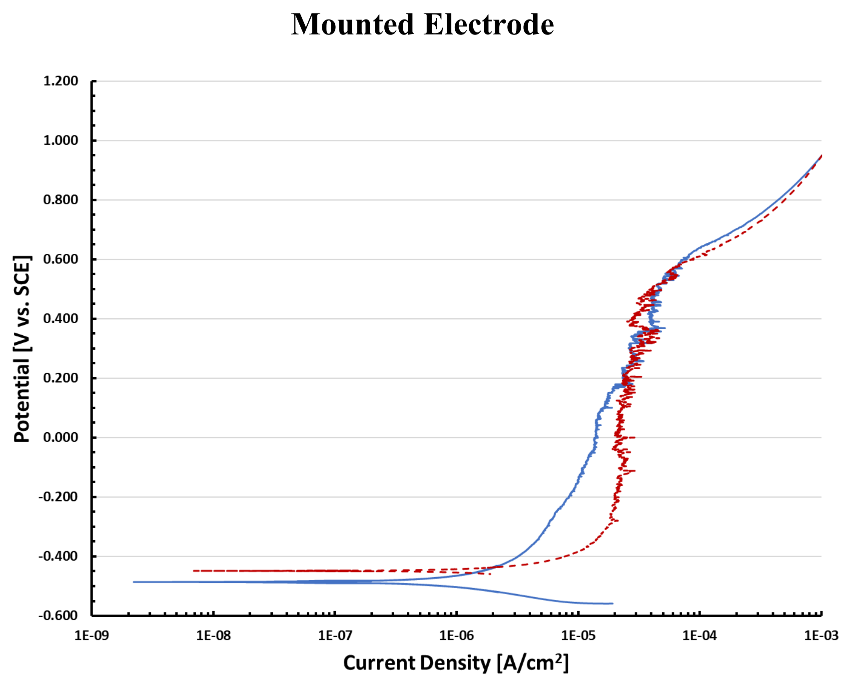
Mounted Electrode
Potential [V vs. SCE]
1.200
1.000
0.800
0.600
0.400
0.200
0.000
-0.200
-0.400
-0.600
1E-09
1E-08
1E-07
1E-06
1E-05
1E-04
1E-03
Current Density [A/cm²]

Trial 87

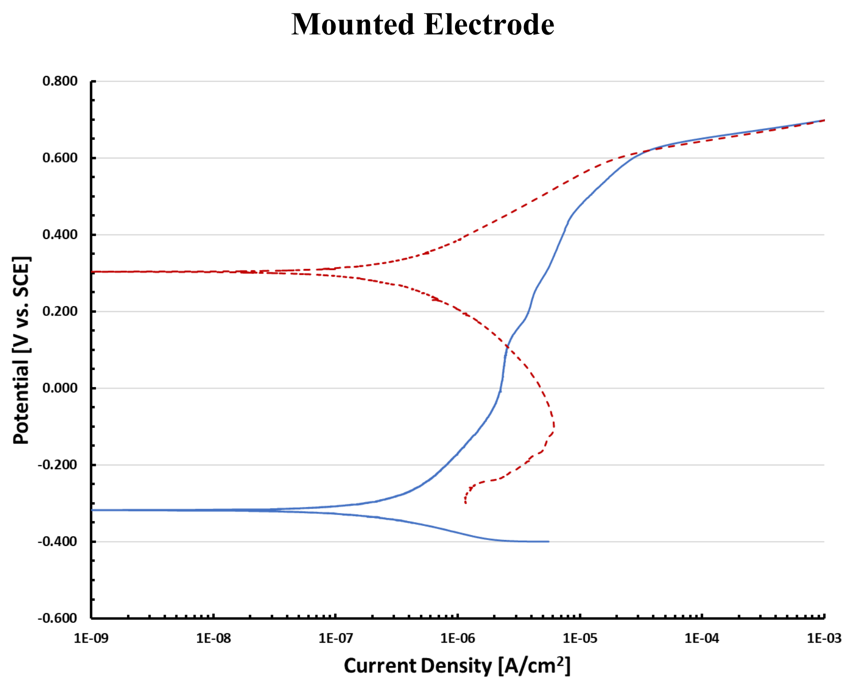
Mounted Electrode
0.800
0.600
0.400
0.200
0.000
-0.200
-0.400
-0.600
Potential [V vs. SCE]
1E-09
1E-08
1E-07
1E-06
1E-05
1E-04
1E-03
Current Density [A/cm²]

Trial 88

Mounted Electrode

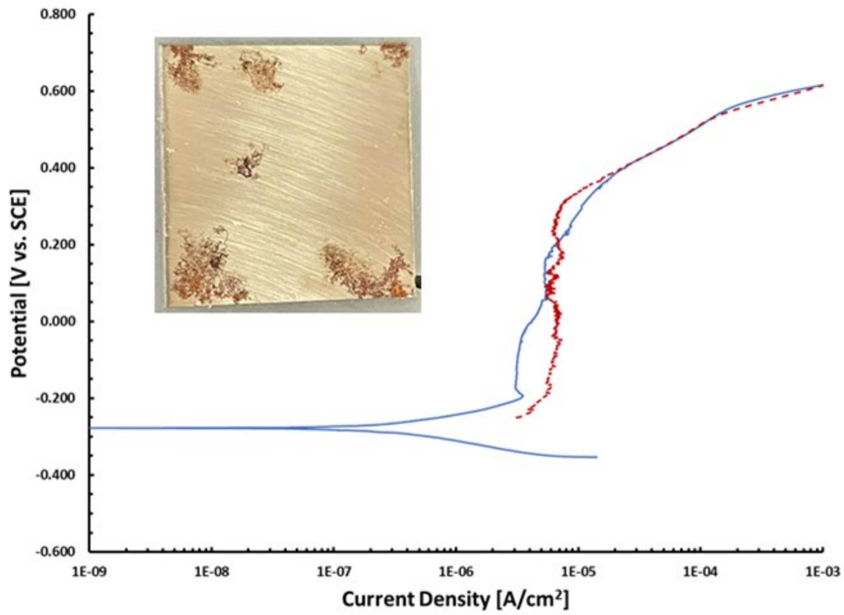

Bullet Electrode

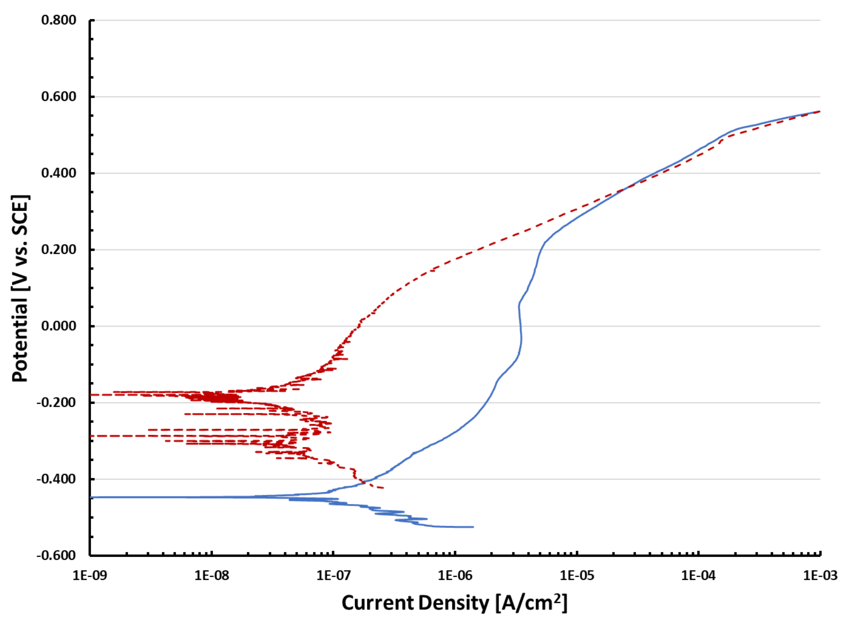

Trial 88 (Continued)

Modified ASTM G192

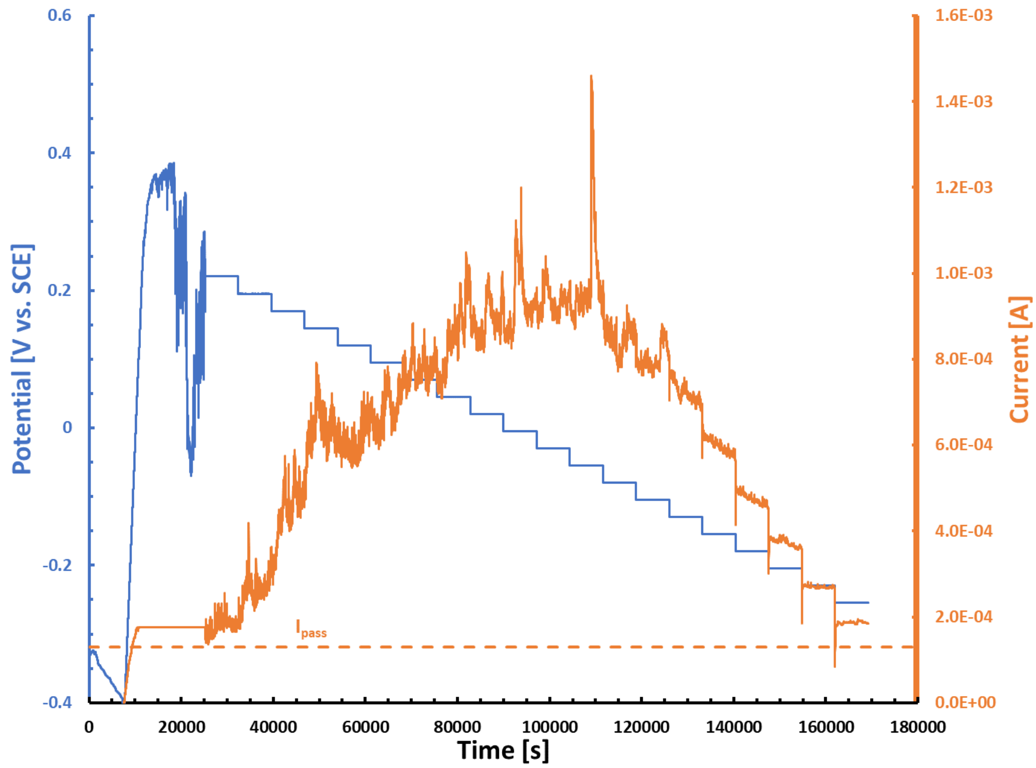

Trial 89

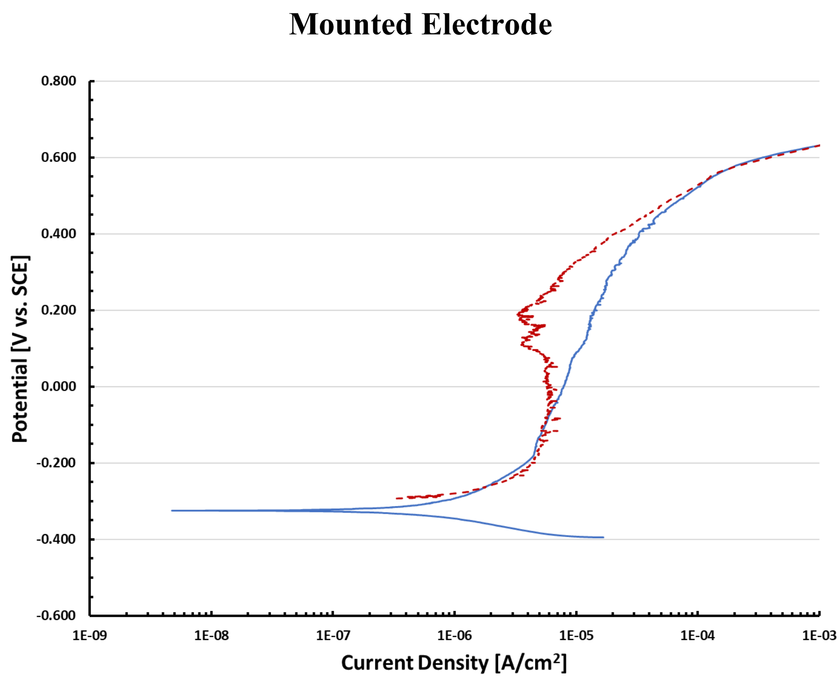
Mounted Electrode
0.800
0.600
0.400
0.200
0.000
-0.200
-0.400
-0.600
Potential [V vs. SCE]
1E-09
1E-08
1E-07
1E-06
1E-05
1E-04
1E-03
Current Density [A/cm2]

Trial 90

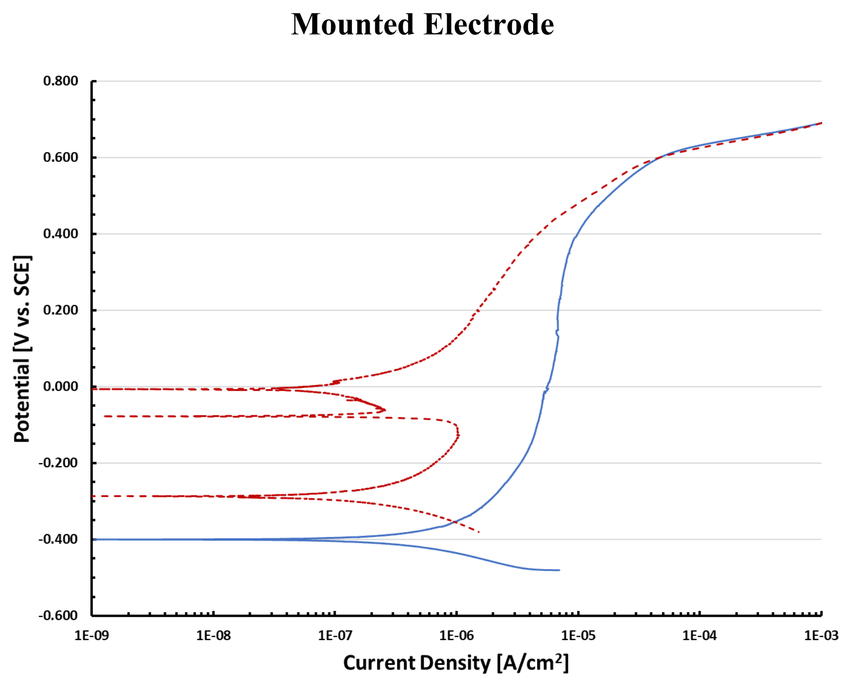
Mounted Electrode
0.800
0.600
0.400
0.200
0.000
-0.200
-0.400
-0.600
Potential [V vs. SCE]
1E-09
1E-08
1E-07
1E-06
1E-05
1E-04
1E-03
Current Density [A/cm²]

Trial 91

Mounted Electrode

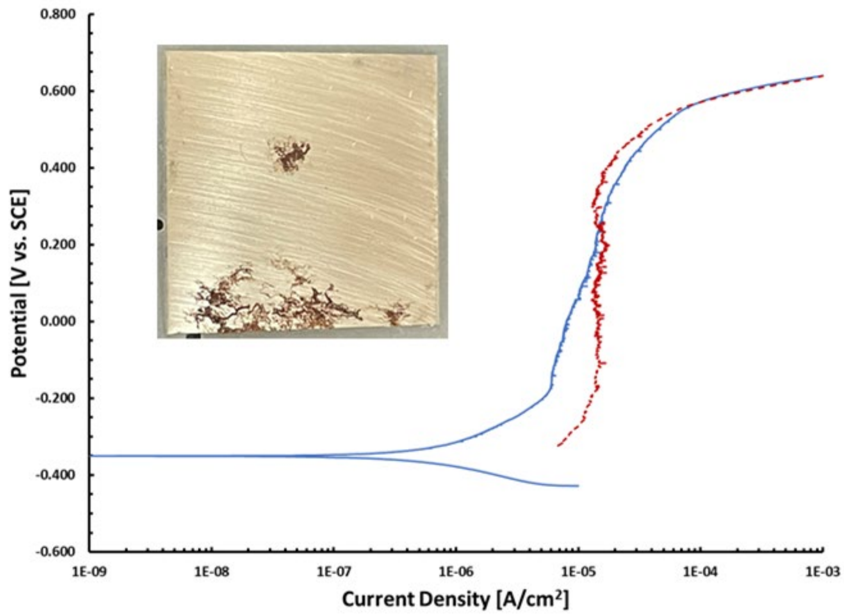

Bullet Electrode

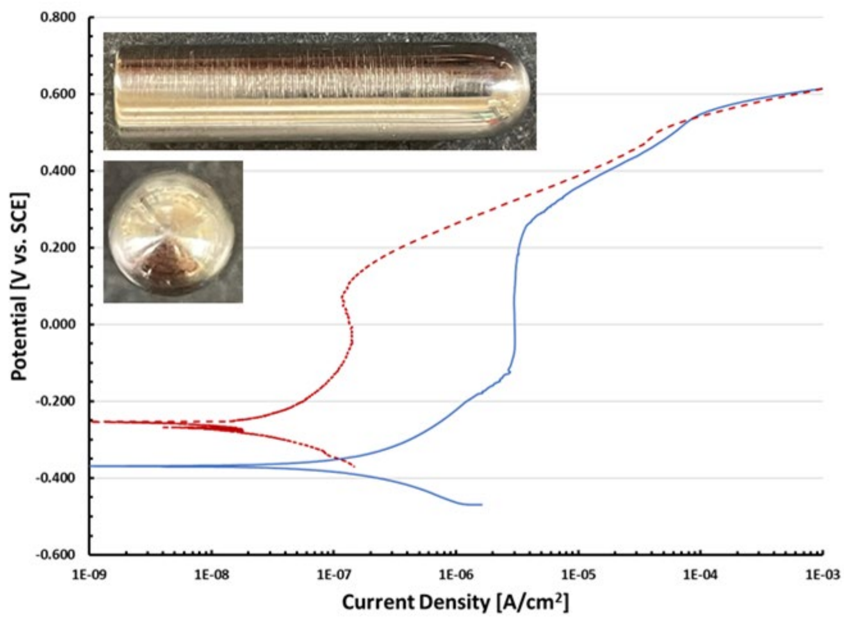

Trial 91 (Continued)

Modified ASTM G192

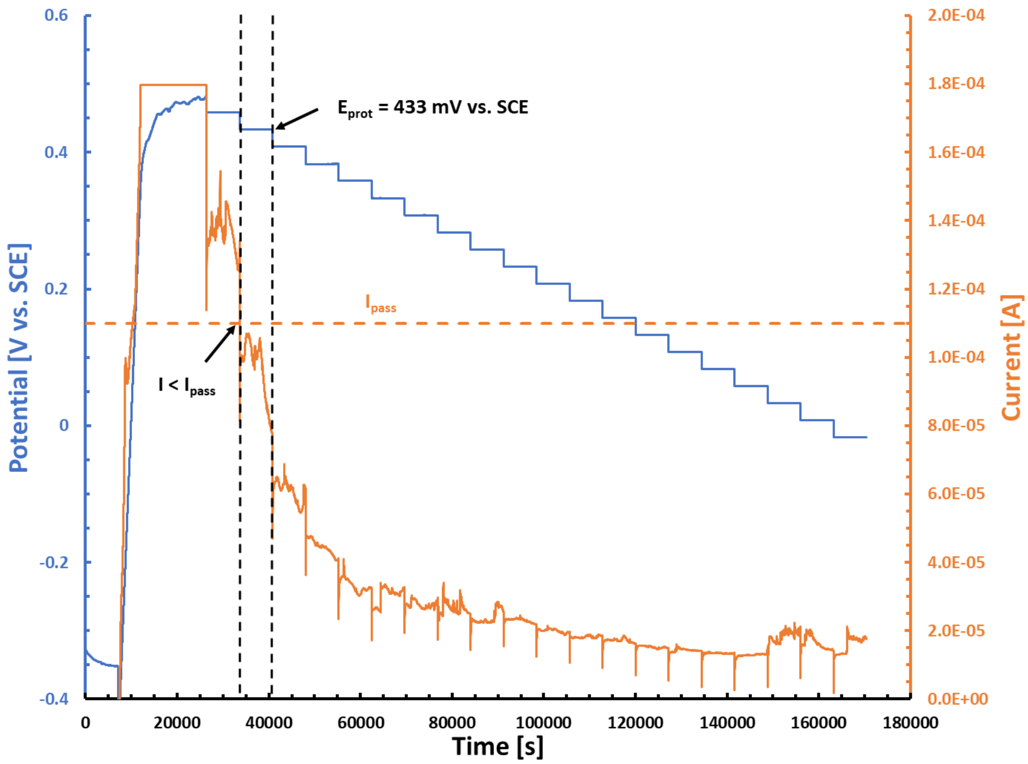

Trial 92

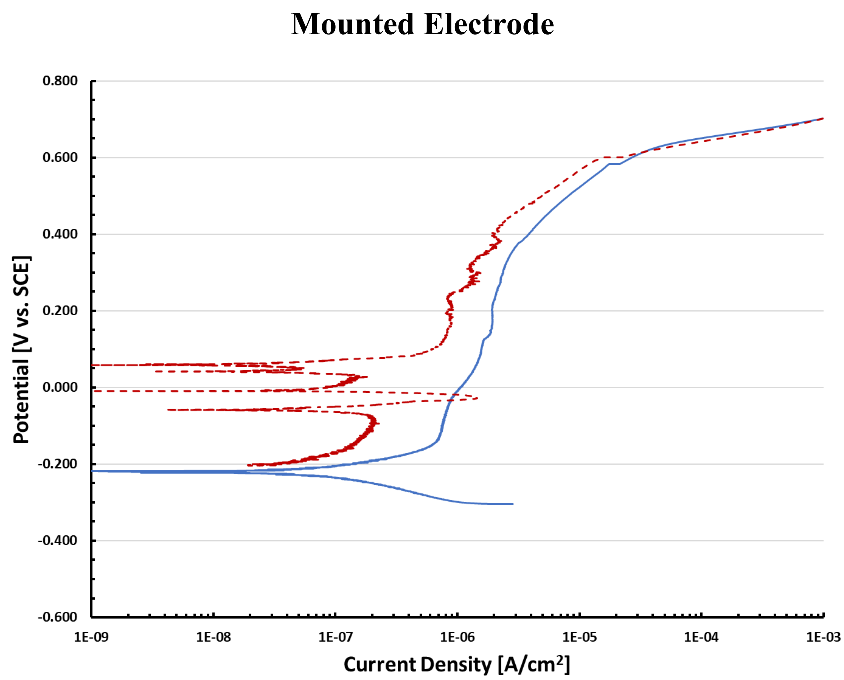
Mounted Electrode
0.800
0.600
0.400
0.200
0.000
-0.200
-0.400
-0.600
Potential [V vs. SCE]
1E-09
1E-08
1E-07
1E-06
1E-05
1E-04
1E-03
Current Density [A/cm2]

Trial 93

Mounted Electrode

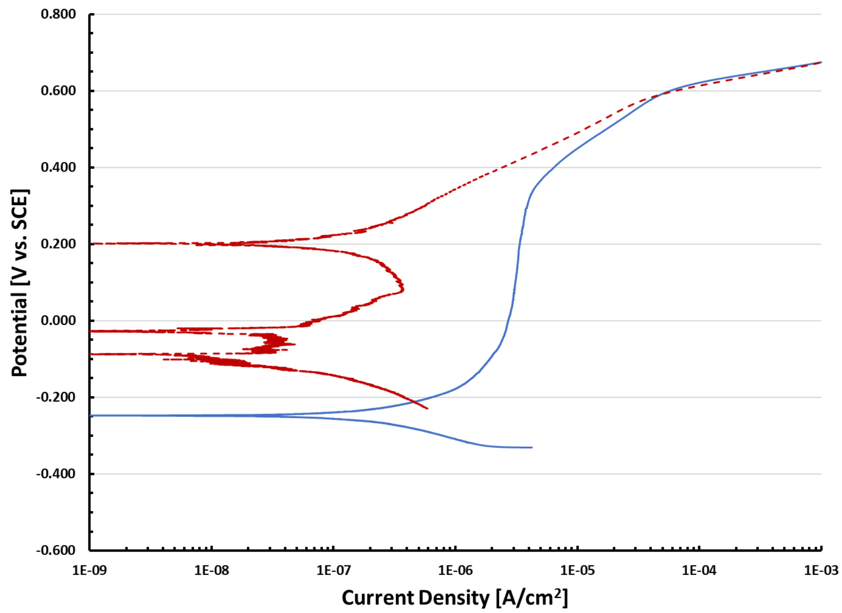

Trial 94

Mounted Electrode

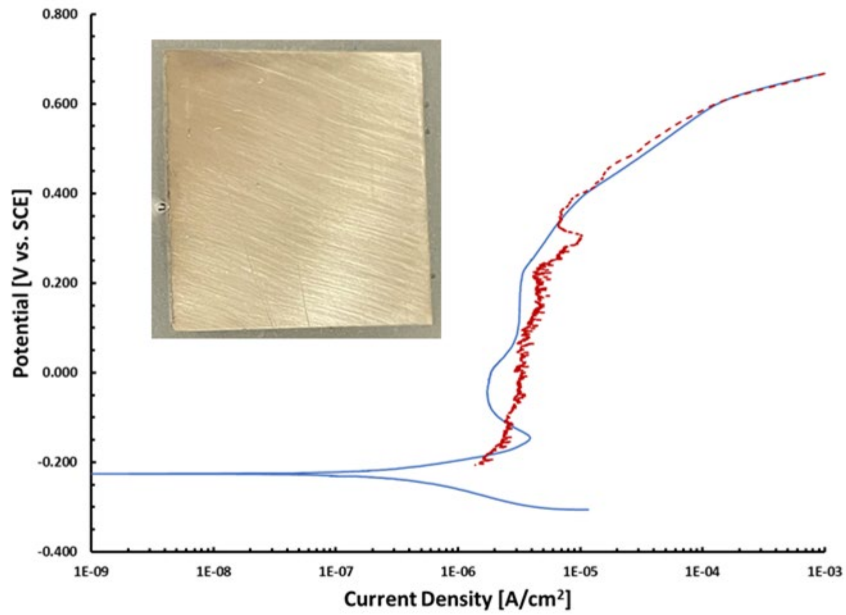

Modified ASTM G192

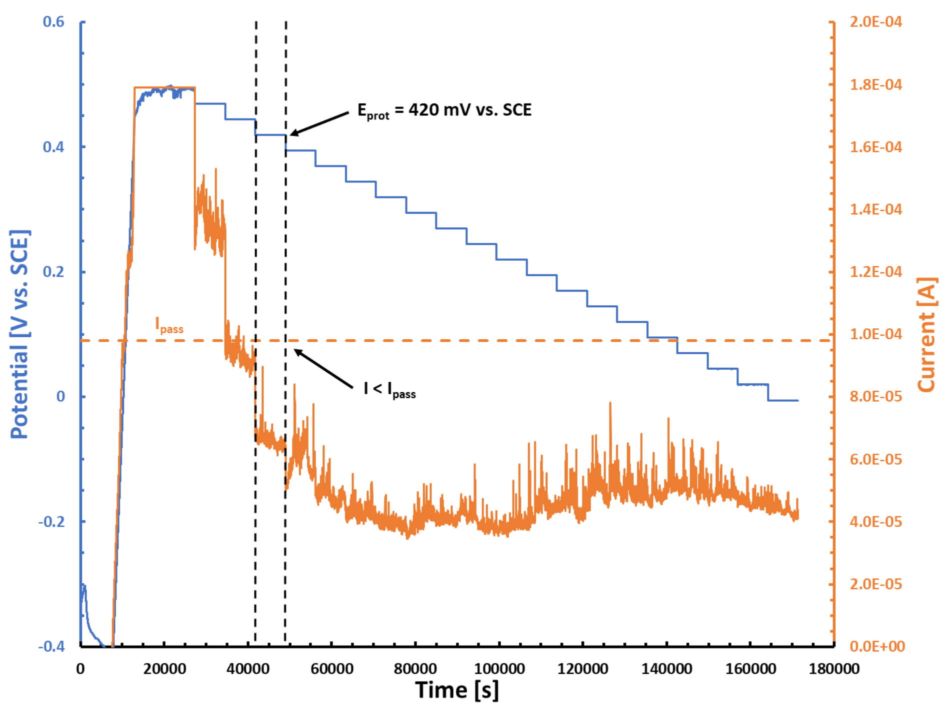

Trial 95

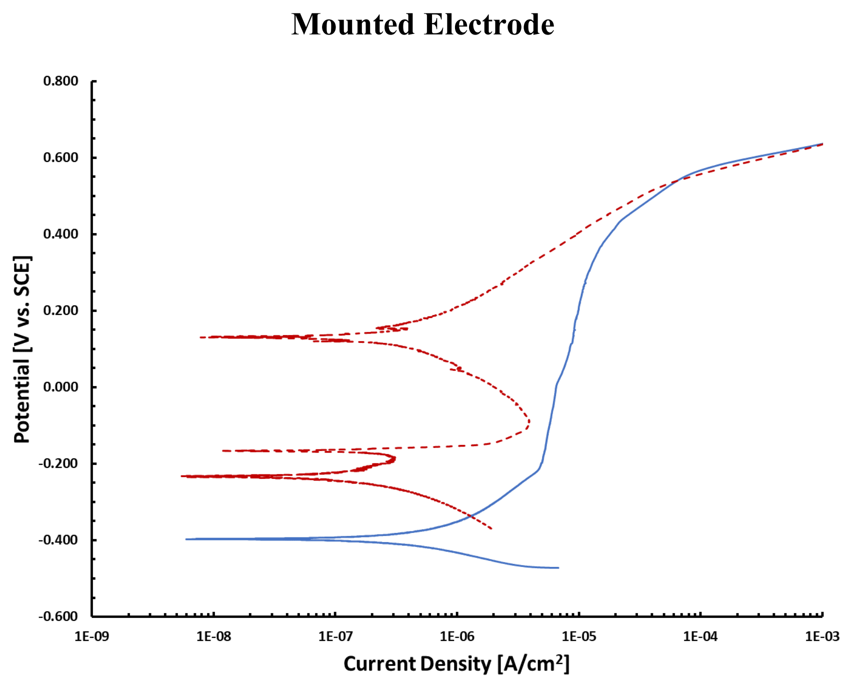
Mounted Electrode
0.800
0.600
0.400
0.200
0.000
-0.200
-0.400
-0.600
Potential [V vs. SCE]
1E-09
1E-08
1E-07
1E-06
1E-05
1E-04
1E-03
Current Density [A/cm2]

Trial 96

Mounted Electrode

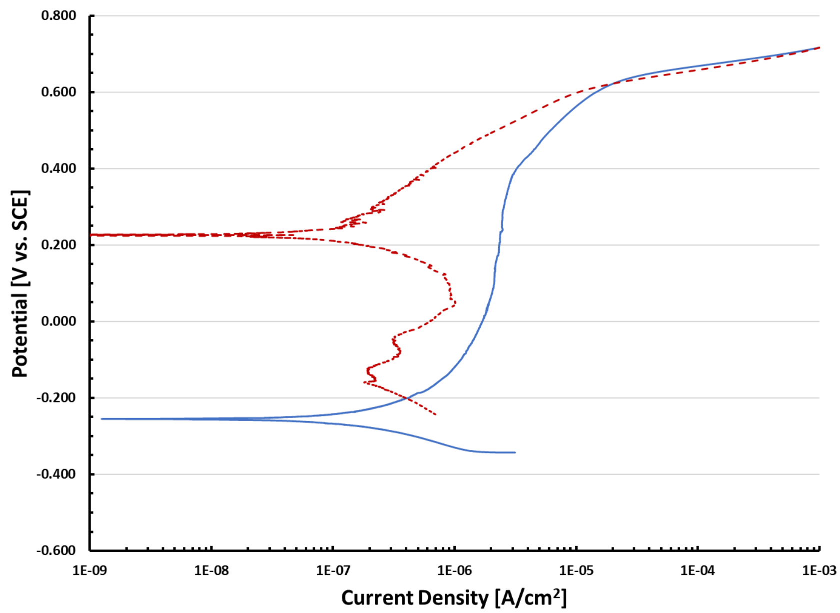

Trial 97

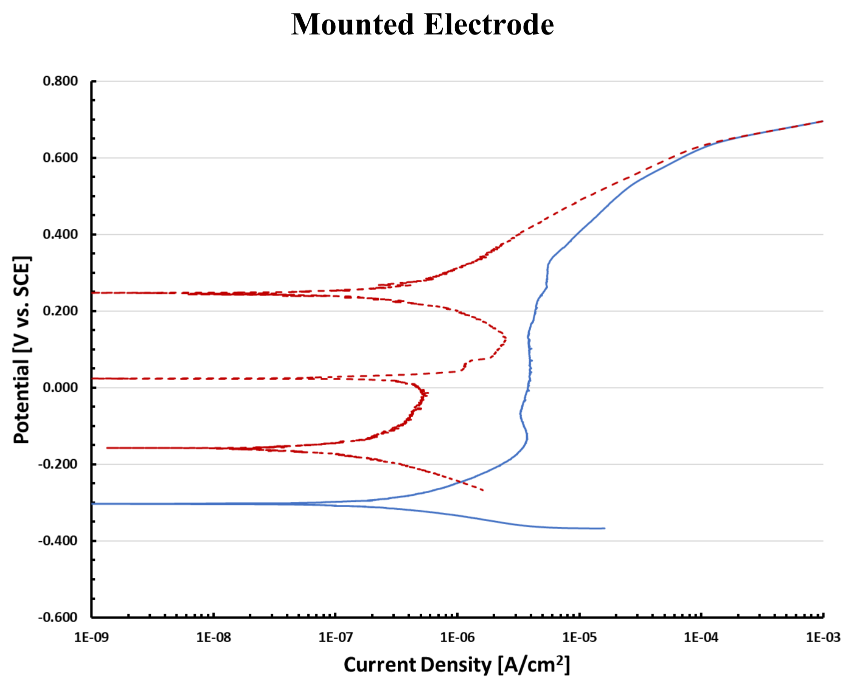
Mounted Electrode
0.800
0.600
0.400
0.200
0.000
-0.200
-0.400
-0.600
Potential [V vs. SCE]
1E-09
1E-08
1E-07
1E-06
1E-05
1E-04
1E-03
Current Density [A/cm²]

Trial 98

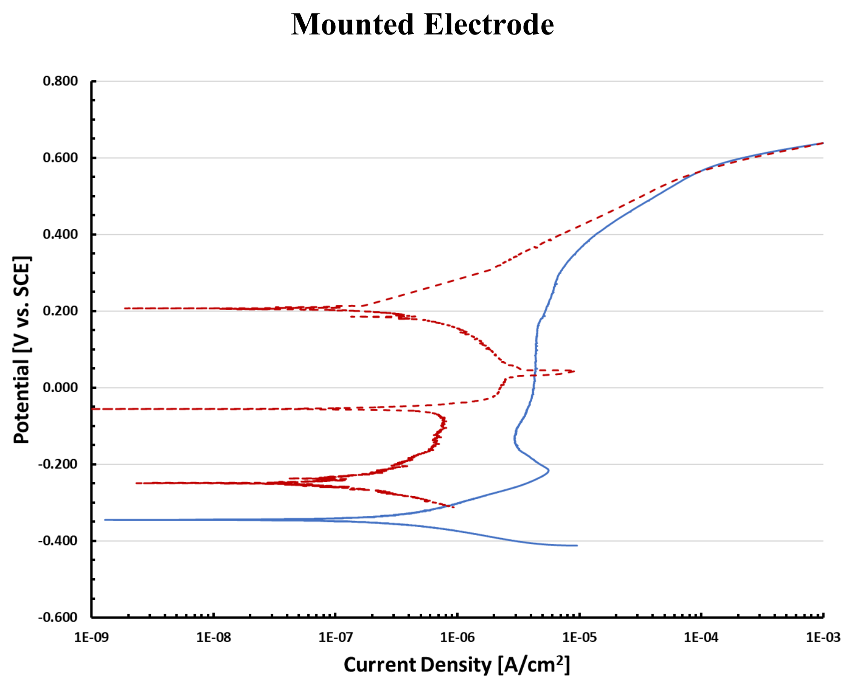
Mounted Electrode
0.800
0.600
0.400
0.200
0.000
-0.200
-0.400
-0.600
Potential [V vs. SCE]
1E-09
1E-08
1E-07
1E-06
1E-05
1E-04
1E-03
Current Density [A/cm²]

Trial 99

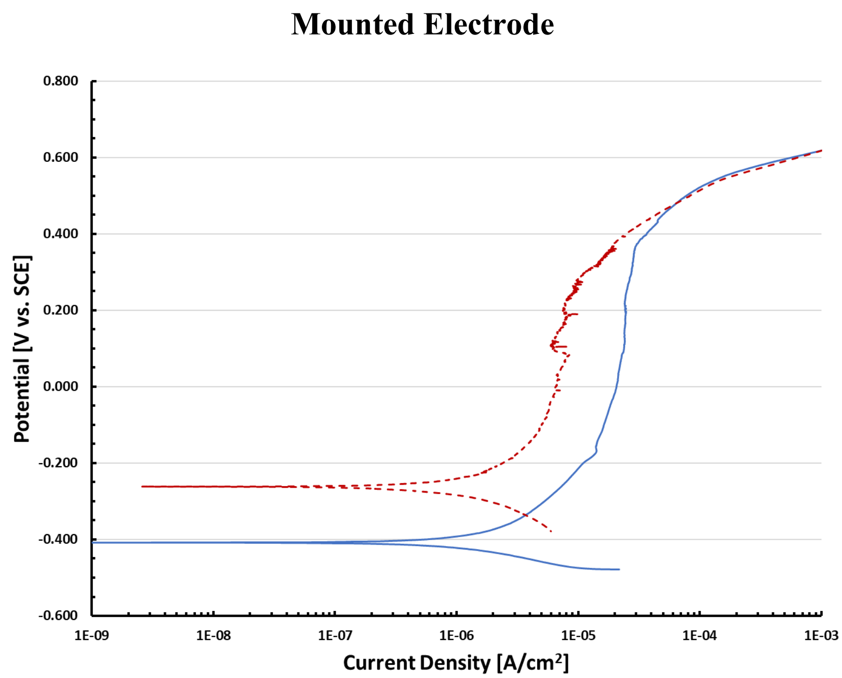
Mounted Electrode
Potential [V vs. SCE]
0.800
0.600
0.400
0.200
0.000
-0.200
-0.400
-0.600
1E-09
1E-08
1E-07
1E-06
1E-05
1E-04
1E-03
Current Density [A/cm²]

Trial 100

Mounted Electrode

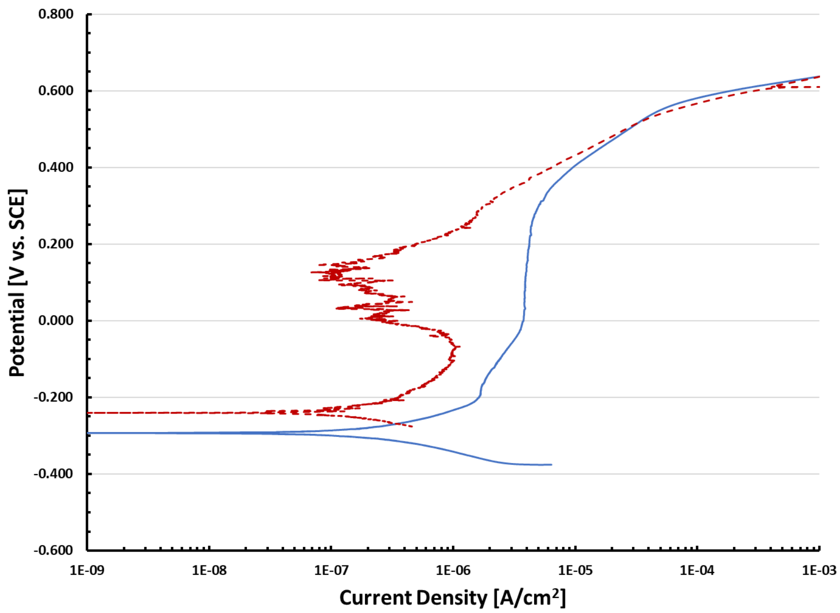

Trial 101

Bullet Electrode

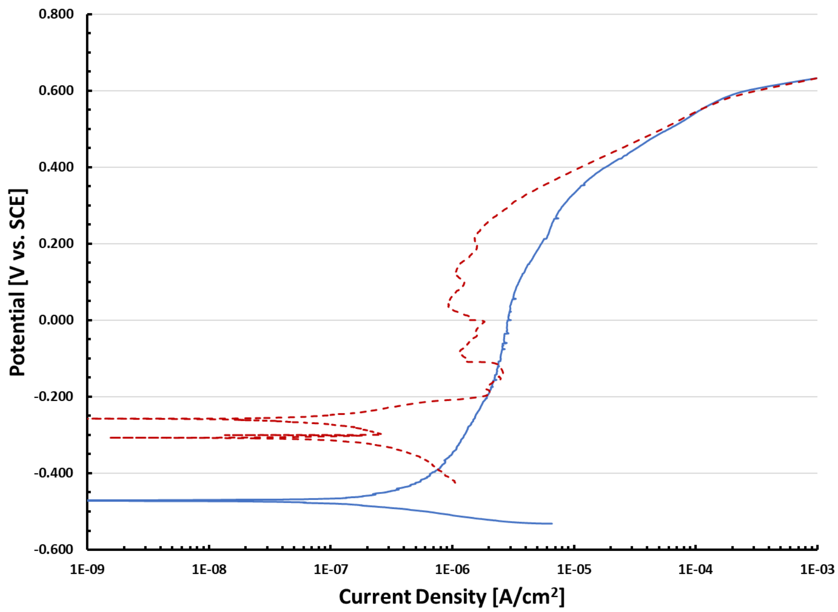

Trial 102

Bullet Electrode

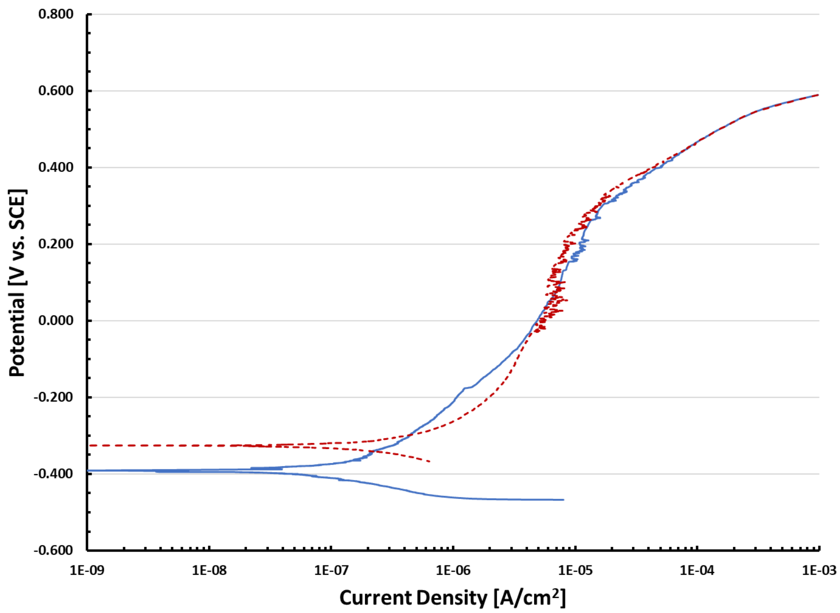

Trial 103

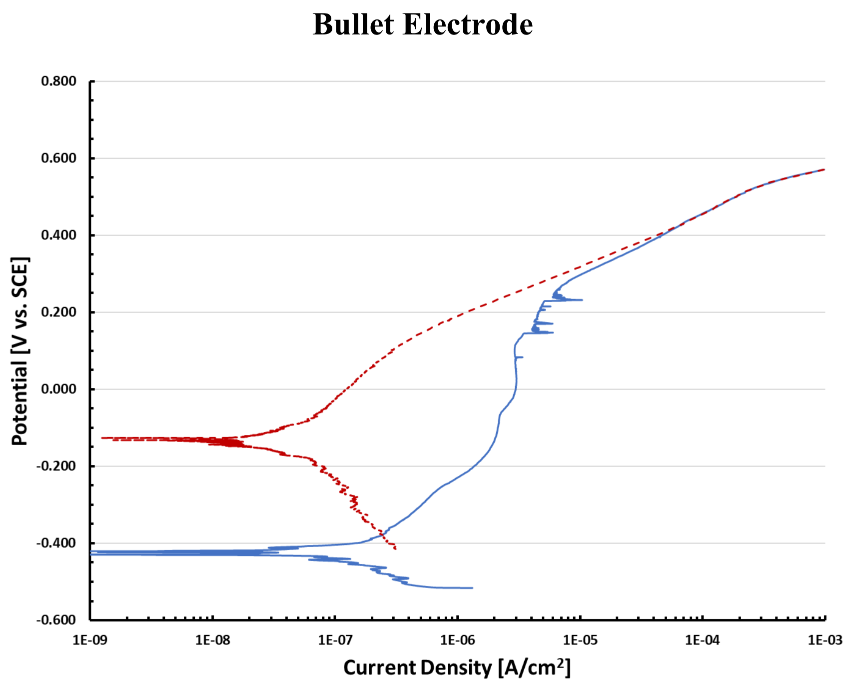
Bullet Electrode
0.800
0.600
0.400
0.200
0.000
-0.200
-0.400
-0.600
Potential [V vs. SCE]
1E-09
1E-08
1E-07
1E-06
1E-05
1E-04
1E-03
Current Density [A/cm2]

Trial 104

Bullet Electrode

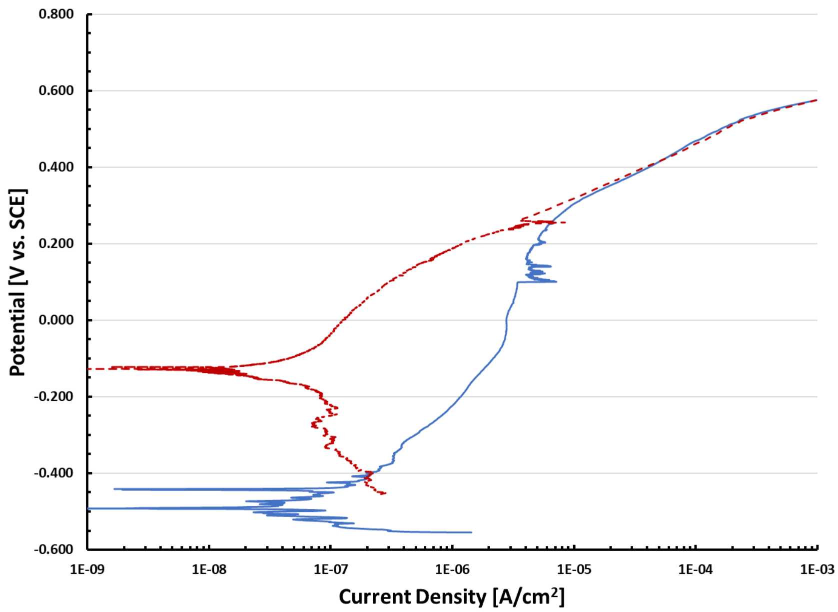

Trial 105

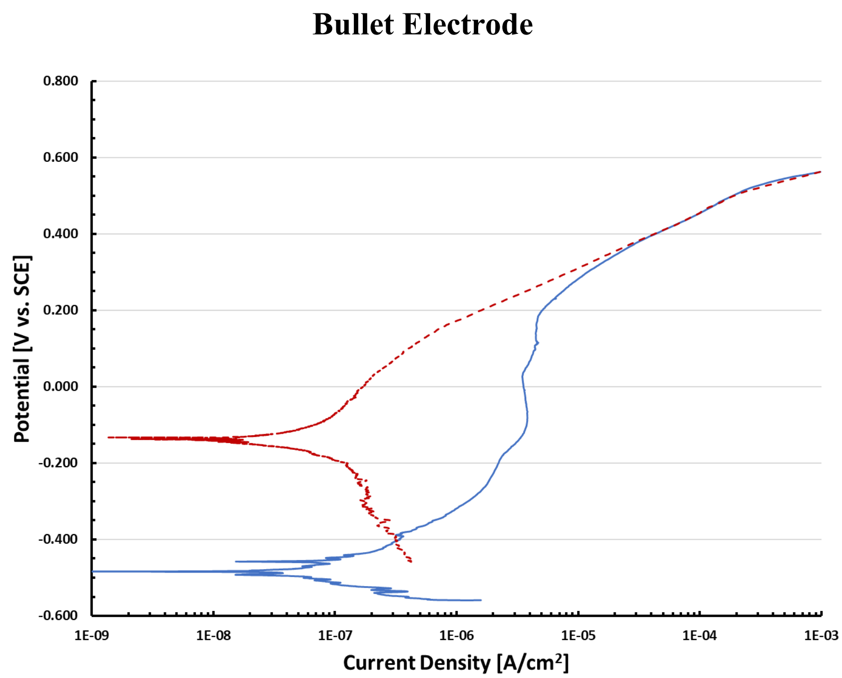
Bullet Electrode
0.800
0.600
0.400
0.200
0.000
-0.200
-0.400
-0.600
Potential [V vs. SCE]
1E-09
1E-08
1E-07
1E-06
1E-05
1E-04
1E-03
Current Density [A/cm²]

Appendix B. Technical Report Design Checklist

WSRC-IM-2002-00011, Revision 2

Figure 1. Technical Report Design Checklist

Report Title: Refinement of Pitting Factor Basis to Support the Corrosion Control Program - Interim Report

Reviewer: B. J. Wiersma

Activity Code: 0HOL3MC054

Document No. SRNL-STI-2023-00061

Current Date: 2/22/2023

Author(s): J. T. Boerstler

Date Needed: 2/24/2023

Location of report and supplemental information: Report and Supplemental Information Sent as an Email Attachment

☑ Analytical/Experimental Approach	Instruction:	Review the experimental approach(es) to determine their validity in evaluating the scope of work.
☐ Mathematical Check	Instruction:	
☑ Inputs	Instruction:	Review information incorporated into the report (charts, figures, equations) to ensure that errors have not occurred in the preparation of data.
☐ Assumptions	Instruction:	
☑ Output	Instruction:	Review results and conclusions to determine if the results are within reason and conclusions have been drawn properly and are supported.
☑ Transcription	Instruction:	Review information/values drawn from figures and charts and used within the text to prevent transcription errors.

Design Check Completed By: BRUCE WIERSMA (Affiliate) Digitally signed by BRUCE WIERSMA (Affiliate) Date: 2023.02.23 15:54:36 -05'00' Date: 02/23/2023

Comment Resolution Accepted By: BRUCE WIERSMA (Affiliate) Digitally signed by BRUCE WIERSMA (Affiliate) Date: 2023.05.15 16:51:09 -04'00' Date: 05/15/2023

JOSHUA BOERSTLER (Affiliate) Digitally signed by JOSHUA BOERSTLER (Affiliate) Date: 2023.05.16 09:10:06 -04'00' Date: 5/16/2023

Distribution:

Joshua.boerstler@srnl.doe.gov
Bruce.wiersma@srnl.doe.gov
Alex.cozzi@srnl.doe.gov
Keisha.martin@srs.gov
Andrea.bridges@srs.gov
Andrew.marvel@srs.gov
Frank.pennebaker@srnl.doe.gov
cj.bannochie@srnl.doe.gov
William.bates@srnl.doe.gov
marion.cofer@srnl.doe.gov
connie.herman@srnl.doe.gov
brady.lee@srnl.doe.gov
Joseph.Manna@srnl.doe.gov
Gregg.Morgan@srnl.doe.gov
William.Ramsey@srnl.doe.gov
eric.skidmore@srnl.doe.gov
michael.stone@srnl.doe.gov
boyd.Wiedenman@srnl.doe.gov
sarah.hodges@srnl.doe.gov
kalyn.loudermilk@srnl.doe.gov
heather.capogreco@srnl.doe.gov
celia.aponte@srs.gov
timothy.baughman@srs.gov
Azikiwe.hooker@srs.gov
Ryan.McNew@srs.gov
phillip.norris@srs.gov
Christine.Ridgeway@srs.gov
Azadeh.Samadi-Dezfouli@srs.gov
Vijay.Jain@srs.gov
arthur.wiggins@srs.gov
Records Administration (EDWS)